AD-A058 611 EXXON RESEARCH AND ENGINEERING CO LINDEN NJ PRODUCTS--ETC F/G 20/11
SELF-GENERATED VOLTAGES AND THEIR RELATIONSHIP TO WEAR UNDER BO--ETC(U)
JUL 78 I L GOLDBLATT N00014-75-C-1080
UNCLASSIFIED EXXON/RL.6PH.78 NL

1 OF 2
AD
A058611

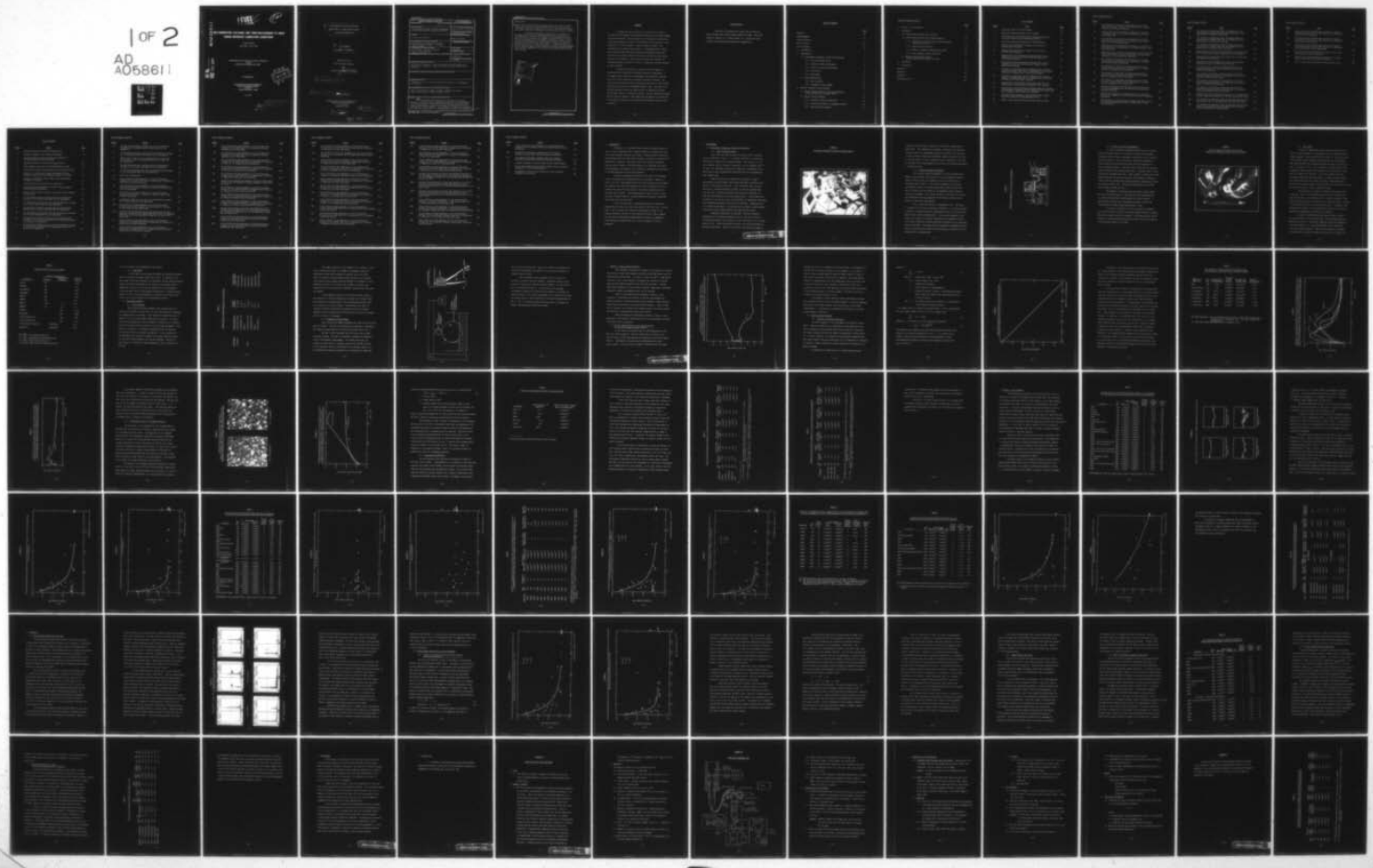

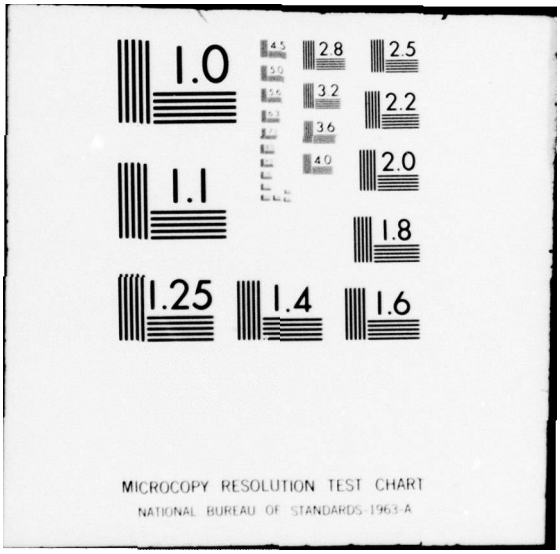
1.0
1.1
1.25
1.4
1.6
1.8
2.0
2.2
2.5
2.8
3.2
3.6
4.0
MICROCOPY RESOLUTION TEST CHART
NATIONAL BUREAU OF STANDARDS-1963-A

LEVEL II

12

SELF-GENERATED VOLTAGES AND THEIR RELATIONSHIP TO WEAR UNDER BOUNDARY LUBRICATED CONDITIONS

FINAL REPORT

MAY 1975 – JULY 1978

SPONSORED BY THE OFFICE OF NAVAL RESEARCH
UNDER
CONTRACT No. N00014-75-C-1080

I.L. GOLDBLATT

EXXON RESEARCH AND ENGINEERING CO.
PRODUCTS RESEARCH DIVISION
P.O. BOX 51
LINDEN, NEW JERSEY 07036

JULY 1978

New

410840

(6) SELF-GENERATED VOLTAGES AND THEIR RELATIONSHIP TO WEAR UNDER BOUNDARY LUBRICATED CONDITIONS.

(9) Final Report.
May 1975 — July 1978.

Sponsored by the
Office of Naval Research
Under
Contract No. N00014-75-C-1080
(15)

(14) Exxon/RL.6PH.78

(10) Irwin Leonard [redacted]/Goldblatt

Exxon Research and Engineering Co.
Products Research Division
P. O. Box 51
Linden, NJ 07036

(12) 190 p.

(11) Jul[redacted]78

410 840

not

Unclassified

SECURITY CLASSIFICATION OF THIS PAGE (When Data Entered)

REPORT DOCUMENTATION PAGE		READ INSTRUCTIONS BEFORE COMPLETING FORM
1. REPORT NUMBER	2. GOVT ACCESSION NO.	3. RECIPIENT'S CATALOG NUMBER
4. TITLE (and Subtitle) SELF-GENERATED VOLTAGES AND THEIR RELATIONSHIP TO WEAR UNDER BOUNDARY LUBRICATED CONDITIONS		5. TYPE OF REPORT & PERIOD COVERED Final, May 1975 - July 1978 6. PERFORMING ORG. REPORT NUMBER Exxon/RL.6PH.78
7. AUTHOR(s) Irwin Leonard Goldblatt		8. CONTRACT OR GRANT NUMBER(s) N00014-75-C-1080
9. PERFORMING ORGANIZATION NAME AND ADDRESS Exxon Research and Engineering Company Products Research Division, P.O. BOX 51 Linden, NJ 07036		10. PROGRAM ELEMENT, PROJECT, TASK AREA & WORK UNIT NUMBERS
11. CONTROLLING OFFICE NAME AND ADDRESS Power Program, Materials Sciences Office of Naval Research Arlington, VA 22217		12. REPORT DATE July 1978 13. NUMBER OF PAGES 177
14. MONITORING AGENCY NAME & ADDRESS(if different from Controlling Office)		15. SECURITY CLASS. (of this report) Unclassified 15a. DECLASSIFICATION/DOWNGRADING SCHEDULE

16. DISTRIBUTION STATEMENT (of this Report)

Reproduction in whole or in part is permitted for any purposes of the United States Government. Approved for public release; distribution unlimited.

17. DISTRIBUTION STATEMENT (of the abstract entered in Block 20, if different from Report)

18. SUPPLEMENTARY NOTES

Presented in part at the MIT International Conference on Fundamentals of Tribology.

19. KEY WORDS (Continue on reverse side if necessary and identify by block number)

Wear, Self-Generated Voltage, Voltage, Boundary Lubrication, Aromatic Hydrocarbons, Ball-on-Cylinder Device

20. ABSTRACT (Continue on reverse side if necessary and identify by block number)

A program has been carried out to determine the relationship which exists between Self-Generated Voltages and wear under Boundary Lubricated Conditions. The observation that voltages are generated between wearing members is shown to be unrelated to such factors as fluid conductivity or fluid viscosity. These voltages are shown to be associated with the wear process itself. A relationship has, indeed, been obtained

DD FORM 1 JAN 73 1473 EDITION OF 1 NOV 65 IS OBSOLETE

Unclassified

SECURITY CLASSIFICATION OF THIS PAGE (When Data Entered)

(Block # 20)

between wear and Self-Generated Voltages and has been found for both a steel-on-steel system and an aluminum-on-steel system under dry air blanketing. Under these conditions, at low wear, the measured voltages are several millivolts in magnitude, and they decrease as wear increases.

A preliminary mechanism to explain how the voltages are generated under the Boundary Lubricated Conditions is discussed. It is suggested that there are two fundamental electrochemical processes which occur under conditions of Boundary Lubrication and wear. One is an electron transfer process involving the shifting of a near surface electron from the metal to an adsorbed surface layer. The other is an oxidation process in which the metal surface is chemically oxidized while another species is chemically reduced. The Self-Generated Voltages and the relative changes in their magnitude and polarity are determined by the relative importance of the above noted processes under the test conditions.

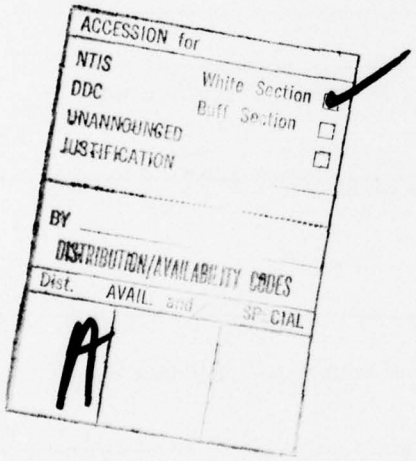

ABSTRACT

A program has been carried out to determine the relationship which exists between Self-Generated Voltages and wear under Boundary Lubricated Conditions. The observation that voltages are generated between wearing members is shown to be unrelated to such factors as fluid conductivity or fluid viscosity. These voltages are shown to be associated with the wear process itself. A relationship has, indeed, been obtained between wear and Self-Generated Voltages and has been found for both a steel-on-steel system and an aluminum-on-steel system under dry air blanketing. Under these conditions, at low wear, the measured voltages are several millivolts in magnitude, and they decrease as wear increases.

A preliminary mechanism to explain how the voltages are generated under the Boundary Lubricated Conditions is discussed. It is suggested that there are two fundamental electrochemical processes which occur under conditions of Boundary Lubrication and wear. One is an electron transfer process involving the shifting of a near surface electron from the metal to an adsorbed surface layer. The other is an oxidation process in which the metal surface is chemically oxidized while another species is chemically reduced. The Self-Generated Voltages and the relative changes in their magnitude and polarity are determined by the relative importance of the above noted processes under the test conditions.

ACKNOWLEDGMENTS

This work was sponsored by a grant from the Office of Naval Research under Contract Number N00014-75-C-1080. The author wishes to thank Dr. R. S. Miller and Mr. G. L. Harting for many valuable and interesting discussions and suggestions.

TABLE OF CONTENTS

Table of Contents (Cont'd)

LIST OF TABLES

List of Tables (Cont'd)

List of Tables (Cont'd)

List of Tables (Cont'd)

LIST OF FIGURES

List of Figures (Cont'd)

List of Figures (Cont'd)

List of Figures (Cont'd)

List of Figures (Cont'd)

List of Figures (Cont'd)

1. INTRODUCTION

Tribology is a technology largely based upon empiricism and as such, currently possesses only a limited capability to predict what will occur when operating conditions are varied. Recently several models have been proposed which have been used to explain a portion of the body of the lubrication technology. These models fall into two broad categories. Some are purely chemical, involving primarily the lubricant, and others are metallurgical or physical, often involving a mathematical description of the phenomenological process being modeled.

In order to adequately describe the real nature of tribology, a model incorporating both approaches will be necessary. However, in order to do this, relationships between the metal surfaces and lubricants are required, and these relationships could well be defined by electrochemical processes which take place at the surface involving both the lubricant and the metal. Such understanding may then be used to relate the purely chemical models to the metallurgical and physical transformations which have been described.

It will be shown that a relationship between self-generated voltages and wear may exist which could serve to fill this role. Furthermore, it will be shown that a detailed investigation of some of the chemical parameters involved in the lubrication process tend to support the idea that self-generated voltages might be related to fundamental electrochemical processes which can in turn be related to the wear mechanism.

2. EXPERIMENTAL

2.1 Experimental Equipment, Fluids and Metallurgy

2.1.1 Ball-on-Cylinder Device

Wear tests have been carried out using the Ball-on-Cylinder device, illustrated in Fig. 1. It consists basically of a stationary ball which is loaded onto a rotating cylinder. The test ball is 1.27 cm in diameter and the cylinder is nominally 4.4 cm in diameter and 1.7 cm long. Any specimens satisfying the dimensional requirements of the device may be used, although AISI 52100 steel has been the metallurgy most commonly used.

Both the ball and the cylinder are enclosed in a small environmental control chamber, which under lubricated conditions, also serves as the lubricant reservoir. In the lubricated case, the test lubricant is contained below the cylinder, so that the cylinder dips into the fluid. The wetted cylinder then carries the lubricant as a film into the conjunction of the two wearing parts. A dead weight load is applied on the end of a lever system having a 2:1 mechanical efficiency, and the maximum permissable load is 4 Kg or 1400 MPa. Through the use of a variable speed motor, the cylinder can be rotated at speeds between 1 rpm (0.23 cm/sec sliding velocity) and 1000 rpm (230 cm/sec).

Additional flexibility is available. Various blanketing atmospheres may be employed through the use of a gas inlet system to the enclosing chamber and/or operation of the entire device in a suitably purged dry box. Under lubricated conditions, tests may be performed at elevated temperatures. Heaters in the base of the enclosing chamber or

FIGURE 1

Photograph Showing the Ball-on-Cylinder Device

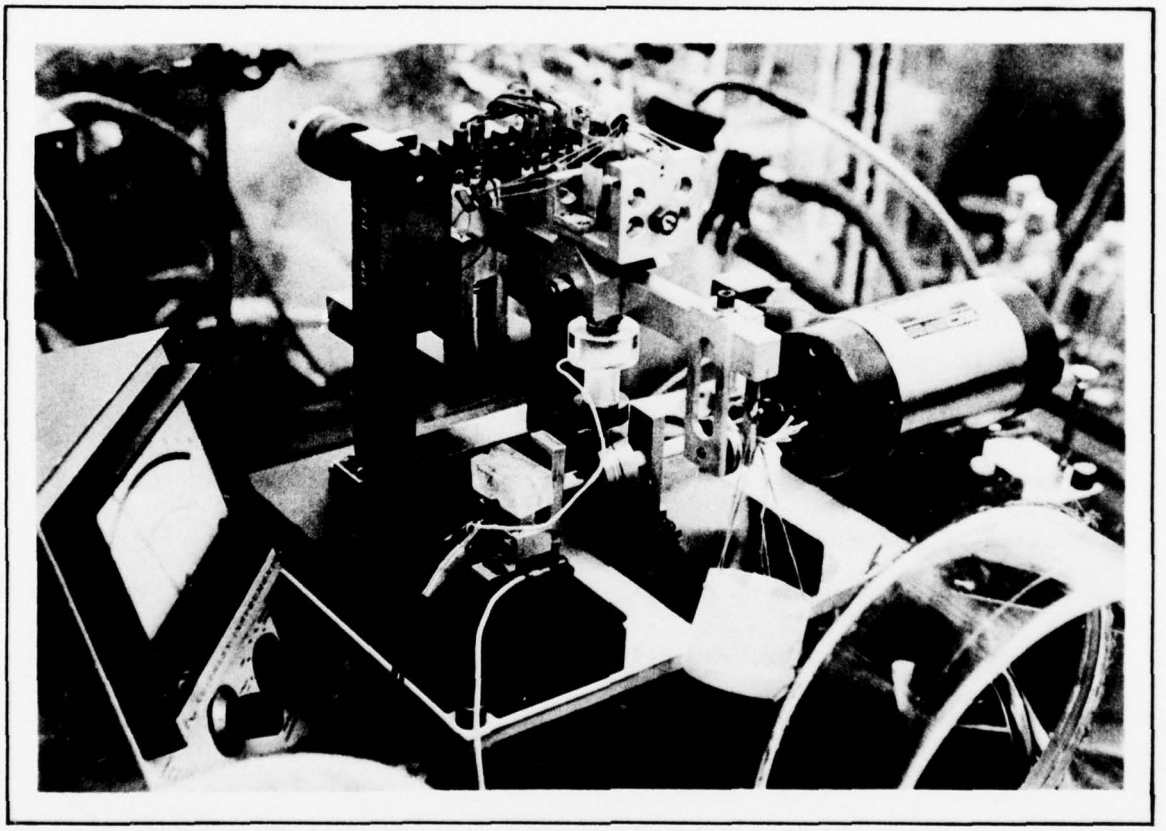

lubricant reservoir permit testing up to bulk fluid temperatures of about 200°C. The temperature is recorded continuously and controlled during testing via a thermocouple placed in the base of the reservoir. A linear variable differential transformer (LVDT), attached at the end of the ball mount, is used to measure friction continuously. The LVDT is activated by the displacement of the central core which works against a calibrated spring.

2.1.2 Talysurf Surface Profilometer

The Talysurf surface profilometer, used for assessing wear damage on the cylinder is an electrical stylus instrument in which a sharply pointed stylus rests lightly on the metal surface and is traversed slowly across it. The vertical movements of the stylus are measured relative to a datum which usually takes the form of a skid in contact with the surface or an independent datum contained within the instrument. The vertical motions of the stylus are electrically amplified and plotted against the horizontal position of the stylus to obtain the final profile.

Fig. 2 shows the Talysurf in diagrammatic form. The stylus T, actuates in this case an electrical transducer, Q, a device producing a current or voltage according to displacement, which is carried in the end of a motor driven sliding shaft E. The vertical movements of the stylus as it passes over surface irregularities are measured relative to the path followed by the shaft which must therefore be of a very high order of precision. The output from the transducer is amplified (A) and sent to a pen recorder (B) which plots the shape of the profile of the surface and its irregularities.

FIGURE 2

Schematic Diagram of the Talysurf Profilometer

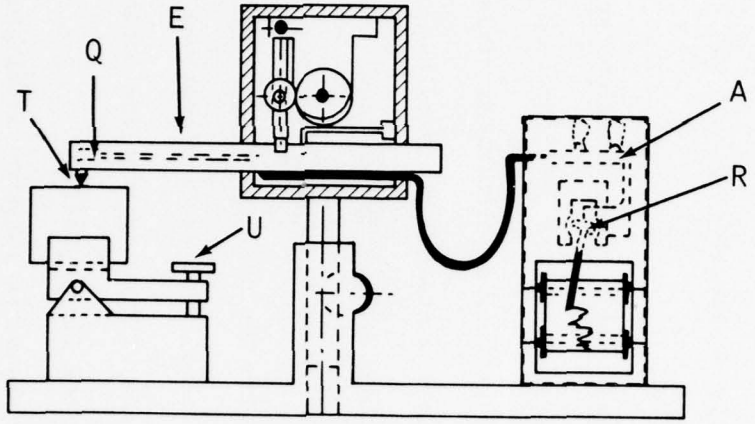

2.1.3 Electric Potential Measurements

In order to measure the magnitude and polarity of the Self-Generated Voltages (SGV's), the ball and cylinder were thoroughly insulated from each other, from ground, and from the rest of the Ball-on-Cylinder device. The test balls were insulated by mounting in special adaptors fabricated either from Lexan (polycarbonate) or Lucite (polymethacrylate). Electrical contact with the ball was then effected using 0.07 mm stainless steel wire. A special collar to lock the balls was machined from nylon. Steel spindles, covered with a nylon sheath 0.083 mm thick, served to insulate the cylinders. Electrical contact with the cylinders was obtained through a conducting set screw via a mercury contact cell. The ball mounting adaptor and covered steel spindle are shown in Fig. 3.

Measurements of potential were made using a Keithly Model 602 Solid State Electrometer. The output from the Keithly was fed to a Hewlett-Packard Model 7100B Moseley Strip Chart Recorder. A Tektronix Type 502 Dual Beam ocsilloscope was used to record the "instantaneous" voltages using Polaroid Type 47 film.

It should be noted that it is not necessary to establish the absolute polarity of either of the test members relative to ground. Only their relative polarity is required. The convention that will be adopted for reporting the polarities of the SVG's will be the polarity of the cylinder relative to the ball.

FIGURE 3

The Ball Adaptor and Nylon Covered Steel
Spindle for Insulating the Ball and the Cylinder

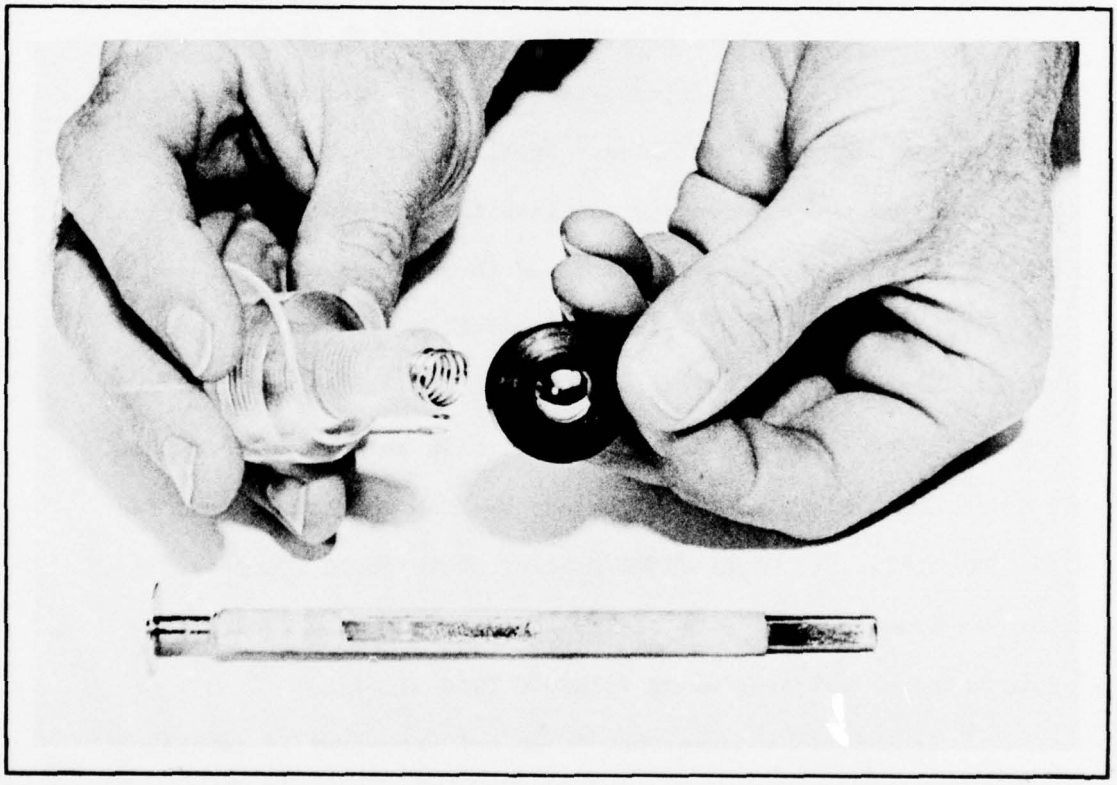

2.1.4 Test Fluids

A variety of hydrocarbon liquids have been tested, Table 1. The list includes members of a homologous series of paraffinic hydrocarbons ranging in carbon number from 10 through 16. Also tested were several highly refined saturated petroleum white oils designated as LVWO, IVWO and HVWO with viscosities ranging from about 2.43 mPa·S at 25°C to 35.8 mPa·S at 25°C. Also included is a lighly refined fluid designated as HVLRO somewhat more typical of the type used as a base stock for mineral oil lubricants. This fluid contains about 65% saturated hydrocarbons and 35% aromatics. A number of pure aromatic type hydrocarbons were also tested, including 1-Chloronaphthalene. The list also includes several ester base stocks (Di-2-Ethylhexl Sebacate, Hercolube J) typical of those in commercial usage.

The fluids were, in general, purified to some degree prior to testing. Some of the fluids were percolated over silica gel and then filtered with a 0.3μ Millipore filter. Others, because of their higher viscosity were only filtered with 0.3μ Millipore filter. Several of the fluids were tested in the as-received state. In general, their performance was similar to the treated fluid; however, in the case of dodecane the performance was significantly different.

A number of additives have been used in order to modify the characteristics of the fluids tested. These included antistatic agents such as ASA-3, a proprietary antistatic agent sold commercially by Shell Chemical Co., and antiwear agents such as isostearic acid and tricresyl phosphate. (Not all these systems are reviewed in the body of this report to enhance the clarity of the report, but

TABLE 1

Lubricants Used in the Test Program

Lubricant	Percent Concentration		Viscosity (mPa·S)
	Saturates	Unsaturates + Aromatics	
Decane	100		0.859
Dodecane	100		1.37
Tetradecane	100		2.06
Hexadecane	100		3.09
LVWO(1)	100		2.43
IVWO(2)	100		17.7
HVWO(3)	99.8	0.2	35.8
HVLRO(4)	65	35	37
Toluene		100	0.536
Mesitylene		100	0.855
1-Methylnaphthalene		100	2.69
1-Chloronaphthalene		100	3.14
Di-2-Ethylhexyl Sebacate	100% Ester		17.1
Hercolube J	100% Ester		39.4

(1) LVWO = Low Viscosity White Oil

(2) IVWO = Intermediate Viscosity White Oil

(3) HVWO = High Viscosity White Oil

(4) HVLRO = High Viscosity Lightly Refined Oil

all are included in the supplementary data tables.)

2.1.5 Metallurgy

As noted above, any specimen satisfying the dimensional requirements of the Ball-on-Cylinder device may be used. In addition to the more common 52100 steel (ferrous) test specimens, several nonferrous metallurgies have been investigated in the course of this program (Table 2). Summarized in Table 2, are the alloys employed for the test members, their hardnesses, and the metallurgical combinations or couples selected. (Again, not all of these metallurgies are reviewed in the body of this report, but all are included in the supplementary tables.)

2.2 Experimental Method

2.2.1 Test Procedure

The procedure followed throughout this program consists of starting the cylinder rotating and at the same time purging the lubricant and blanketing the test chamber. After purging the system for about 15 minutes, the ball is dead weight loaded upon the cylinder. For tests under inerted atmospheres, the test chamber is blanketed for 30 minutes and the surrounding dry box filled with a dry nitrogen atmosphere. Test duration, in general, is 32 minutes, during which time the friction force and the SGV's are recorded continuously. At the conclusion of the experiment, the cylinder is stopped, the contact potential between the ball and cylinder measured, and the ball unloaded. The ball is then removed, is retained for visual examination, and is replaced by a new ball.

TABLE 2

Metallurgical Systems Employed in Test Program

Test Member	Metallurgy/Alloy	Rockwell Hardness	Metallurgical Couples Used
Cylinders	Steel/AISI 52100	R_c 20-22	Ball/Cylinder
	Aluminum/AMS 4150	R_b 54.5	Steel/Aluminum
	Copper	R_b 40	Steel/Steel
Balls	Steel/AISI 52100	R_c 62-64	Copper/Steel
	Aluminum/AMS 2017	R_b 58	Bronze/Steel
	Copper	R_b 53	Aluminum/Steel
	Bronze/SAE 65	R_b 47	Aluminum/Aluminum

The sample reservoir is then emptied of its contents, in the case of lubricated studies; the chamber is thoroughly rinsed with hydrocarbon solvent such as hexane or heptane, and is air dried. Next, the cylinder is moved along its axis by about 1 mm to another track position, and a sample of fresh lubricant is introduced. After completion of about 8 to 12 tests, the cylinder is removed, and a Talysurf profile of the surface is recorded, from which the track wear is assessed.

A very important feature of the Ball-on-Cylinder device is the capability of multiple testing upon a single test cylinder since the cylinder may be moved along on its axis permitting several tests to be carried out on each cylinder. This minimizes the impact of cylinder-to-cylinder variations by permitting the use of standard reference fluids to measure the relative severity of each test cylinder prior to its use in the program.

2.2.2 Assessment of Wear Damage

After testing wear damage assessments are made on both the ball and the cylinder. The need to do this may be recognized by considering the schematic representation of the Ball-on-Cylinder device, Fig. 4.

The ball is held stationary and its contact zone is under continuous loading. The ball is, therefore, considered the monotonically or continuously loaded member. In contrast with this, the cylinder is under cyclic or periodic stress as the cylinder rotates. If one considers a point on the surface of the cylinder, point A, it is periodically loaded and unloaded as it is brought into, under and

FIGURE 4

Schematic Diagram of the Ball-on-Cylinder Device

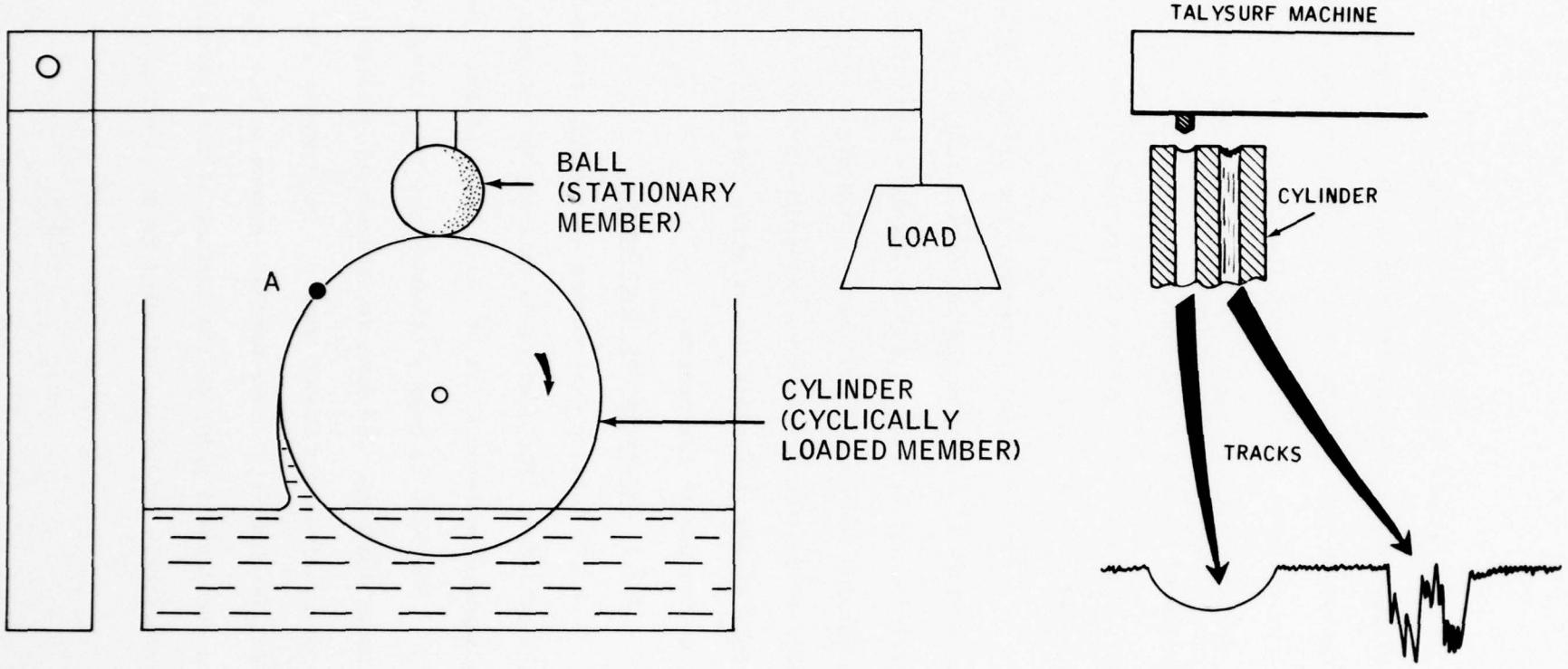

out of contact with the ball. Hence, the cylinder is considered the cyclically loaded member, and points on its surface are subject to repeated stress cycling.

Wear assessment on the stationary ball is carried out optically in terms of the scar diameter. Evaluation of wear on the cylinder is carried out using the Talysurf machine. The way this is done is illustrated in Fig. 4. As the stylus of the talysurf profilometer traverses the surface of the cylinder, it outlines the overall features of the surface topography of the cylinder wear tracks. Two tracks typical of those obtained are illustrated schematically in Fig. 4. One is relatively smooth, while the other is irregular and ragged, possessing many furrows and troughs.

3. RESULTS - General System Variables

The experimental program was designed to investigate the relationship which may exist under boundary lubricated conditions between wear and Self-Generated Voltage (SGV). In order to relate the SGV's to wear models currently in use, it was decided to determine the influence of certain operating and chemical parameters upon both SGV's and wear. Included among these parameters are load, moisture (water), temperature, metallurgy, atmosphere (oxygen) and chemical nature of the lubricant.

Prior to investigating these parameters, however, it was necessary to investigate the influence of several other germane non-readily controlled or measured general system variables, namely lubricant conductivity, fluid motion and lubricant film thickness. Each of these latter variables could influence the voltages generated and thus confound the detection of relationships between wear and SGV.

Before describing the experimental results in detail, a brief description of the general characteristics of the time dependent variation of the SGV's will be presented.

3.1 General Characteristics of the Time Dependence of the Self-Generated Voltages (SGV's)

In this study, two general types of time dependences for the SGV's have been recognized. Both are characterized, usually, by an initial break-in period, during which the magnitude of the SGV increases (Fig. 5). Differences in behavior can be encountered after this initial period. The first type of response, illustrated by the results

FIGURE 5

Time Dependent Variation of the Self-Generated Voltage
(Test Conditions: Ball-on-Cylinder Device, HVWO 1,000 g Load,
240 rpm, 25°C, 32 minutes, 52100 Steel-on-52100 Steel, Atmospheres as Noted)

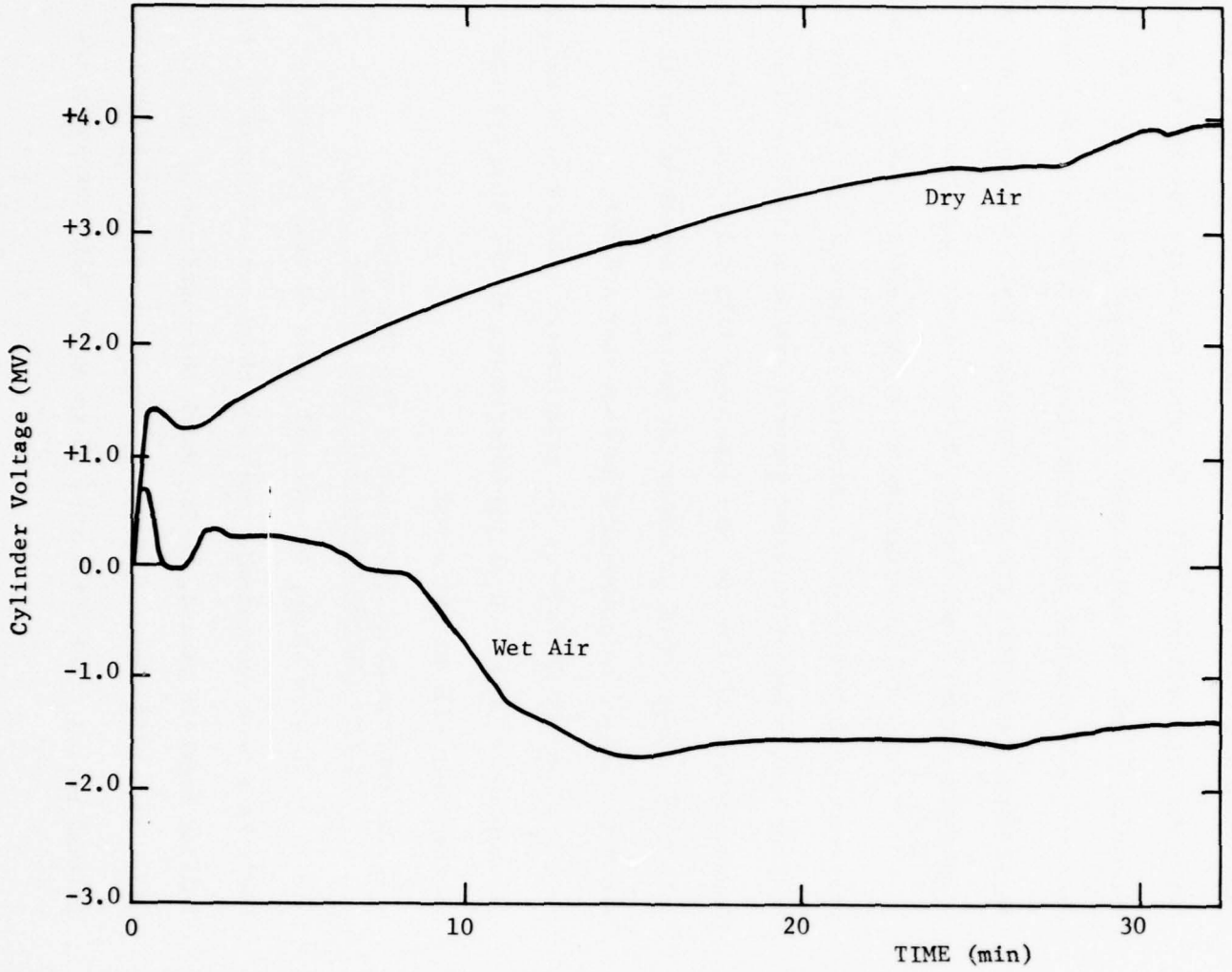

obtained in dry air, is typified by a brief decrease in the magnitude of the SGV after the break-in period, in this example to 1.2 mv (Fig. 5). There is then a gradual approach towards a higher asymptotic value of SGV, in this case about +4.65 mv after 32 minutes. The second type of behavior is exhibited under wet air blanketing in which an initial rise in the SGV to about 0.9 mv is observed. This falls to about 0 mv, increases to about 0.3 mv, then decreases to the point where the polarity of the cylinder relative to the ball changes. The SGV at the end of a 32 minute test period is about -1.5 mv.

The behavior of other lubricant and/or metallurgical systems are in general similar to one of the above examples. The actual magnitude and polarity will depend, however, upon the particular system under investigation. A rationale for the appearance of these two cases will become apparent in Section 5.

3.2 General System Variables

3.2.1 Influence of Fluid Conductivity

The first parameter to be investigated was lubricant conductivity. Lubricant conductivity is recognized as being important in the static charging of flowing liquids since fluid conductivity influences the charge relaxation process and thereby the magnitude of charge build-up. In order, therefore, to establish the relationship between SGV and wear under boundary lubricated conditions, it is of importance to determine if changes in charge relaxation or fluid conductivity contribute to the measured voltage.

The magnitude of charge decay in a flowing system follows

Equation 1.

$$\frac{Q_t}{Q_o} = e^{-tk/\varepsilon\varepsilon_o} \qquad (1)$$

where Q_t = charge after time, t (e.g., C/m^3)

Q_o = initial charge (e.g., C/m^3)

t = elapsed time (seconds)

k = fluid conductivity (Siemens/meter)

ε = relative dielectric constant, a dimensionless quantity which varies only slightly for hydrocarbons and has a value of about 2,

and ε_o = the absolute dielectric constant of a vacuum (8.854×10^{-12} ampere-seconds/volt-meter).

It is common practice to define a relaxation time, τ, as the time required for the original charge to decay $1/e$ of its original value

$$\frac{Q_\tau}{Q_o} = e^{-1} = 0.368 \qquad (2)$$

Therefore, τ is related to k by the following relationship

$$\tau = \frac{\varepsilon\ \varepsilon_o}{k} = \frac{17.7 \times 10^{-12}}{k} \qquad (3)$$

The dependence of relaxation time upon fluid conductivity derived from equation 3 is presented graphically in Fig. 6. It is evident that a change in fluid conductivity from 0.01 Picosiemens/meter to 1000 Picosiemens/meter produces a change in the relaxation time from 1770 sec to 0.0177 sec.

FIGURE 6

Relationship Between Fluid Conductivity and Relaxation Time

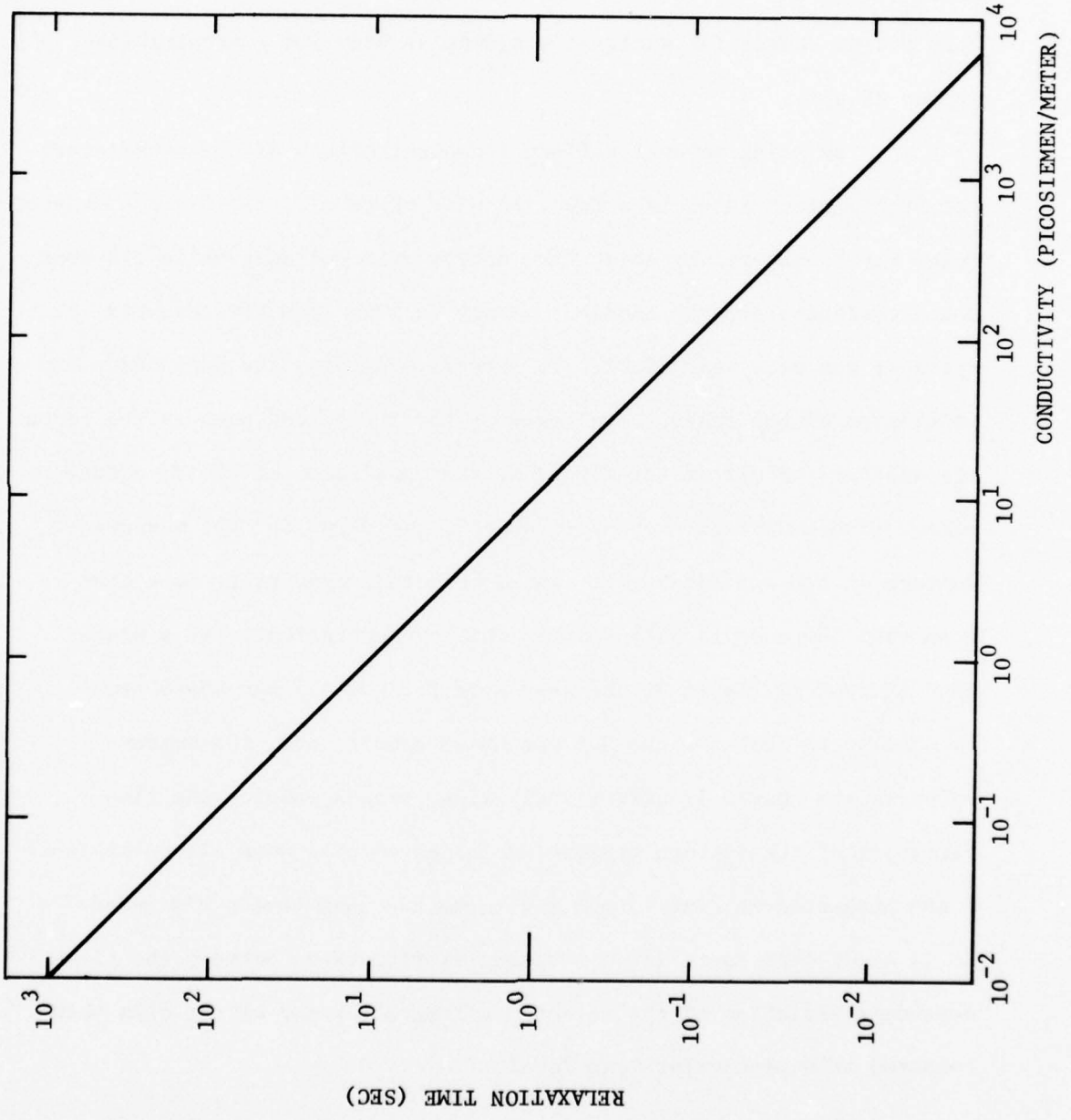

Evaluation of the influence which fluid conductivity has upon the voltage measured is best performed under experimental conditions in which the wear parameters remain essentially constant while only conductivity is varied. Such conditions may best be achieved by using very potent commercial antistatic agents at very low concentrations (under 20 ppm).

By using several different concentrations of the proprietary antistatic agent ASA-3 in a low viscosity white oil, the fluid's conductivity may be altered by about five orders of magnitude, while its wear characteristics are not changed, as may be seen from the measured cylinder and ball wear (Table 3). Correspondingly, the magnitudes and polarities of the measured voltages at the 500 g load used in the tests are similar for all of the fluids at the conclusion of the 32 minute test. (There appears to be one "sport", the value for the measured voltage at 1.5 ppm ASA-3. It should be noted, that there is a concommitant increase in ball wear at this concentration.) At a higher load of 2000 gm (Table 3) the wear rate for the 1.5 ppm ASA-3 sample is similar to that for the 0.4 ppm ASA-3 sample, and, the measured voltages are nearly identical. Likewise, traces showing the time variation of the average measured voltages for the runs listed in Table 3 are presented in Figs. 7 and 8 for the two load levels discussed. It is clear that there is no substantial difference between the time dependent variation of the measured voltages for any of the oils when compared at a particular load level.

TABLE 3

The Influence of Fluid Conductivity Modified Using ASA-3 Antistatic Additive Upon the Measured Voltage

Additive to Bayol 35	Load (g)	Conductivity (Picosiemens/m)	Ball Wear Volume (cm^3)(2)	Cylinder Wear Volume (cm^2)	Measured Voltage (mv)
None	500	0.017	3.77×10^{-7}	0.08×10^{-5}	+ 0.5
0.05 ppm ASA-3	500	4.59	2.64×10^{-7}	0.08×10^{-5}	+ 0.6
0.4 ppm ASA-3	500	50.51	2.64×10^{-7}	0.12×10^{-5}	+ 0.6
1.5 ppm ASA-3	500	215.0	3.77×10^{-7}	0.09×10^{-5}	+ 0.2
15 ppm ASA-3	500	2066.0	2.41×10^{-7}	0.008×10^{-5}	+ 0.7
0.4 ppm ASA-3	2000	50.51	12.18×10^{-7}	0.11×10^{-5}	+ 0.06
1.5 ppm ASA-3	2000	215.0	11.4×10^{-7}	0.12×10^{-5}	+ 0.06

(1) Test Conditions : Ball-on-Cylinder device, Loads as noted, IVWO as base fluid, 240 rpm, Dry Air Atmosphere, 25°C., 32 Minute, 52100 Steel-on-52100 Steel.

(2) Ball Wear Volume calculated as $7.73 \times WSD^4 \times 10^{-2}$ (cc).

FIGURE 7

Influence of the Antistatic Agent ASA-3 Upon the Time Dependent Variation of the Measured Voltages of the LVWO (Test Conditions: Ball-on-Cylinder Device, 500 g Load, Dry Air Atmosphere, 240 rpm, 25°C, 32 minutes, 52100 Steel-on-52100 Steel)

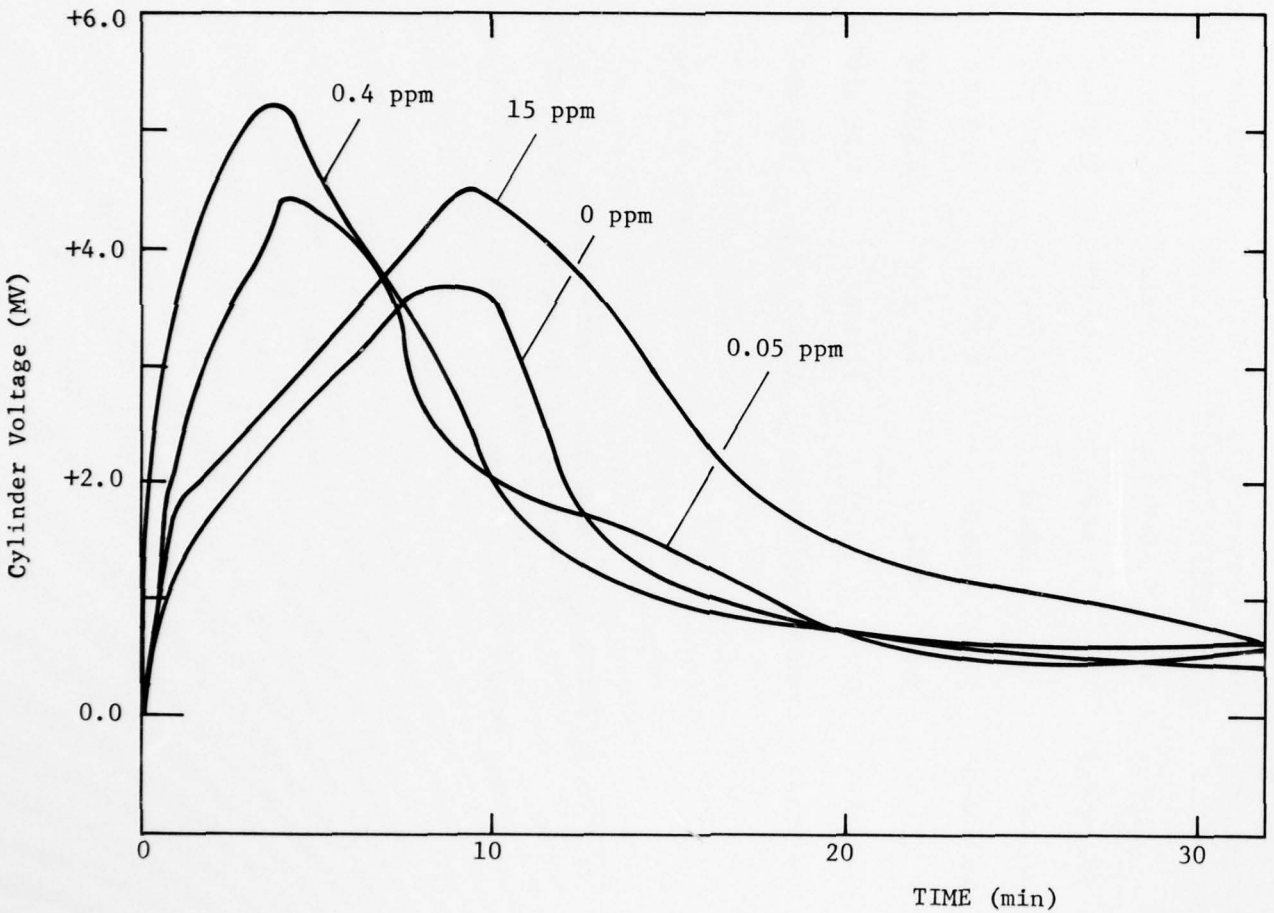

FIGURE 8

Influence of Antistatic Agent, ASA-3, Upon the Measured Voltages of the LVWO (Test Conditions: Ball-on-Cylinder Device, 2,000 g Load, Dry Air Atmosphere, 240 rpm, 25°C, 52100 Steel-on-52100 Steel)

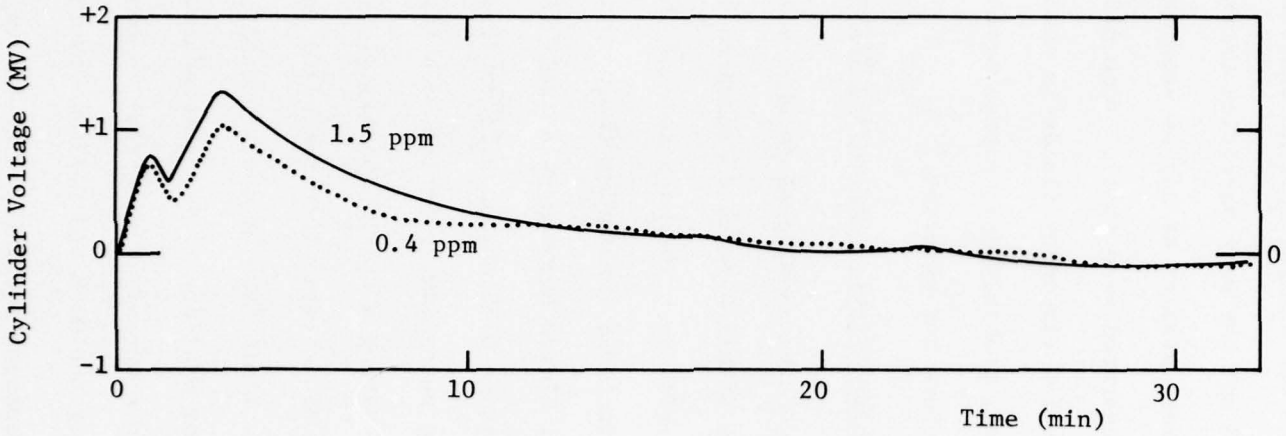

The evidence suggests that measured voltages are not dependent upon fluid conductivity. In order to confirm that the wear process for the tests with added ASA-3 was similar to that without the additive, the test fluids were filtered and the wear particles examined. The particles from all of the samples were similar as may be seen in Fig. 9. In general, the particles generated were small. (One difficulty which has been encountered with the low viscosity fluids is that many of the particles which are formed, probably precipitate prior to filtration or Ferrography and are therefore not observed.)

3.2.2 Fluid Motion Effects - Streaming Potential

The next aspect to be considered is what voltages might be generated due to the flow of oil between a separated ball and cylinder, i.e. streaming potential effects. The magnitude of the streaming potential effect was estimated by measuring the potentials developed during tests in which oil flowed between relatively large ball and cylinder separations of about 0.55 mm and 0.25 mm (Fig. 10), separations which prevented any wear from occurring. In these tests, an ester base stock, Hercolube J, having a charge density of 1280 $\mu c/m^3$ as measured using the Exxon Mini-Static Test Procedure was used, a value which represents an upper limit for the charge density. (See Appendix A for details of the Exxon Mini-Static Test Procedure.)

The values of the streaming potential as measured at 400 rpm were 1.45 v and 0.58 v for the 0.55 and 0.25 mm spacings, respectively. These measured voltages compare favorably with the values 5.5 v and 1.1 v which are calculated using Equation (4), which predicts the potential

FIGURE 9

Filtered Particles From Tests With Added ASA-3
(Test Conditions: Ball-on-Cylinder Device, 500 g Load, Dry Air Atmosphere, 240 rpm, 25°C, 32 Minutes, 52100 Steel-on-52100 Steel)

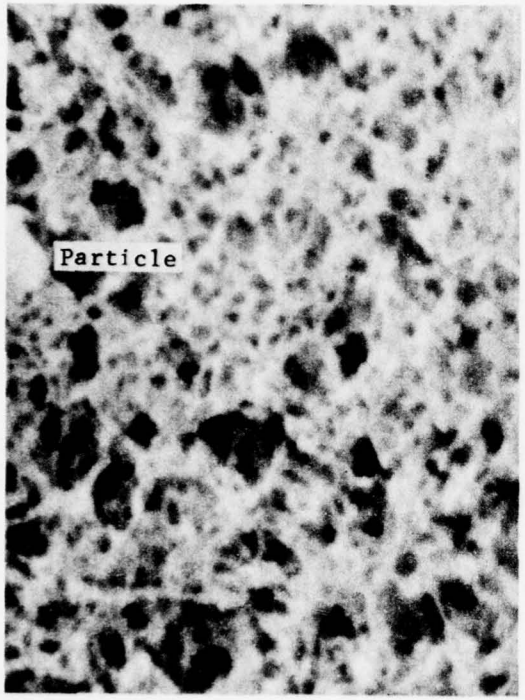

9a - 0.40 ppm ASA-3

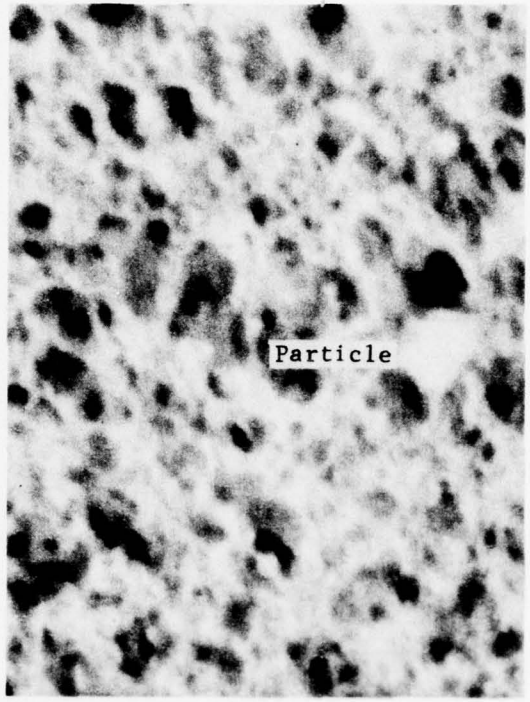

9b - 15 ppm ASA-3

FIGURE 10

Measured Voltage Generated Due to Flow of Fluid Between a Separated Ball and Cylinder (Test Condition: Ball-on-Cylinder Device, Hercolube J, Dry Air Atmosphere, 25°C, 52100 Steel-on-52100 Steel)

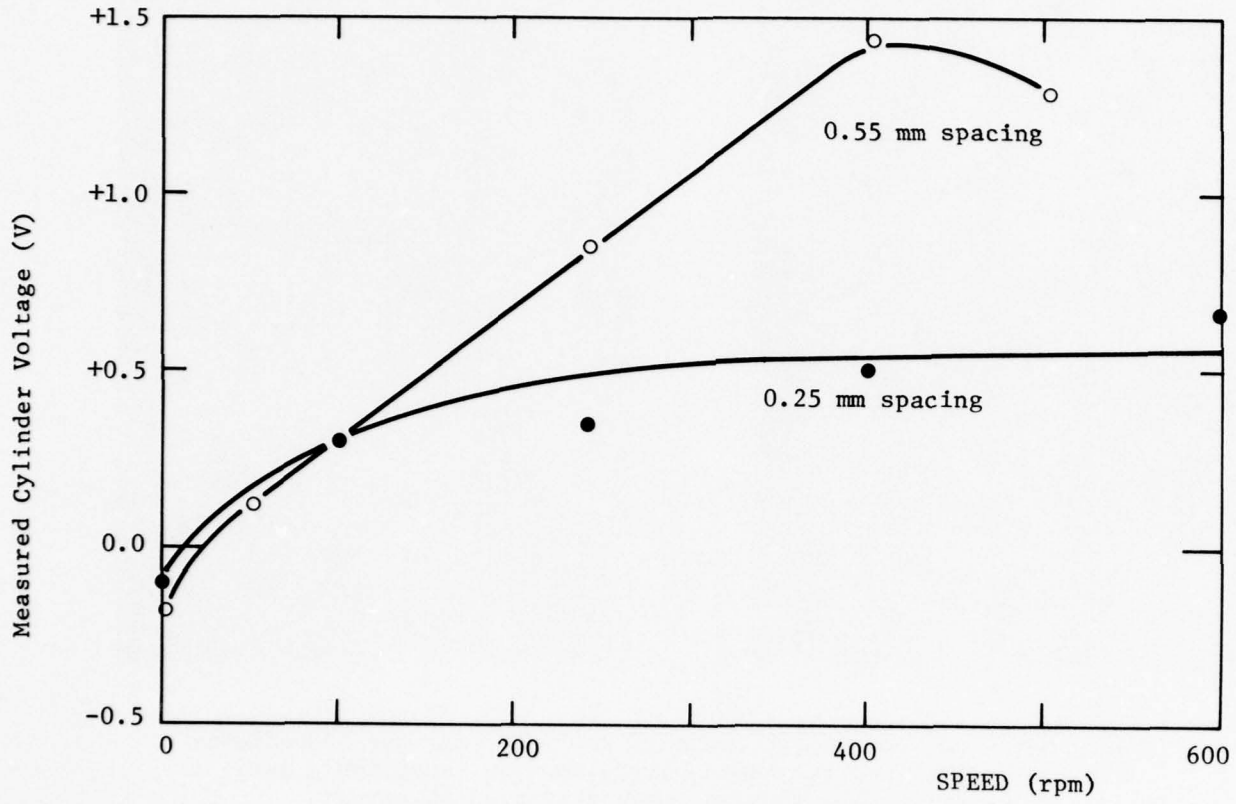

difference developed between the wall and the core of a flowing liquid.

$$V_{axis} - V_{wall} = sR^2/4\ \varepsilon\varepsilon_o \quad (4)$$

V = Voltage (volts)

s = charge density (c/m^3)

R = distance between core of fluid and wall (taken in this case as the distance between the ball and the cylinder) (m)

and ε and ε_o have the same meanings as in Equation 3.

(These calculations assumed that the fluid moves with the rotating cylinder, and thus R equals the separation between the ball and the cylinder.)

Since Equation 4 seems to predict the magnitude of the streaming potential due to the flow of relatively thick films, the magnitude of the streaming potentials to be expected using the various fluids employed in the program may also be computed using this equation. Gathered in Table 4 are the measured charge densities for several fluids used in this study, and the streaming potentials calculated from Equation 4 assuming a relatively thick fluid film of 0.5 μm. In general the streaming potentials are computed to be less than 10^{-2} mv. This value is small in comparison to the measured voltages. Hence, the recorded voltages are probably not related to streaming potentials.

3.2.3 Lubricant Film Thickness

The next parameter which may affect the measured voltages is lubricant film thickness. Experimentally, it was decided to vary lubricant viscosity and thereby film thickness, and thus probe the influence which lubricant film thickness has upon measured voltages. This has been done using two different lubricant systems, one, a group of hydrocarbons from a homologous paraffinic series and the other, two similar, but less well

TABLE 4

Calculated Streaming Potentials for Several Fluids

Lubricant	Charge Density (1) ($\mu C/m^3$)	Computed Measured Voltages Due to Streaming (mv)
Bayol 35	35	0.124×10^{-3}
HVWO	18.13	0.064×10^{-3}
HVLRO	2200	7.8×10^{-3}
Dodecane	9.18	0.032×10^{-3}
Cetane	8.21	0.028×10^{-3}
Hercolube J	1280	4.52×10^{-3}

(1) Measured Using the Exxon Mini-Static Test Procedure.

characterized hydrocarbons, investigated individually and in combination with one another. With either approach, chemical and structural differences between the lubricant of each group are maintained at a minimum.

In the first series of tests, using a steel ball sliding on a steel cylinder, it has been found that at low viscosities, wear being maintained nearly constant, the measured voltages are essentially independent of viscosity and therefore film thickness, Table 5.

Over a viscosity range of about 0.86 $x10^{-3}$ to 2.06 $x\ 10^{-3}$ mPa·S corresponding to a relative film thickness increase of about 89% the measured voltages are nearly constant. With a 150% increase in fluid film thickness (with hexadecane) the measured voltage appears to rise. This increase in measured voltage may be related to the large decline in the ball wear rate observed, suggesting that a change in wear mechanism has occurred. In general, for moderate changes in film thickness and viscosity, measured voltages are similar if wear rates are nearly equivalent.

In the second series of experiments to study the influence of film thickness and/or viscosity upon the measured voltages, two white oils, the LVWO and the IVWO, having viscosities of 2.43 $x\ 10^{-3}$ mPa·S and 17.7 $x\ 10^{-3}$ mPa·S, respectively, and mixtures thereof were used. The metallurgical combination selected in order to ensure nearly constant wear rate over the range of film thicknesses (or viscosities) investigated is an aluminum ball on a steel cylinder. It is clear, Table 6, that the measured voltages are essentially independent of film thickness and/or

TABLE 5

Measured Wear and Measured Voltages as a Function of Relative Film Thickness (1)

Lubricant	Load (g)	Viscosity (mPa·S)	Relative Film Thickness(2) (ho/ho')	Ball Wear Scar Diameter (mm)	Ball Wear Volume (cc)	Track Cross Sectional Area (cm^2)	Cylinder Wear Volume (cc)	Measured Voltage (mv)
Decane	500	0.859	1.00	0.83	36.69×10^{-7}	0.04	0.05×10^{-5}	+0.21
Dodecane	500	1.37	1.39	0.72	20.77×10^{-7}	0.14	0.18×10^{-5}	+0.20
Tetradecane	500	2.06	1.86	0.63	12.18×10^{-7}	0.09	0.12×10^{-5}	+0.24
Hexadecane	500	3.09	2.48	0.48	4.10×10^{-7}	0.20	0.26×10^{-5}	+1.65
HVWO	500	35.8	14.12	0.27	0.41×10^{-7}	0.18	0.24×10^{-5}	+4.9

(1) Test Conditions: Ball-on-Cylinder device, Paraffinic Hydrocarbons 240 rpm, 25°C, 32 minutes, Dry Air Atmosphere, 52100 Steel-on-52100 Steel.

(2) $ho/ho' = (\eta o/\eta o')^{0.725}$ as per Cheng, H. S., "A Numerical Solution of the EHD Film Thickness in an Elliptical Contact", Trans. ASME, J. Lub. Tech., 92, pgs. 155-162, (assumed nearly circular contact).

TABLE 6

Measured Wear and Measured Voltages as a Function of Relative Film Thickness[1]

Lubricant	Load (g)	Viscosity (mPa·S)	Relative Film Thickness ho/ho'[2]	Ball Wear Scar Diameter (mm)	Ball Wear Volume (cc)	Track Cross Sectional Area (cm^2)	Cylinder Wear Volume (cc)	Measured Voltage (mv)
LVWO	500	2.43	1.0	0.62	11.42×10^{-7}	0.88	1.16×10^{-5}	+ 0.3
50:50 LVWO:IVWO	500	5.6	1.81	0.55	7.07×10^{-7}	0.90	1.19×10^{-5}	+ 0.45
30:70 LVWO:IVWO	500	8.2	2.37	0.50	4.83×10^{-7}	0.63	0.83×10^{-5}	+ 0.6
15:85 LVWO:IVWO	500	11.3	2.98	0.50	4.83×10^{-7}	0.53	0.70×10^{-5}	+ 0.51
IVWO	500	17.7	4.10	0.48	4.10×10^{-7}	0.52	0.69×10^{-5}	+ 0.33

(1) Test Conditions: Ball-on-Cylinder Device, Mixtures of LVWO and IVWO, 240 rpm, 25°C, 32 Minutes, Wet Air Atmosphere, Aluminum-on-Steel

(2) $ho/ho' = (\eta o/\eta o')^{0.725}$ as per Cheng, H. S., "A Numerical Solution of the EHD Film Thickness in an Elliptical Contact", Trans. ASME, J. Lub. Tech., 92, pgs. 155-162, (assumed nearly circular contact).

viscosity over a reasonably broad range of the film thicknesses. As may be seen from Table 6, both ball and cylinder wear are virtually identical for all of these fluids.

From both of the above series of tests, it is evident that the measured voltages, under conditions in which wear rates (and presumably wear mechanism) are similar, are not affected by changes in film thickness.

4. RESULTS - Test Variables

This program has essentially a two-fold objective, firstly to determine if a general relationship exists between SGV's and the amount of wear which takes place within a fixed interval of time, and secondly, to determine if the SGV's are related to the mechanisms by which wear takes place. Two groups of experiments have been performed in order to evaluate these relationships. In order to assess if a relationship between SGV's and wear exists, tests have been carried out using different lubricant base stocks under varied loads, while maintaining other operating parameters such as metallurgy, speed and temperature constant for each group of experiments. In the other, in order to assess if SGV's are related to wear mechanism, the influence upon SGV's of change in chemical parameter, primarily lubricant, have been examined.

Gathered in Table 7 are the calculated wear and measured SGV's for tests with 52100 steel under dry air blanketing at room temperature using several base stocks, including paraffinic hydrocarbons, aromatic type hydrocarbons, mixtures of aromatics and paraffins, the HVWO, the HVLRO and esters. A complete set of data including all of the measured wear data and curves illustrating the time dependent variations of the SGV's are included in the appended Data Tables.

Included in Table 7 is a parameter labeled the Surface Fatigue Demerit Rating (SFDR) which reflects the nature and character of the track surface profile. This system is illustrated graphically in Fig. 11. A relatively smooth track, showing no apparent cracking is assigned

TABLE 7

Measured Wear and Self-Generated Voltages Under Dry Air Blanketing for AISI 52100 Steel Balls Sliding on AISI 52100 Steel Cylinders(1)

Lubricant	Load (g)	Wear Volume		Surface Fatigue Demerit Rating	Self-Generated Voltage (mv)	Appendix Table No.
		Ball (cc)	Cylinder (cc)			
HVWO	200	0.08×10^{-7}	0.11×10^{-5}	1	+6.3	1B
Decane	500	36.69×10^{-7}	0.05×10^{-5}	2	+0.21	18B
Dodecane	500	20.77×10^{-7}	0.18×10^{-5}	1+	+0.20	18B
Tetradecane	500	12.18×10^{-7}	0.12×10^{-5}	1	+0.24	18B
LVWO	500	3.17×10^{-7}	0.08×10^{-5}	1	+0.50	17B
Hexadecane	500	2.64×10^{-7}	0.26×10^{-5}	3	+1.65	18B
1-Methylnaphthalene	500	1.16×10^{-7}	0.50×10^{-5}	1	+3.0	19B
HVWO	500	0.41×10^{-7}	0.24×10^{-5}	1	+4.9	1B
HVLRO	500	0.18×10^{-7}	0.24×10^{-5}	1	+2.6	20B
20/80 Toluene/LVWO	1000	12.18×10^{-7}	0.33×10^{-5}	3	+0.15	26B
20/80 Mesitylene/LVWO	1000	10.02×10^{-7}	0.22×10^{-5}	1	+0.40	26B
LVWO	1000	6.10×10^{-7}	0.30×10^{-5}	1	+0.18	17B
HVWO	1000	0.71×10^{-7}	0.50×10^{-5}	1	+4.3	1B
HVLRO	1000	0.30×10^{-7}	0.40×10^{-5}	1	+2.3	20B
20/80 1-Methylnaphthalene/LVWO	1000	1.16×10^{-7}	0.17×10^{-5}	2	+3.0	26B
20/80 1-Chloronaphthalene	1000	8.16×10^{-7}	0.42×10^{-5}	1	+4.0	26B
LVWO	2000	27.17×10^{-7}	0.45×10^{-5}	3	-0.05	17B
20/80 1-Methylnaphtlalene/LVWO	2000	4.83×10^{-7}	1.11×10^{-5}	3	-0.15	26B
20/80 1-Chloronaphthalene/LVWO	2000	16.53×10^{-7}	1.83×10^{-5}	3	+0.8	26B
HVWO	2000	0.92×10^{-7}	0.54×10^{-5}	1+	+0.55	1B
Di-2-Ethylhexyl Adipate	2000	0.71×10^{-7}	1.25×10^{-5}	1	+0.20	29B
Hercolube J	2000	0.63×10^{-7}	0.50×10^{-5}	3	+1.50	29B
HVLRO	2000	1.61×10^{-7}	1.15×10^{-5}	3	-0.06	20B
20/80 1-Chloronaphthalene/LVWO	4000	31.66×10^{-7}	2.31×10^{-5}	3	+0.45	26B
HVWO	4000	3.77×10^{-7}	2.35×10^{-5}	3	-0.30	1B
HVLRO	4000	4.10×10^{-7}	2.82×10^{-5}	3	-0.24	20B

(1) Test Conditions: Ball-on-Cylinder Device, Loads as noted, 240 rpm, 25°C, 32 min.

FIGURE 11

Surface Profiles Which Illustrate the Surface Fatigue Demerit Rating System

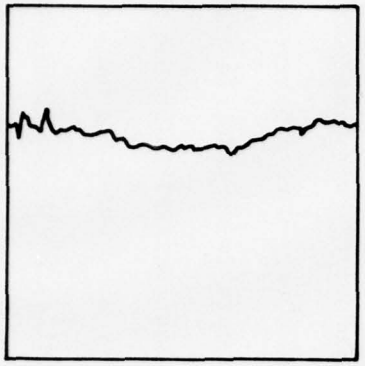

Surface Fatigue Demerit
Rating = 1

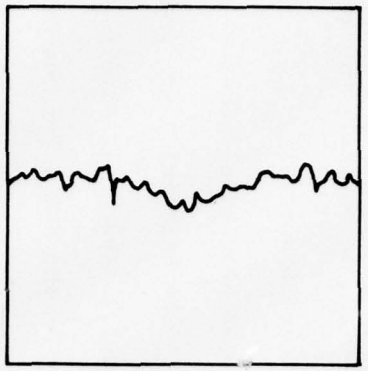

Surface Fatigue Demerit
Rating = 1+

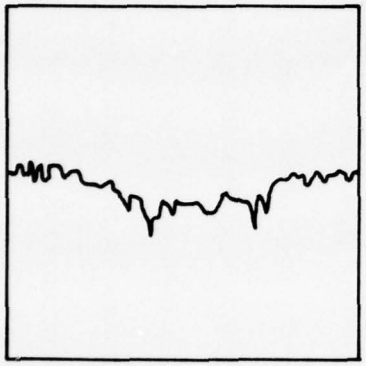

Surface Fatigue Demerit
Rating = 2

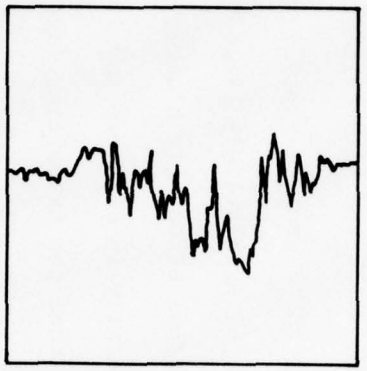

Surface Fatigue Demerit
Rating = 3

a demerit rating of 1. One which exhibits some damage is assigned a value of 2. A surface profile which exhibits extensive "cracking", is jagged and non-symmetric, is assigned a value of 3. A rating of 1^{+} indicates slight damage within the wear track.

Presented graphically in Figs. 12 and 13 are the relationships between SGV's and both cylinder and ball wear. In general, the magnitudes of the SGV's decline rapidly with an increase in wear.

A relatively large body of data has also been gathered under conditions of wet air blanketing, Table 8. The data which are presented graphically in Figs. 14 and 15 show no general trend. It should also be noted that the polarities (and magnitudes) of the SGV's for the HVWO are different from those for the other base stocks investigated under this atmospheric environment.

The relationships between wear and SGV seem to exist at elevated temperatures also. Increased temperature, under dry air blanketing, leads, in general to increased wear and either relatively more negative or unchanged, negative, SGV's, Table 9. This data is included in Figs. 12 and 13 and presented in Figs. 16 and 17. The same general influence of increased temperature as that noted for test under dry air blanketing have been noted for tests carried out under wet air blanketing, Table 10. These data have not been included in Figs. 14 and 15.

Data are also available for the aluminum-on-steel metallurgy using the HVWO, HVLRO and mixed aromatic-LVWO base stocks under dry air blanketing (Table 11). The general relationships which emerge using this metallurgy, Figs. 18 and 19 for cylinder and ball wear, respectively as a function of SGV's,

FIGURE 12

The Relationship Between Cylinder Wear and Self-Generated Voltages for the Steel System Under Dry Air Blanketing

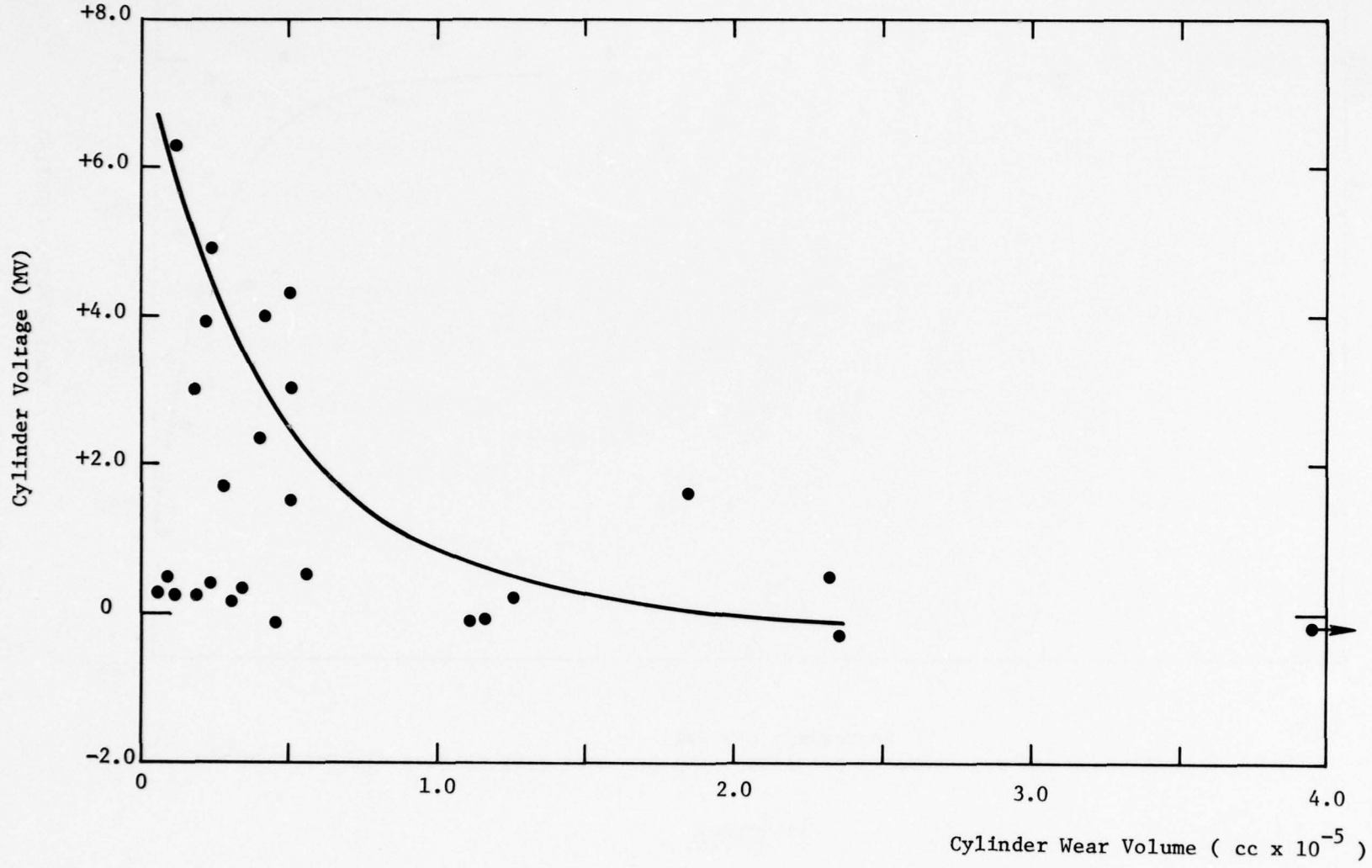

FIGURE 13

The Relationship Between Ball Wear and Self-Generated Voltages for the Steel System Under Dry Air Blanketing

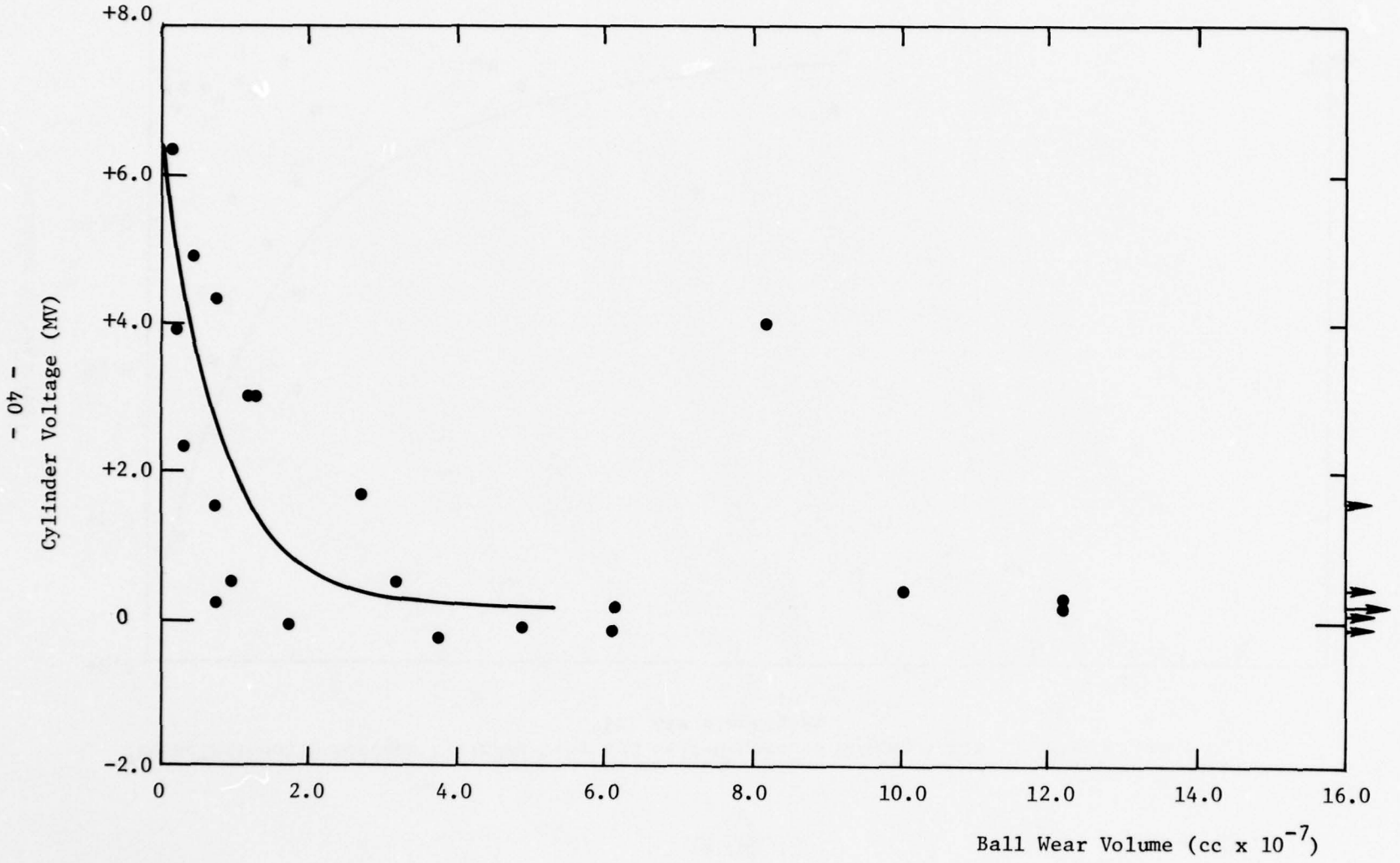

TABLE 8

Measured Wear and Self-Generated Voltages Under Wet Air Blanketing for AISI 52100 Steel Balls Sliding on AISI 52100 Steel Cylinders(1)

Lubricant	Load (g)	Wear Volume		Surface Fatigue Demerit Rating	Self Generated Voltage (mv)	Appendix Table No.
		Ball (cc)	Cylinder (cc)			
HVWO	200	0.48×10^{-7}	0.08×10^{-5}	1	-0.84	3B
Hexadecane	250	24.46×10^{-7}	0.04×10^{-5}	1+	+0.09	18B
HVWO	350	0.92×10^{-7}	0.12×10^{-5}	1	-1.50	3B
LVWO	500	10.70×10^{-7}	0.33×10^{-5}	1	+0.20	17B
Hexadecane	500	44.28×10^{-7}	1.06×10^{-5}	3	+0.09	18B
HVWO	500	1.16×10^{-7}	0.24×10^{-5}	1	-1.80	3B
1-Methylnaphthalene	500	6.10×10^{-7}	0.37×10^{-5}	1	+2.9	19B
HVLRO	500	0.63×10^{-7}	0.13×10^{-5}	1	+2.8	21B
Di-2-Ethylhexyl Sebacate	500	0.26×10^{-7}	0.15×10^{-5}	+	+0.69	29B
HVWO	700	1.45×10^{-7}	0.22×10^{-5}	1	-2.19	3B
1-Chloronaphthalene	1000	83.67×10^{-7}	0.59×10^{-5}	1	+0.6	19B
LVWO	1000	24.46×10^{-7}	0.95×10^{-5}	3	+0.15	17B
20/80 Toluene/LVWO	1000	44.28×10^{-7}	0.32×10^{-5}	3	+0.0	27B
20/80 Mesitylene/LVWO	1000	44.28×10^{-7}	0.79×10^{-5}	2	+0.01	27B
20/80 1-Methylnaphthalene/LVWO	1000	15.58×10^{-7}	0.59×10^{-5}	1	+0.18	27B
20/80 1-Chloronaphthalene/LVWO	1000	241.87×10^{-7}	0.59×10^{-5}	3	+0.02	27B
HVWO	1000	1.98×10^{-7}	0.33×10^{-5}	1+	-1.38	3B
HVLRO	1000	0.63×10^{-7}	0.69×10^{-5}	1	+0.66	21B
Di-2-Ethylhexyl Sebacate	1000	0.30×10^{-7}	0.24×10^{-5}	+	+0.57	29B
HVWO	1500	1.61×10^{-7}	0.53×10^{-5}	1+	-0.90	3B
LVWO	2000	323.32×10^{-7}	163.68×10^{-5}	3	+0.06	17B
HVWO	2000	2.41×10^{-7}	1.02×10^{-5}	1+	+0.15	3B
HVLRO	2000	1.80×10^{-7}	0.90×10^{-5}	1	+0.46	21B
Di-2-Ethylhexyl Sebacate	2000	0.48×10^{-7}	0.25×10^{-5}	1	+0.24	29B
Di-2-Ethylhexyl Adipate	2000	0.92×10^{-7}	0.71×10^{-5}	3	+0.06	29B
Hercolube J	2000	0.81×10^{-7}	0.49×10^{-5}	3	+1.41	29B
1-Chloronaphthalene	4000	160.29×10^{-7}	6.07×10^{-5}	3	0.0	19B
HVWO	4000	6.10×10^{-7}	4.54×10^{-5}	1+	+0.30	3B
HVLRO	4000	3.46×10^{-7}	1.97×10^{-5}	1+	+0.09	21B
Di-2-Ethylhexyl Azelate	4000	1.45×10^{-7}	2.55×10^{-5}	1+	+0.24	29B

(1) Test Conditions: Ball-on-Cylinder Device, Loads as noted, 240 rpm, 25°C, 32 minutes.

FIGURE 14

The Relationship Between Cylinder Wear and Self-Generated Voltages for the Steel System Under Wet Air Blanketing

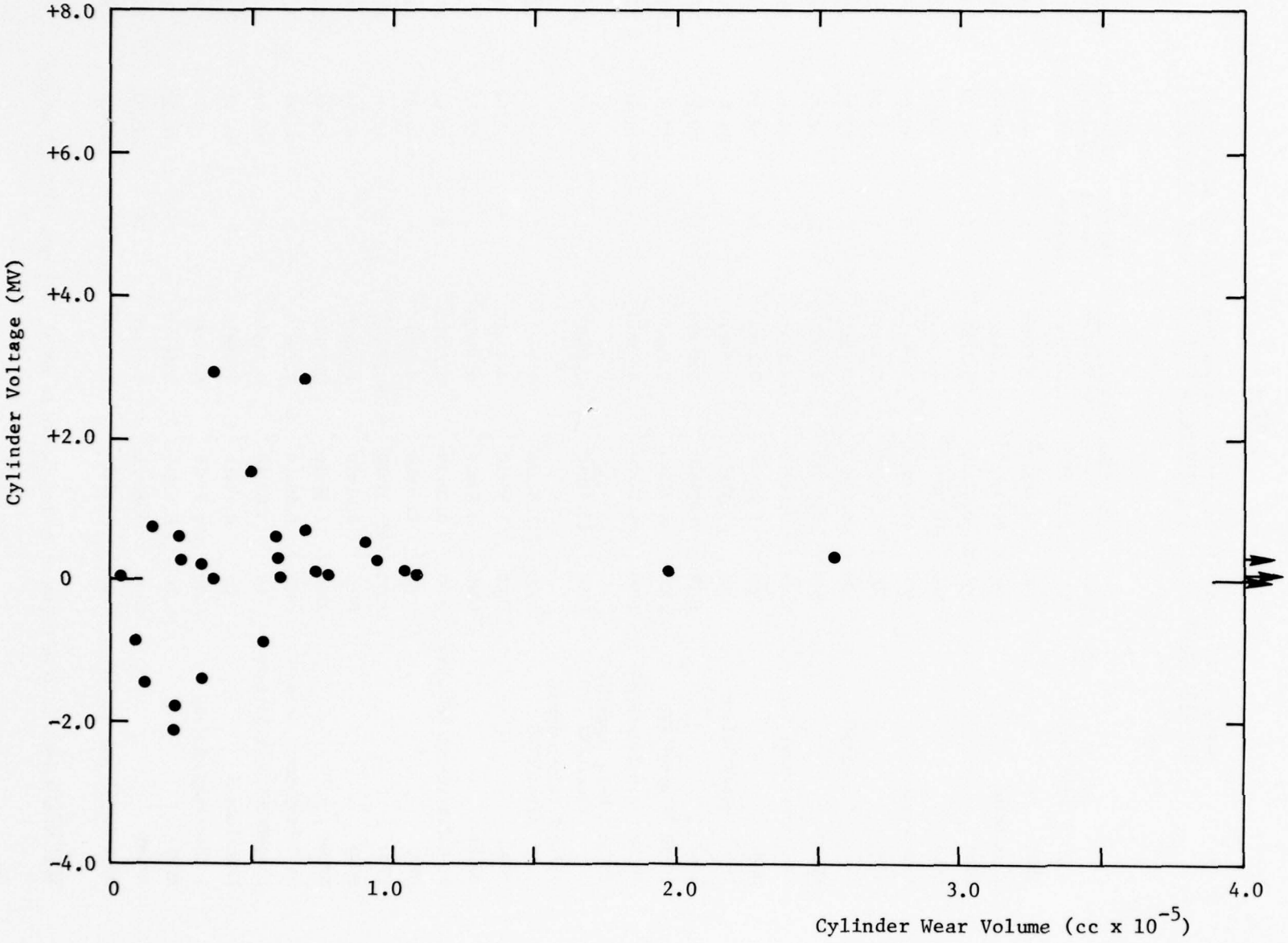

FIGURE 15

The Relationship Between Ball Wear and Self-Generated Voltages for the Steel System Under Wet Air Blanketing

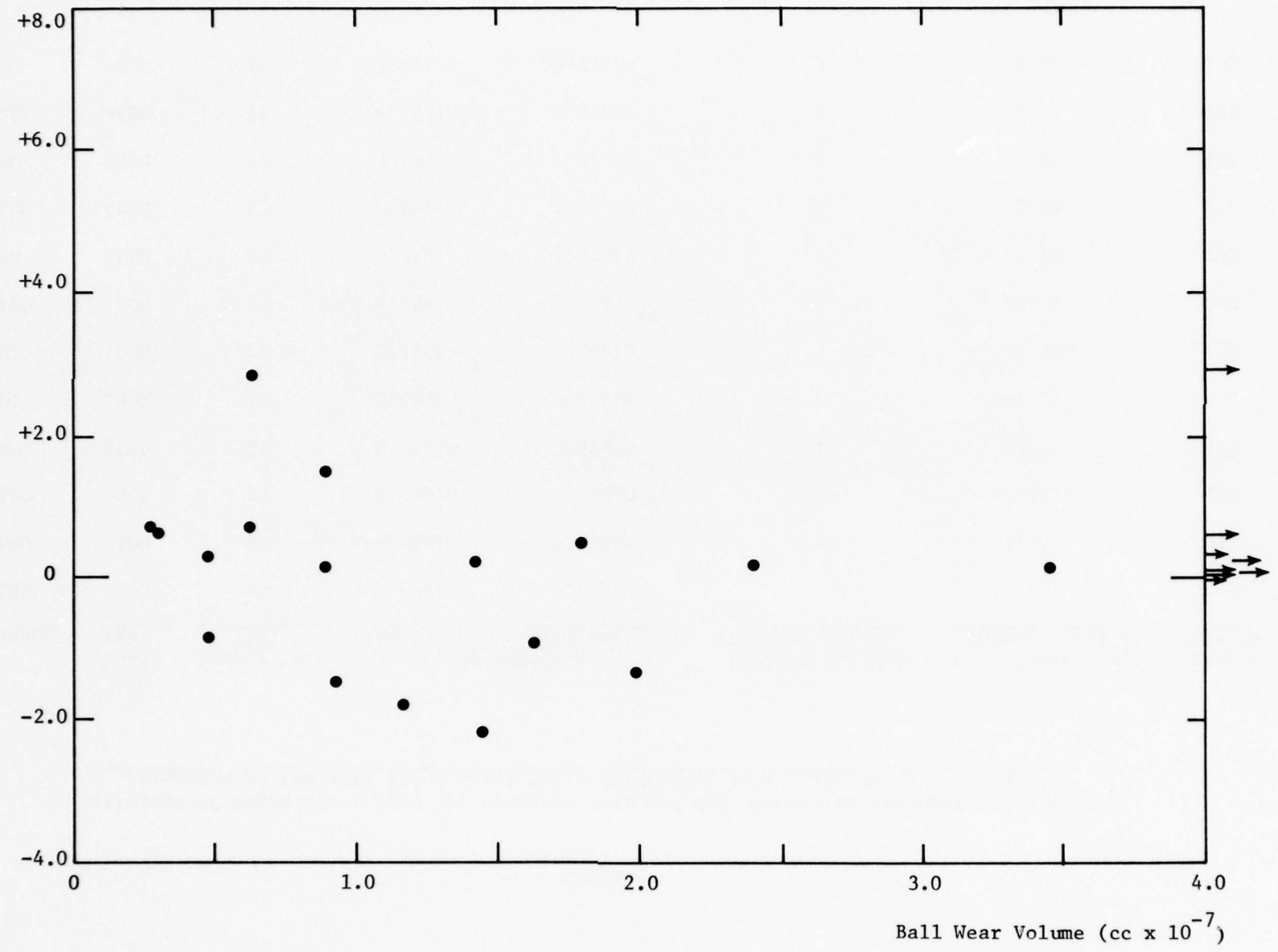

TABLE 9

Influence of Temperature Upon the Measured Wear and Self-Generated Voltages Under Dry Air Atmospheres for AISI 52100 Steel Balls Sliding on AISI 52100 Steel Cylinders(1)

Lubricant	Load (g)	Temperature (°C)	Wear Volume		Surface Fatigue Demerit Rating	Self-Generated Voltage (mv)(2)	Appendix Table No.
			Ball (cc)	Cylinder (cc)			
HVLRO	500	25	0.18×10^{-7}	0.24×10^{-5}	1	+2.6	24B
HVLRO	500	52	0.63×10^{-7}	0.60×10^{-5}	2	+1.2	24B
HVLRO	500	79	1.30×10^{-7}	0.13×10^{-5}	1+	erratic	24B
HVWO	1000	25	0.71×10^{-7}	0.50×10^{-5}	1	+4.3	13B
HVWO	1000	52	0.48×10^{-7}	0.95×10^{-5}	1	+1.11	13B
HVWO	1000	79	2.64×10^{-7}	0.44×10^{-5}	2	+0.78	13B
HVLRO	4000	25	4.10×10^{-7}	2.82×10^{-5}	3	-0.24	24B
HVWO	4000	25	3.77×10^{-7}	2.35×10^{-5}	3	-0.30	13B
HVLRO	4000	52	6.10×10^{-7}	3.50×10^{-5}	3	-0.18	24B
HVWO	4000	52	3.77×10^{-7}	1.81×10^{-5}	3	-0.21	13B
HVLRO	4000	79	8.75×10^{-7}	3.05×10^{-5}	3	-0.15	24B
HVWO	4000	79	19.64×10^{-7}	10.23×10^{-5}	3	-0.19	13B

(1) Test Conditions: Ball-on-Cylinder Device, 240 rpm, 32 minutes.

(2) The zero for the SGV's in the steel-on-steel system is temperature dependent and follows the relationship SGV (MV) = $0.209 - 6.96\times10^{-3}$ T (°C) over the temperature range 25°C - 160°C. SGV's have been temperature corrected.

FIGURE 16

The Relationship Between Cylinder Wear and Self-Generated Voltages for the Steel System Under Dry Air Blanketing Showing the Influence of Temperature

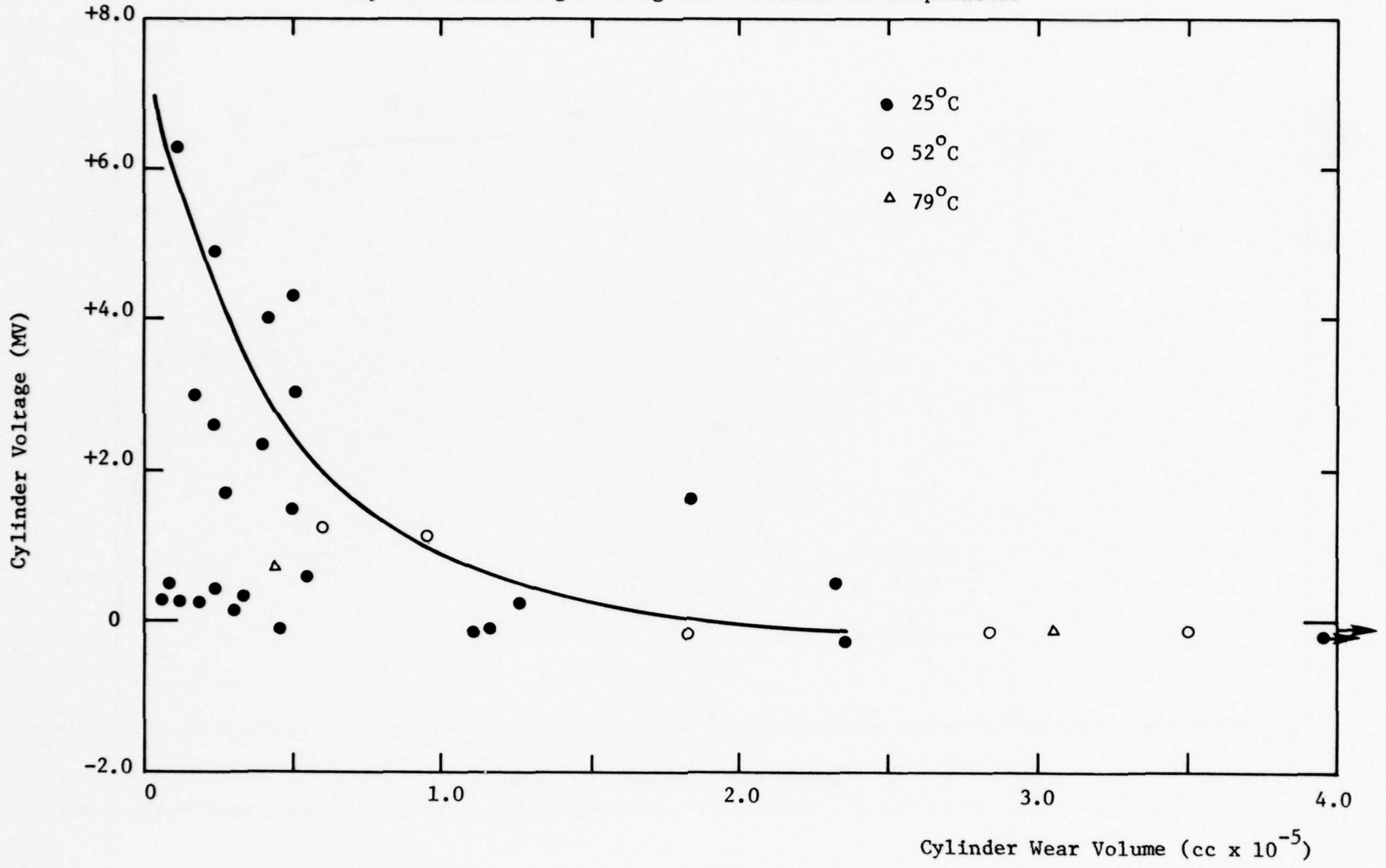

FIGURE 17

The Relationship Between Ball Wear and Self-Generated Voltages for the Steel System Under Dry Air Blanketing Showing the Influence of Temperature

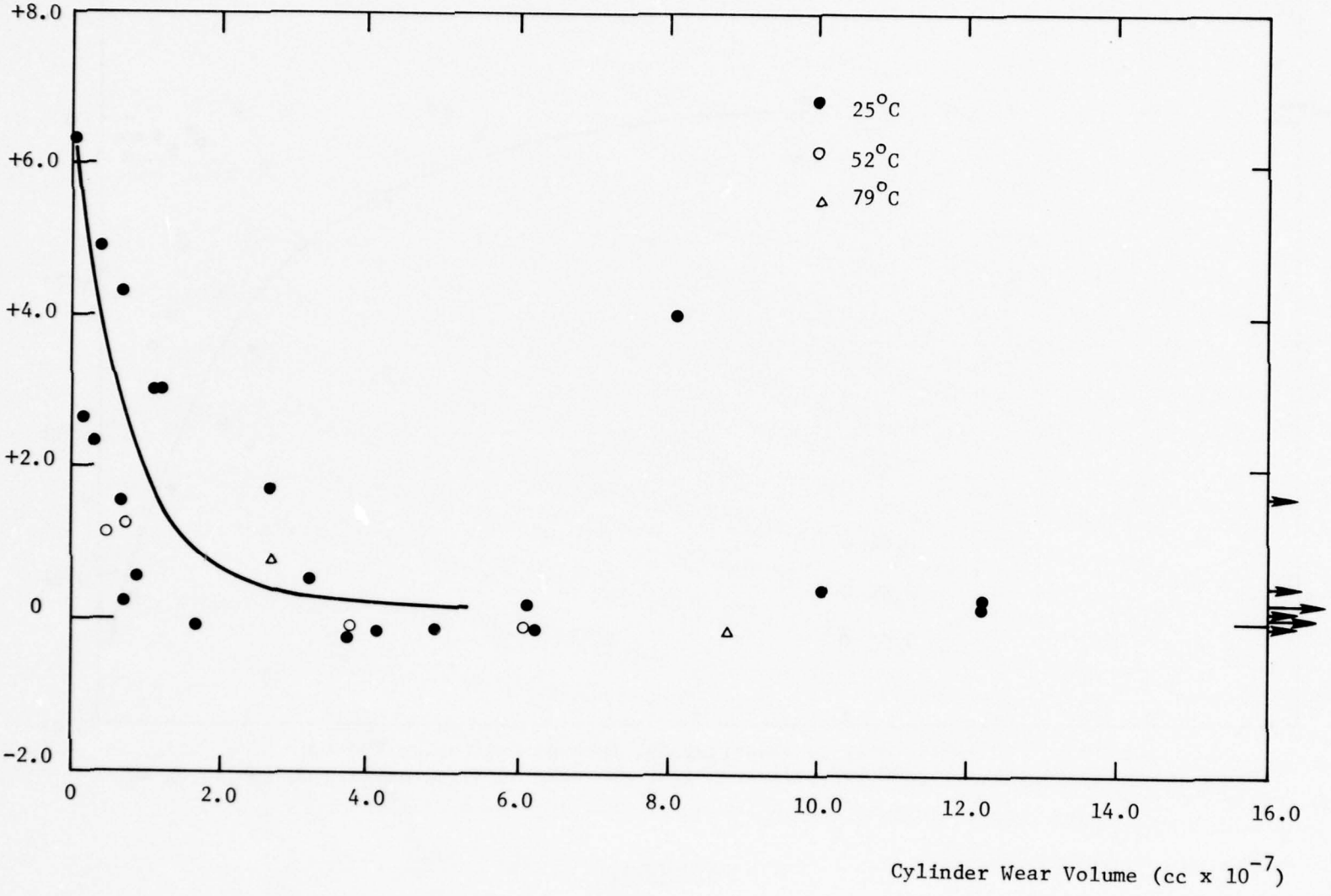

TABLE 10

Influence of Temperature Upon the Measured Wear and Self-Generated Voltages Under Wet Air Atmospheres for AISI 52100 Sliding on AISI 52100 Steel Cylinders[1]

Lubricant	Load (g)	Temperature (°C)	Wear Volume Ball (cc)	Wear Volume Cylinder (cc)	Surface Fatigue Demerit Rating	Self-Generated Voltage (mv)[2]	Appendix Table No.
HVLRO	500	25	0.41×10^{-7}	0.08×10^{-5}	1	+2.8	24B
HVLRO	500	52	1.03×10^{-7}	0.38×10^{-5}	2	+0.41	24B
HVLRO	500	79	0.92×10^{-7}	2.02×10^{-5}	1+	+0.42	24B
HVWO	1000	25	0.81×10^{-7}	0.59×10^{-5}	1	[illegible].2	14B
HVWO	1000	52	0.63×10^{-7}	1.03×10^{-5}	1	+0.78	14B
HVWO	1000	79	4.83×10^{-7}	1.07×10^{-5}	2	+0.42	14B
HVLRO	4000	25	3.45×10^{-7}	1.97×10^{-5}	1+	+0.09	24B
HVWO	4000	25	6.10×10^{-7}	4.54×10^{-5}	1+	+0.30	14B
HVLRO	4000	32	4.10×10^{-7}	1.20×10^{-5}	2	-0.09	24B
HVLRO	4000	52	3.17×10^{-7}	3.97×10^{-5}	2	-0.23	24B
HVLRO	4000	79	4.83×10^{-7}	6.40×10^{-5}	2	-0.24	24B
HVWO	4000	79	62.96×10^{-7}	11.48×10^{-5}	3	-0.14	14B

(1) Test Conditions: Ball-on-Cylinder Device, 240 rpm, 32 minutes.
(2) The zero for the SGV's in the steel-on-steel system is temperature dependent and follows the relationship SGV (MV) = $0.209 - 6.96\times10^{-3}$ T (°C) over the temperature range 25°C - 160°C. SGV's have been temperature corrected.

TABLE 11

Measured Wear and Self-Generated Voltages Under Dry Air Blanketing for Aluminum Balls Sliding on Steel Cylinders(1)

Lubricant	Load (g)	Wear Volume Ball (cc)	Wear Volume Cylinder (cc)	Surface Fatigue Demerit Rating	Self-Generated Voltage (mv)	Appendix Table No.
HVWO	200	0.63×10^{-7} (2)	$<0.09\times10^{-5}$ (2)	1	+10.8	7B
20/80 Toluene/LVWO	500	1.16×10^{-7}	0.11×10^{-5}	1	+ 5.8	28B
HVLRO	500	0.63×10^{-7}	0.11×10^{-5}	1	+ 3.6	22B
LVWO	1000	2.41×10^{-7}	0.26×10^{-5}	3	+ 0.45	28B
20/80 Toluene/LVWO	1000	2.64×10^{-7}	0.13×10^{-5}	1+	+ 0.48	28B
20/80 Mesitylene/LVWO	1000	2.41×10^{-7}	0.29×10^{-5}	3	+ 0.45	28B
20/80 1-Methylnaphthalene/LVWO	1000	2.41×10^{-7}	0.17×10^{-5}	1	+ 2.6	28B
HVWO	1000	1.45×10^{-7} (2)	$<0.12\times10^{-5}$ (2)	1	+ 4.9	7B
HVLRO	1000	1.03×10^{-7}	0.13×10^{-5}	1	+ 3.1	22B
HVWO	2000	2.90×10^{-7} (2)	0.18×10^{-5} (2)	1	+ 3.8	7B
HVLRO	2000	3.77×10^{-7}	0.30×10^{-5}	1	+ 1.9	22B
20/80 1-Chloronaphthalene/LVWO	4000	15.58×10^{-7}	1.74×10^{-5}	3	+ 0.24	28B
HVLRO	4000	4.83×10^{-7}	0.59×10^{-5}	1	+ 0.7	22B
HVWO	4000	4.83×10^{-7}	0.46×10^{-5}	1	+ 0.7	7B

(1) Test Conditions: Ball-on-Cylinder Device, 240 rpm, 25°C, 16 minute tests (see Note 2).

(2) Measured Wear after 32 minutes of Testing, Self-Generated Voltages as read at 16 minutes.

FIGURE 18

The Relationship Between Cylinder Wear and Self-Generated Voltages for an Aluminum-on-Steel System Under Dry Air Blanketing

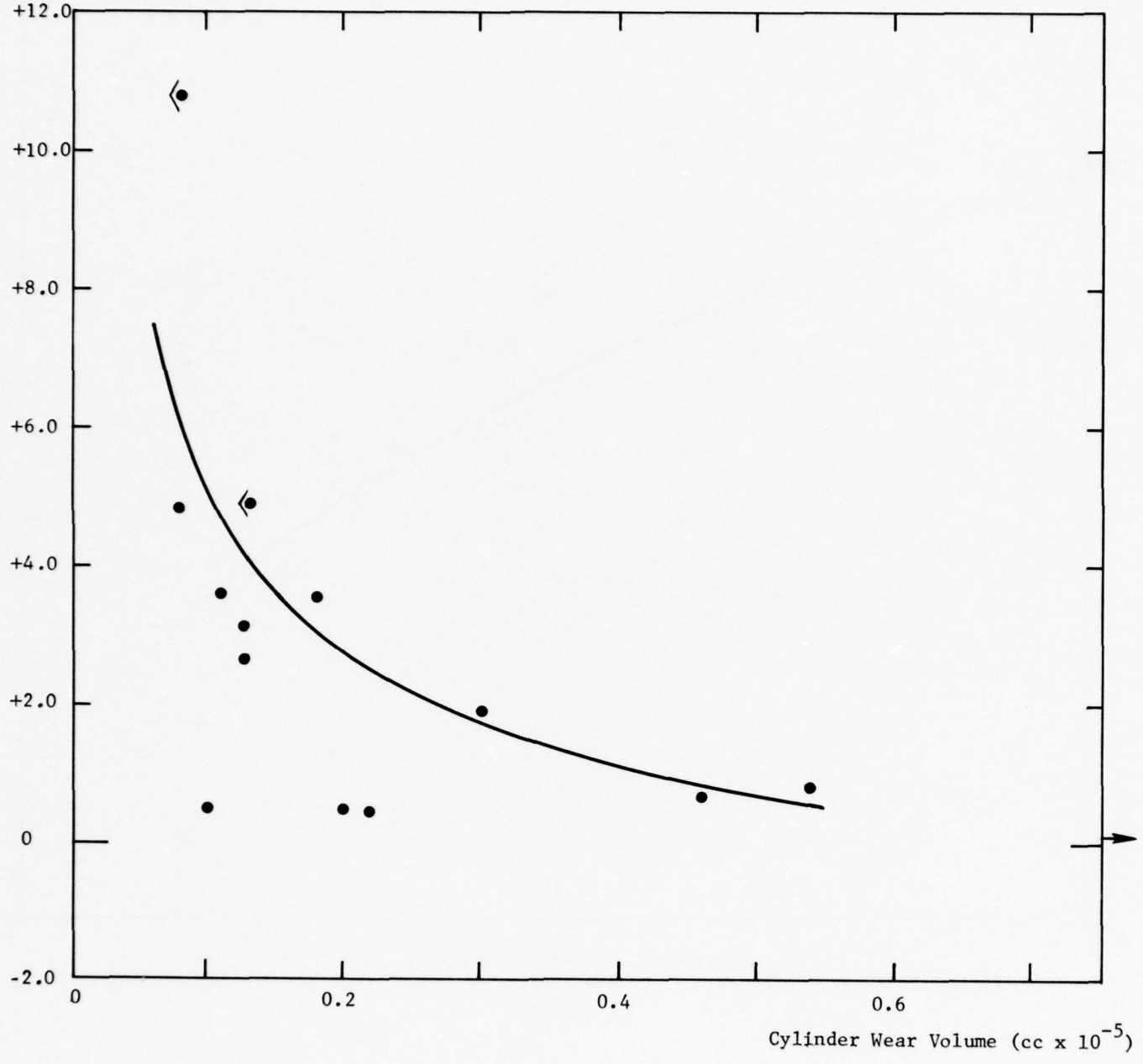

FIGURE 19

The Relationship Between Ball Wear and Self-Generated Voltages for an Aluminum-on-Steel System Under Dry Air Blanketing

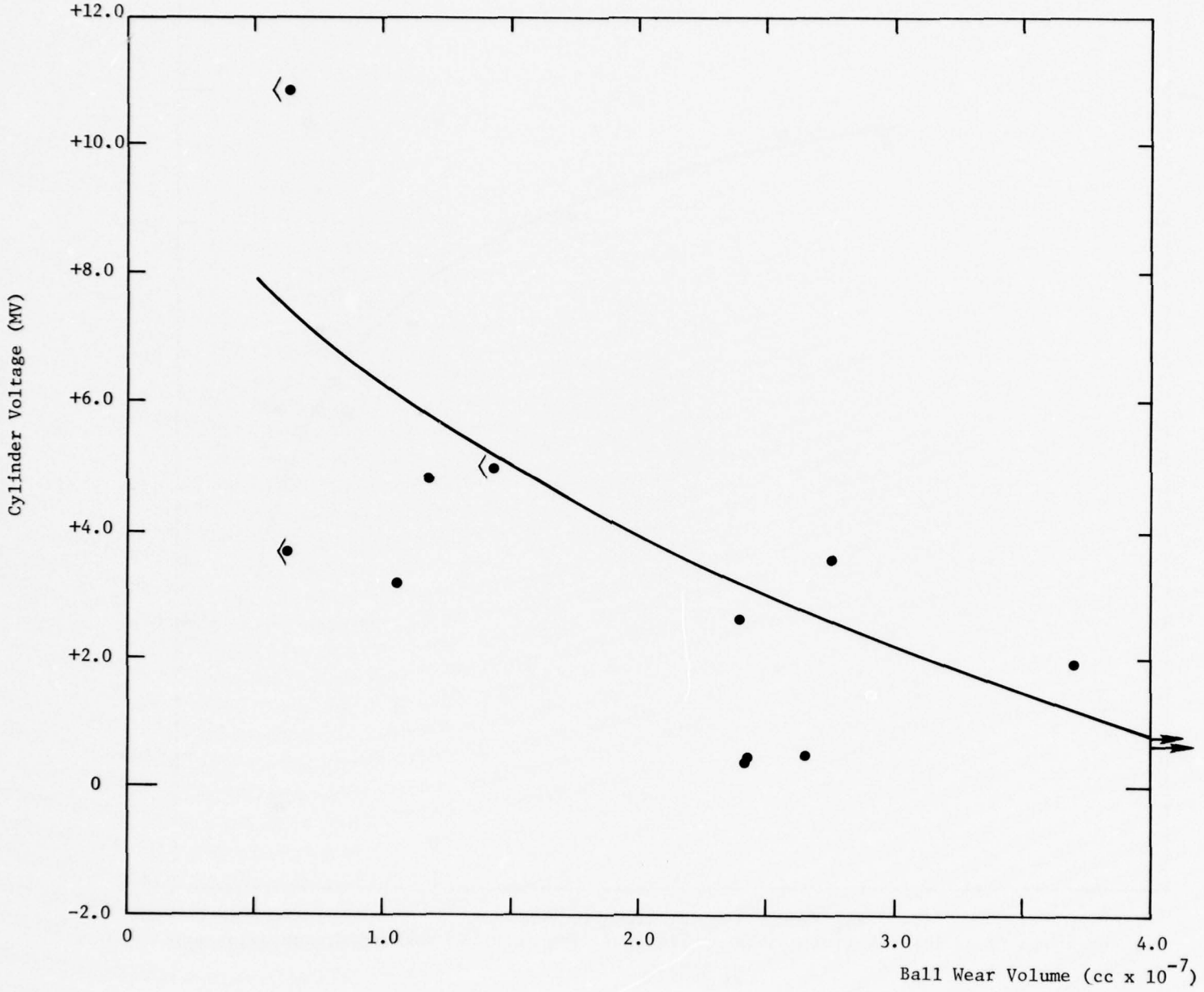

are generally similar to those presented in Figs. 12 and 13 namely that higher SGV's give rise to lower wear.

The influence of oxygen availability upon the development of SGV's was investigated by studying systems under Argon or partially inerted atmospheres, Table 12. Oxygen availability is clearly necessary for the development of SGV's since in its absence, the SGV's are all nearly zero, even though wear may be substantial.

TABLE 12

Measured Wear and Self-Generated Voltages Under Both Inerted and Oxygenated Atmospheres for the HVWO Using AISI 52100 Steel Balls Sliding on AISI 52100 Steel Cylinders[1]

Load	Metallurgy (Ball/Cylinder)	Time (min)	Argon			Air		
			Ball Wear Volume (cc)	Cylinder Wear Volume (cc)	Self-Generated Voltage (mv)	Ball Wear Volume (cc)	Cylinder Wear Volume (cc)	Self-Generated Voltage (mv)
			DRY CONDITION					
200	Aluminum/Steel	32	--	--	--	0.63×10^{-7}	0.13×10^{-5}	+14.1
250	Aluminum/Steel	32	1.98×10^{-7}	0.23×10^{-5}	-0.19	--	--	--
500	Aluminum/Steel	32	7.07×10^{-7}	--	-0.08	1.98×10^{-7}	0.22×10^{-5}	+ 2.5
500	Steel/Steel	36	0.22×10^{-7}	0.30×10^{-5}	+0.06	0.40×10^{-7}	0.24×10^{-5}	+ 4.9
500	Steel/Steel	360	0.22×10^{-7}	0.21×10^{-5}	+0.18	--	--	--
2000	Steel/Steel	36	0.81×10^{-7}	0.66×10^{-5}	0.00	0.92×10^{-7}	0.54×10^{-5}	+ 0.55
			WET CONDITION					
200	Steel/Steel	32	--	--	--	0.48×10^{-7}	0.08×10^{-5}	- 0.84
350	Steel/Steel	32	--	--	--	0.92×10^{-7}	0.12×10^{-7}	- 1.5
500	Steel/Steel	32	0.30×10^{-7}	0.20×10^{-5}	+0.05	1.16×10^{-7}	0.24×10^{-5}	- 1.8
2000	Steel/Steel	32	0.63×10^{-7}	0.91×10^{-5}	+0.03	2.41×10^{-7}	1.02×10^{-7}	+ 0.15

Test Conditions: Ball-on-Cylinder Device, 240 rpm, 25°C, Data taken from Appendix Table 12B.

5. DISCUSSION

5.1 Relationships Between SGV's and Wear

This experimental program was initiated in order to establish if a relationship exists between SGV's and wear, and, in addition, to establish if there is a correlation between the relative polarity and magnitude of the SGV's and wear mechanism. Since demonstration that a general relationship between wear and SGV's exists is the more general of the objectives, it will be discussed first. For this purpose, it is necessary only to recognize that SGV's are developed under boundary lubricated conditions; postponing the question of how such voltages might be generated under boundary lubricated conditions until later.

With increased wear on either the ball or the cylinder, there is a general decline in the magnitudes of the SGV's for the steel-on-steel system under dry air blanketing, Figs. 12 and 13 and for the aluminum-on-steel system, Figs. 18 and 19. The data under wet air blanketing for the steel-on-steel system (Figs. 16 and 17) will not be discussed at the present time. The relationship between ball wear and SGV's for the steel-on-steel system is particularly striking. For example, it may be concluded, based upon the functional relationship which is plotted in Fig. 13, that for ball wear volumes in excess of 2.1×10^{-7} cc (wear scar diameters of 0.41 mm or greater) the SGV's will assume values of 0.5 mv or less.

The relationship between cylinder wear and SGV's for the steel-on-steel system is not as clear because low values of cylinder wear may be associated with either high or low values for the SGV's. However, it

should be noted that the systems which comprise the data base clustering in the low cylinder wear - low SGV's region, all exhibit large values for ball wear. This characteristic, high ball wear, low cylinder wear is typical of systems undergoing severe corrosive wear. There is, therefore, reason to believe that the systems which comprise this set of data are different from the rest of the data presented in Figure 12. The smooth curve drawn in Figure 12, therefore, disregards these values. In so doing, the relationship between SGV's and cylinder wear for the steel-on-steel system is reasonably good. Based upon the smooth curve drawn, it may be concluded that cylinder wear volumes in excess of about 1.2×10^{-5} cc will lead to SGV's of +0.5 mv or less.

For the aluminum-on-steel system, there is also a general trend that increased wear leads to lower SGV's. There are again several systems which lie substantially away from the smooth curves drawn in Figs. 18 and 19, namely those for the LVWO, and the 20/80 blends of toluene and mesitylene in the LVWO. The reason for this failure is apparent, however, upon elemental analysis, performed using EDAX, of the aluminum balls employed in these particular tests (Fig. 20). The major elemental component at the surface of the wear scar in these cases is found to be iron rather than the aluminum metallurgy of the ball (Figs. 20a-20c). Presumably, considerable metal transfer from the cylinder to the ball has taken place, essentially converting the test metallurgy from aluminum-on-steel to steel-on-steel. Indeed, the SGV's measured for the above named systems are close to those noted for the steel-on-steel case, Table 7. Typical surface analysis of the worn

Figure 20

EDAX Analysis of Wear Scar of Aluminum Balls for test with Various Base Stocks for Aluminum-on-Steel Tests Under Dry Air Blanketing

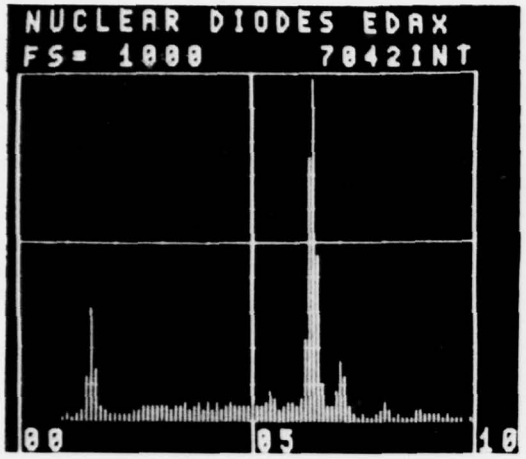

20a. Toluene

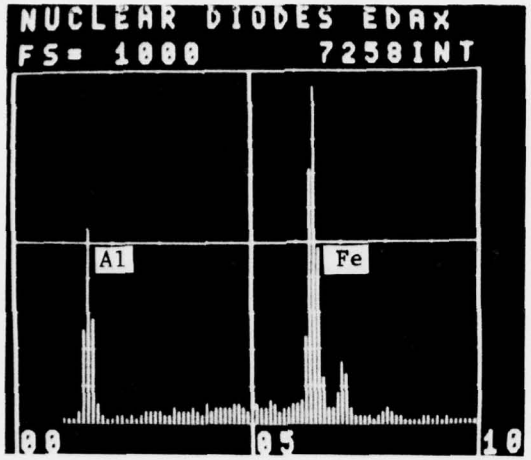

20b. Mesitylene

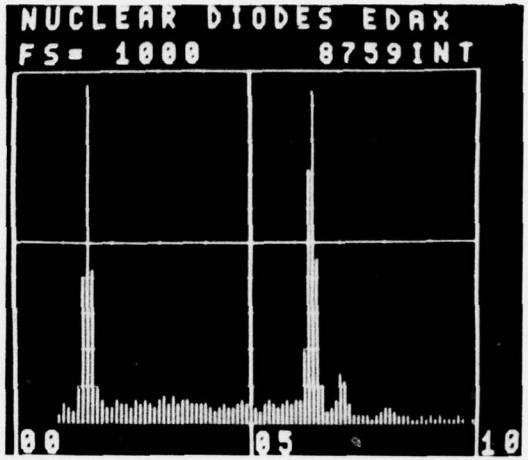

20c. LVWO

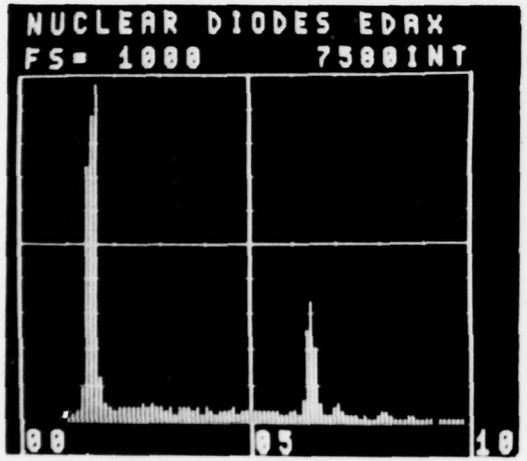

20d. 1-Methylnaphthalene

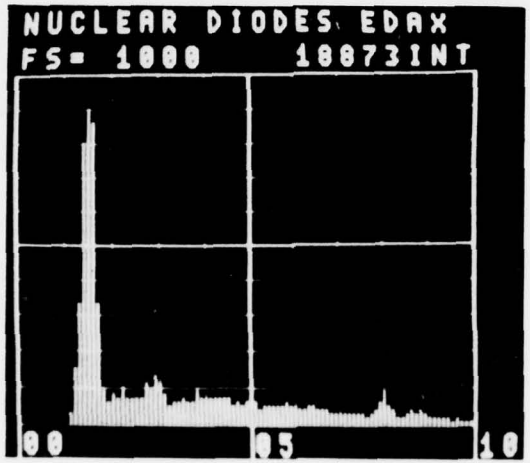

20e. HVWO

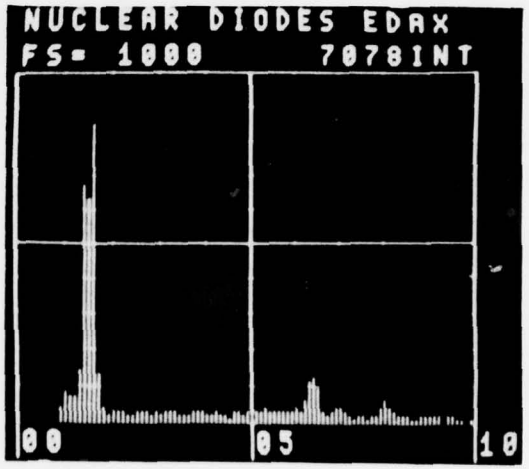

20f. HVLRO

balls from some of the other test systems are shown in Figs. 20d-20f where it is noted that in contrast with Figs. 20a-20c, the dominant element observed is aluminum. Since the three special cases discussed above represent circumstances closer to steel-on-steel wear rather than aluminum-on-steel, it is readily understood why they do not correlate with the relationships presented in Figs. 18 and 19. Disregarding these three values, the smooth curve relationships presented in Figs. 18 and 19 are fairly good.

For the steel-on-steel system under wet air blanketing, Figs. 16 and 17, it is apparent that little correlation exists between wear and the SGV's. There are two difficulties associated with this system, the first is that the SGV's at low wear for the HVWO are much lower in magnitude than (and opposite in polarity from) the other systems investigated. The second difficulty stems from the fact that several of the systems investigated undergo severe corrosive wear, and hence, for example, low cylinder wear may be associated with low SGV's. Discounting these data, there is an indication of a trend towards decreased SGV's with increased wear. However, it is obvious that because of the comingling of competitive wear mechanisms under the wet air, steel-on-steel conditions it would be difficult to obtain a general, unambiguous relationship between wear and SGV's.

Based upon the evidence above, it appears that a relationship between wear and Self-Generated Voltages exists under dry air blanketing conditions. Under dry air conditions for the steel-on-steel system, it was pointed out that there are instances in which low cylinder wear is

associated with low SGV's. If these data are excluded from the smooth curves presented in Figs. 16 and 17 the relationship which is suggested is seen even more clearly, Figs. 21 and 22. It should be noted, however, that only a limited portion of the data obtained under wet air blanketing may be fit to this relationship.

5.2 Relationships Between SGV and Wear Mechanism

5.2.1 Mechanism of Voltage Generation Under Boundary Lubricated Conditions

This work was initiated in order to determine if relationships between wear, wear mechanism and SGV's exist. One aspect of this objective has been demonstrated, namely that a relationship exists between wear and SGV's under dry air atmospheres. Another particularly interesting and important aspect of this work was to demonstrate that wear mechanism, specifically surface fatigue wear, a process in which microcracks form either at or near the surface and thereafter propagate due to the repeated stress cycling, leads to the development of potential differences between the stationary and cyclically loaded members of a lubricated system. This would be consistent with, and therefore tend to confirm that a controlling primary reaction for surface fatigue wear is the electron transfer process, depicted schematically below.

$$M \longrightarrow M^{+\chi} + \chi e^{-} \qquad (1)$$

$$\text{Lubricant} + e^{-} \longrightarrow (\text{Lubricant} \cdot\cdot e)^{-} \qquad (2)$$

in which M is the metal surface. In the above scheme the reaction is written as liberating "χ" electrons. It is suggested that these "χ"

FIGURE 21

The Relationship Between Cylinder Wear and Self-Generated Voltages for the Steel System Under Dry Air Blanketing (Excluding Fluids exhibiting high Ball Wear)

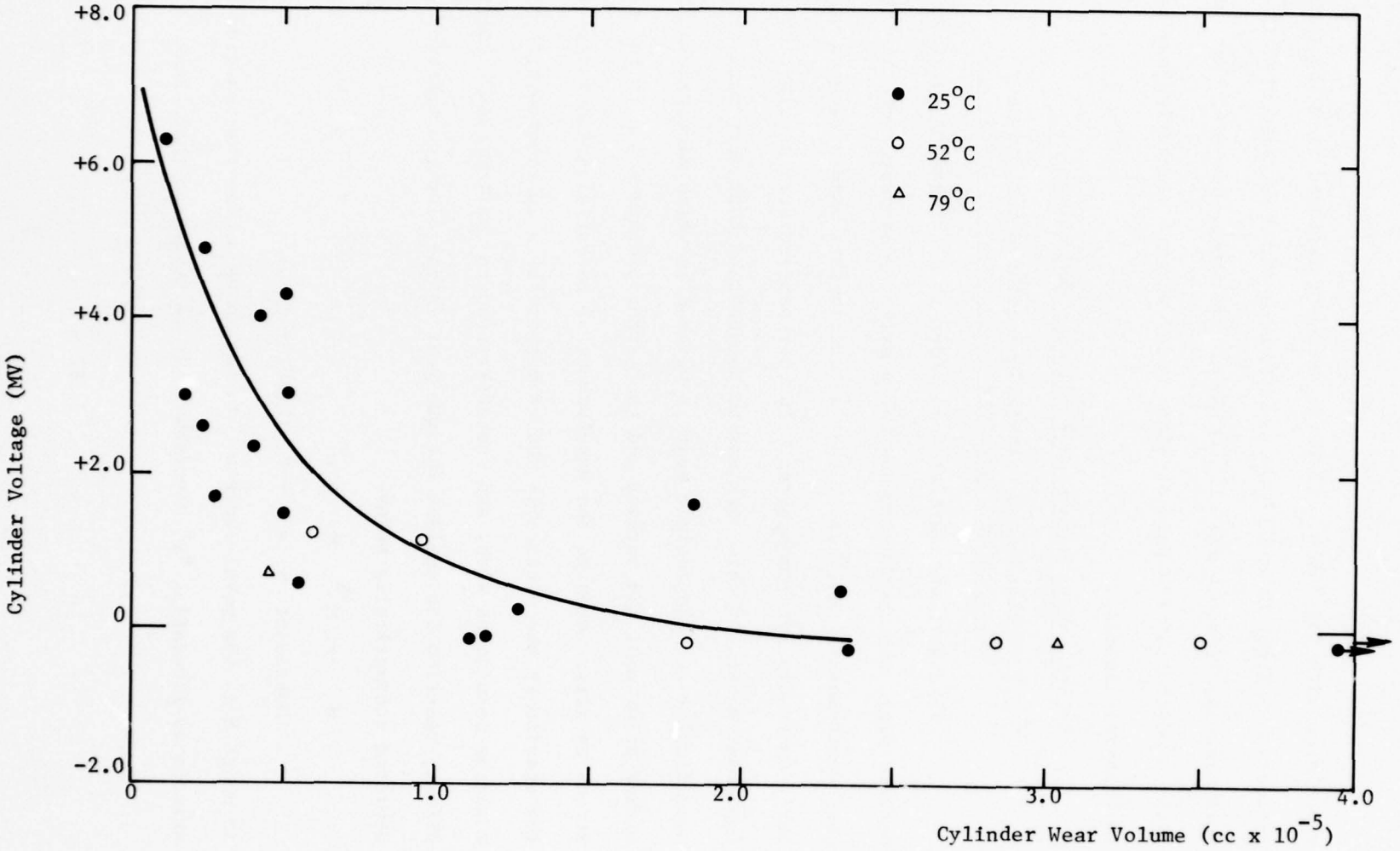

FIGURE 22

The Relationship Between Ball Wear and Self-Generated Voltages of the Steel System Under Dry Air Blanketing
(Excluding Fluids Exhibiting High Ball Wear)

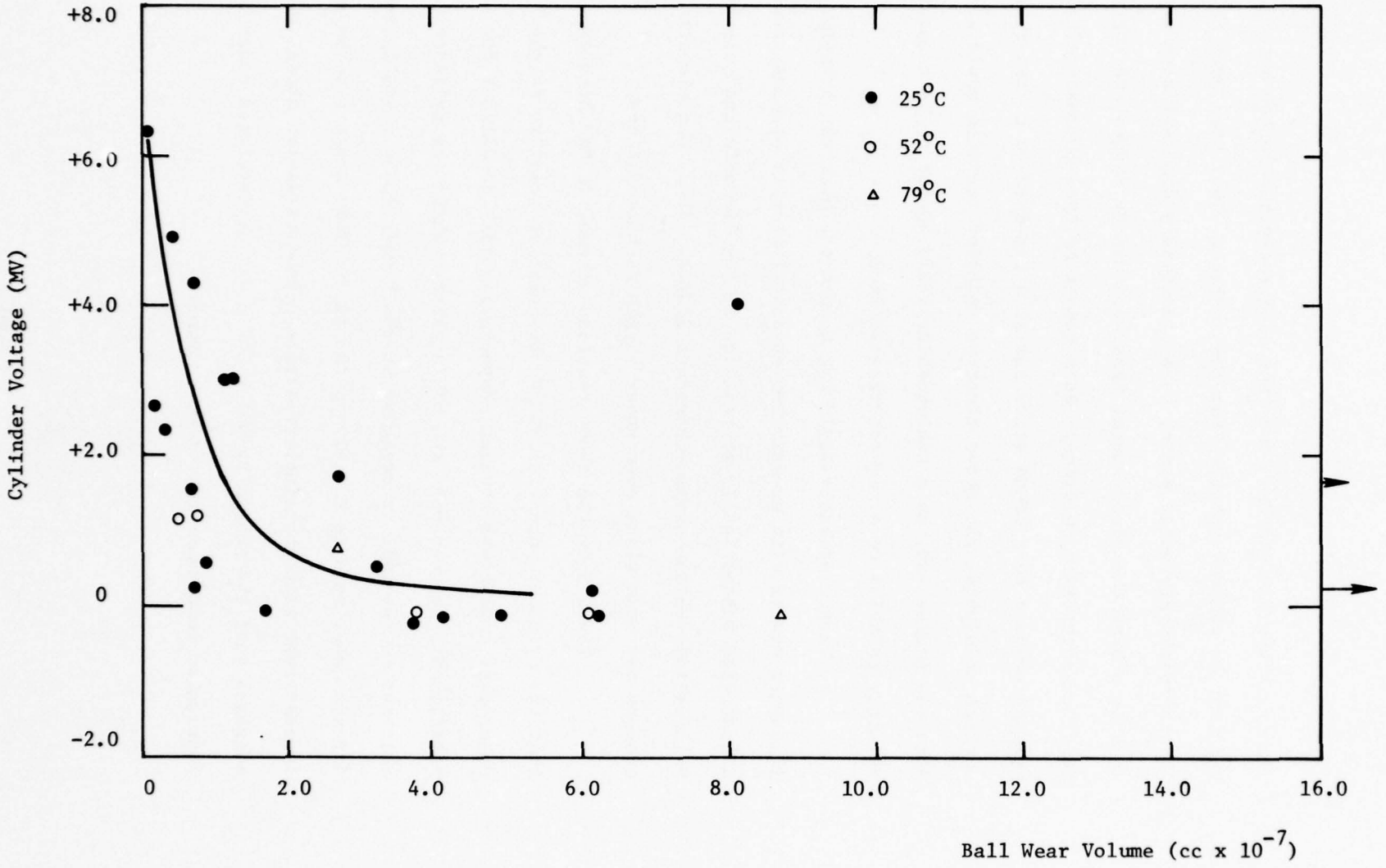

electrons are removed from the free electron-cloud in the metal. They need not be removed totally from the surface. They need only be placed into a relatively bound state, thus essentially demetallizing the surface. In this scheme therefore, metal ions need not be formed and therefore need not enter into solution. As a result of this movement of electrons from an unbound to a bound state and at times even to a free state, a surface undergoing the above electron transfer reaction would act as an electron source and, as a consequence, would appear to be negative in polarity relative to a non-reacting surface.

Oxygen probably would not quench the electron transfer process. If oxygen reacts with an adsorbed anionic lubricant species, such as illustrated schematically in reaction 2, the "transferred" electron could be localized on the oxygen-lubricant adduct. Thus, the electron transfer process may take place even under oxygen rich conditions.

Based upon the above reaction scheme, it had been expected that the cylinder potential would be negative relative to the ball under most conditions studied, especially under conditions for which a relationship between wear and SGV's exist. While the cylinder potential relative to the ball is negative at the higher loads investigated for the dry air case, this is not always the case. This appears to be somewhat inconsistent with the simple reaction scheme presented above, and therefore suggests that the scheme by which SGV's may be developed under boundary lubricated conditions may be more complex.

Reinforcing this idea that the single reaction scheme is not sufficient to explain how SGV's may be developed is the fact that the SGV's under wet air blanketing are in general of different polarity from that observed under dry air blanketing. Referring to Fig. 5 it is evident that the time dependent variation of the SGV's under these two atmospheres are also markedly different. The fact that the polarities of the cylinder are negative under wet air blanketing, a condition known to enhance oxidative or corrosive wear probably indicates that an oxidative electrochemical process should also be included in the reaction mechanism. Such an oxidative electochemical process leading to negative potentials of the reacting surface would probably be controlled by the electrochemical processes outlined below, reactions 3 and 4.

$$M \longrightarrow M^{a+} + ae^- \tag{3}$$

$$ae^- + \frac{a}{2} O_2 + aH_2O \longrightarrow 2aOH^- \tag{4}$$

Electrons are liberated via reaction 3, the metal oxidation step. The surface undergoing this process assumes a negative polarity since it behaves as an electron sink. The electrons may be consumed via a reduction step such as reaction 4. Under conditions in which the metal ions are not free to migrate away from the surface, an oxide/hydroxide film would grow on the metal surface. The net consequence of this oxidation-reduction process would be to cause the reacting test member to assume a negative polarity relative to the nonreacting surface.

There are, therefore, at least two primary electrochemical processes, the electron transfer and the oxidation processes, whereby SGV's may be developed under boundary lubricated conditions. These, as indicated above, are associated with two competitive fundamental wear processes, the surface fatigue wear process and the corrosive wear process, respectively. Therefore, in a wearing system both primary electrochemical processes may be operative simultaneously. Furthermore, it might be expected that the primary electrochemical process responsible for the cylinder wear and therefore the cylinder potential would be different from that encountered on the ball. The potential difference which is measured between the ball and the cylinder is, therefore, the resultant of the single cell potentials for each member. Since systems, in general, do not exhibit a single unique wear mode, it is readily understood that the correlation between wear and SGV's, the latter a function of the combined single cell processes, would exhibit some scatter. Furthermore, a clear relationship between SGV's and any single wear mechanism would be difficult to establish.

It is believed, but not proven, that the ball of the Ball-on-Cylinder device (the continuously loaded member) is susceptible primarily to corrosive wear, while the cylinder (the cyclically stressed member) is susceptible to both corrosive and surface fatigue wear. Thus, to a first approximation, a major change in SGV's for systems under study may be taken as an indication of a change in mechanism by which wear is occurring.

Two other wear mechanisms which are often encountered, adhesive wear and abrasive wear, would probably contribute to the SGV's via so called "second-order" processes. With either of these modes the primary removal of metal would probably not contribute to the SGVs. However, subsequent oxidation of the fresh, nascent metal surface may contribute to the voltage generated.

5.2.2 Oxygen Effects Upon SGV's

The fact that inerting the atmosphere, Argon tests, leads to near zero values for the SGV's, even under conditions in which surface fatigue damage, can also be explained. Based upon the discussion above, reasonably large SGV's might be expected under these circumstances. (Tests using Isostearic Acid in the HVLRO under inerted atmospheres fall into this category.)

It can be assumed that, at a minimum, a thin insulating oxide film is necessary in order to measure the SGV's. With such a film as might be measured under oxygenated atmospheres, a pseudostationary level for the SGV may be measured. However, under inerted atmospheres, the oxide films are sufficiently thin so that voltage discharge between the test member occurs frequently, and a measurable pseudoequilibrium value for the SGV is not established. Since SGV's cannot be measured under these inerted conditions, no relationship to wear can be established, even though electron transfer processes may still be important.

Several reports have appeared describing the relationship between exoelectron emission and wear in general and fatigue in particular. One striking similarity between the two phenomena of exoelectron emission and of SGV's is that, in general, both require

the presence of air (or oxygen) for their observation. Electron activation during the oxidation step is used to rationalize the need for oxygen in order to observe exoelectron emission. Perhaps, therefore, an alternate explanation for the absence of SGV's under inerted atmospheres is that oxygen is necessary in order to activate and free the electrons via chemical reaction.

5.2.3 Effects of Chemical Parameters Upon SGV's

Another set of data consistent with the relationship between wear mechanism and SGV's is obtained by determining the effects of variations in the chemical nature of the lubricant while maintaining the test system under otherwise similar conditions. A selection of data, taken from those presented in Tables 7 and 9, for several different base stocks which exhibit similar (although not identical) wear under identical operating conditions, Table 13, indicates that molecules which are better electron acceptors exhibit relatively more negative cylinder potentials.

The HVWO is the poorest electron acceptor and it, in general, exhibits the highest relative potentials. The polycyclic aromatics (present for example in the HVLRO) which behave as strong electron acceptors appear to lead to the lowest relative potentials. Of the esters tested, Di-2 Ethylhexyl Adipate, leads to potentials intermediate between the HVWO and the aromatics while the ester of pentaerythritol alcohol, Hercolube J, leads to more positive potentials. Of the two tested, the Hercolube J is expected to be the poorer electron acceptor at a freshly abraded surface because it is more sterically hindered and hence can not adsorb upon the metal surface as strongly as the other ester. Possibly

TABLE 13

Self-Generated Voltages for Systems Tested Under Similar Operating Parameters Exhibiting Similar Wear

Lubricant	Load (g)	Wear Volume Ball (cc)	Wear Volume Cylinder (cc)	Surface Fatigue Demerit Rating	Self-Generated Voltage (mv)	Report Table No.
Metallurgy: 52100 Steel-on-52100 Steel						
1-Methylnaphthalene	500	1.16×10^{-7}	0.50×10^{-5}	1	+3.0	7
HVWO	500	0.41×10^{-7}	0.24×10^{-5}	1	+4.9	7
HVLRO	500	0.18×10^{-7}	0.24×10^{-5}	1	+2.6	7
20/80 1-Methylnaphthalene/LVWO	1000	1.16×10^{-7}	0.17×10^{-5}	2	+3.0	7
HVWO	1000	0.71×10^{-7}	0.50×10^{-5}	1	+4.3	7
HVLRO	1000	0.30×10^{-7}	0.40×10^{-5}	1	+2.3	7
HVWO	2000	0.92×10^{-7}	0.54×10^{-5}	1+	+0.55	7
Di-2-Ethylhexyl Adipate	2000	0.71×10^{-7}	1.25×10^{-5}	1	+0.20	7
Hercolube J	2000	0.63×10^{-7}	0.50×10^{-5}	3	+1.50	7
HVLRO	2000	1.61×10^{-7}	1.15×10^{-5}	3	-0.06	7
HVWO	4000	3.77×10^{-7}	2.35×10^{-5}	3	-0.30	7
HVLRO	4000	4.10×10^{-7}	2.82×10^{-5}	3	-0.24	7
Metallurgy: 52100 Steel-on-Aluminum						
20/80 1-Methylnaphthalene/LVWO	1000	2.41×10^{-7}	0.17×10^{-5}	1	+2.6	11
HVWO	1000	1.45×10^{-7}	0.12×10^{-5}	1	+4.9	11
HVLRO	1000	1.03×10^{-7}	0.13×10^{-5}	1	+3.1	11
HVWO	2000	2.90×10^{-7}	0.18×10^{-5}	1	+3.8	11
HVLRO	2000	3.77×10^{-7}	0.30×10^{-5}	1	+1.9	11
HVWO	4000	4.83×10^{-7}	0.59×10^{-5}	1	+0.7	11
HVLRO	4000	4.83×10^{-7}	0.46×10^{-5}	1	+0.7	11

unexpected is that the Hercolube J leads to more positive potentials than the HVWO, perhaps reflecting some additional chemical influences at the surface. Thus, it appears that the relative magnitude (and polarity) of the SGV's are associated with an electrochemical process.

5.2.4 Other Parameter Effects Upon SGV's

Increased loads appear to promote relatively more negative cylinder potentials, however, because, in general wear rate increases with load, the effect is not readily apparent. The effect, if real, may be understood in terms of the "hot-spot" temperature at the surface. Since the rates for the processes probably depend upon $e^{-E_{act}/RT}$, and the activation energy (E_{act}) is probably around 110Kcal/mole for the electron transfer process, and only about 4 Kcal/mole for the oxidation process, it is evident that increased localized contact temperatures would accelerate the electron transfer process more than the oxidation process.

One parameter whose effect should be rationalized is water content. Presumably increased water promotes the electrochemical oxidation process, reactions 3 and 4, greatly. This accentuation of the electrochemical oxidation process is important on both the ball and the cylinder. Previously, it had been indicated that the electron transfer process is relatively more important for the cylinder, however, in the presence of substantial amounts of moisture, this is not the case, and the oxidation process is probably important. Thus, the cylinder's single cell (oxidation) potential with its greater surface area relative to the ball presumably dominates the overall system potential. Increased load may lead to increased importance of the electron transfer process on the

cylinder. This probably would lead to a decrease in the "oxidation" aspect of the cylinder single cell potential, and thereby a relatively more positive SGV.

5.3 Related Metallurgical Studies - Surface and Subsurface Defect Structure

It has been shown that a relationship exists between the SGV's and wear, and the two electrochemical processes which have been assumed to be operative, have been the oxidation process and the electron transfer process. Since either of these processes might be affected by the build-up of surface and subsurface stresses, it was decided to investigate what the role of such stress build-up on the cylinder might be in determining the relative magnitudes and polarities of the SGV's. It should be noted that stress build-up might affect on the one hand the oxidation process because of the increased lattice energy and on the other hand the electron transfer process because of the increased lattice misalignment which would increase the number density of the labile surface and near surface electrons.

In order to study the surface and subsurface defect structure, an X-ray technique in which lattice misalignment is determined by a shift in the size and intensity of the diffraction pattern arising due to a change in the number of coherently reflecting domains, as described in Appendix C. The systems which were investigated primarily were the steel-on-aluminum and aluminum-on-aluminum because the grain sizes of the aluminum cylinder test specimens are relatively large, and hence grain break up is readily assessed. The data presented in Table 14, and described in greater detail in Appendix C, in which β represents the overall rocking curve width,

TABLE 14

Effect of Wear Upon the Build-Up of Near Surface Strain

Lubricant	Metallurgy	Load (g)	Time (min)	Atmosphere	Ball Wear Scar Diameter (mm)	Ball Wear Volume (cc)	Track Cross Sectional Area (cm^2)	Cylinder Wear Volume (cc)	Self-Generated Voltage (mv)	β min of arc	β_m min of arc	$\Delta\psi$ min of arc
HVLRO	Steel/Aluminum	1000	30	Dry Air	0.28	0.48×10^{-7}	1.63	2.15×10^{-5}	-2.4	110.6	108	117.6
HVWO	Steel/Aluminum	1000	0.5	Dry Air	0.27	0.41×10^{-7}	2.72	3.59×10^{-5}	-0.03	115.1	120	126.6
HVLRO	Aluminum/Aluminum	1000	1	Wet Air	0.28	0.48×10^{-7}	1.33	1.76×10^{-5}	-0.01	117.9	120	140.4
HVLRO	Steel/Aluminum	1000	1	Dry Air	0.20	0.12×10^{-7}	0.14	0.18×10^{-5}	-15	97.5	96	112.2
HVLRO	Steel/Aluminum	1000	30	Wet Air	0.27	0.41×10^{-7}	0.03	0.04×10^{-5}	-300	89.4	90	99.1
UNWORN CYLINDER TRACK										85.3	84	77.4

β_m represents the median value of the rocking curve width and $\Delta\Psi$ represents the azimuthal spread, show that the surface and subsurface defect structure builds up very rapidly. Indeed, even when there is virtually no macroscopic wear, surface and subsurface deformation approach their higher damage values. In view of the large differences in the SGV's (Table 14) it is unlikely that there is a direct relationship between the SGV's and surface defect structure. It may be noted, however, that the measured increase in lattice misalignment appears to be correlated with the magnitude of wear.

6. CONCLUSIONS

This program, as described in the Technical Proposal entitled, "The Relationship Between Wear and Self-Generated EMF's During Sliding Under Conditions of Boundary Lubrication", has studied the interrelationship between Self-Generated Voltages and the operating parameters in a boundary lubricated system. The parameters which have been investigated include (1) the lubricant type, (2) metallurgy, (3) temperature, (4) load, (5) speed, (6) moisture, and (7) atmosphere.

Based upon these studies it has been determined that a relationship exists between wear and Self-Generated Voltages. The correlation between these two parameters is not exceptionally strong, however, part of this weakness is associated with the fact that the total wear measured in any system is probably the result of the wear due to any several competing fundamental wear mechanisms occurring simultaneously.

The work tends to indicate that relationships may exist between wear mechanisms and the relative SGV's since much of the experimental data may be rationalized if it is assumed that there are two primary electrochemical processes, the oxidation and the electron transfer processes, occurring under boundary lubricated conditions. The magnitude and polarity of the SGV's are then determined by the relative importance of these fundamental processes under the given set of operating parameters. It has been possible, in general, to explain how changes in operating variables would affect both the SGV's and wear, as well as wear character.

7. Presentation

I. L. Goldblatt, "Self-Generated Voltages Under Boundary Lubricated Conditions," presented at the International Conference on Fundamentals of Tribology, MIT, June 19-22, 1978.

APPENDIX A

EXXON MINI-STATIC TEST PROCEDURE

1. Scope

   1.1 This method is intended to measure the relative static electricity charging tendency of different filter/separator media and/or fuels.

2. Summary of Method

   2.1 The test involves the measurement of static electricity generated by the contact and separation of two dissimilar materials - fuel and filter. Ions of one sign are selectively absorbed on the charge separating surface - the filter, while those of opposite sign are separated and carried along with the flowing fuel. Separated charge is observed by measuring the current that flows to ground from the electrically isolated filter. Level of charge is influenced by filter surface area, filter composition, flow rate, fuel characteristics and impurities. By holding filter area and flow rate constant, charge level or charge density (charge per unit volume of fuel) becomes an indicator of relative charging tendency between fuels when using the same filter composition or between filter media when using the same fuel. In this test, a measured sample of fuel is forced by means of a syringe/plunger to flow through a filter at a constant flow rate using the mechanical drive of the Minisonic Separometer apparatus. Streaming current off the filter is measured in

microamperes (10^{-6} amperes) or nanoamperes (10^{-9} amperes) with a Keithley 600B Electrometer.

3. Apparatus

The apparatus consists of the following (Fig. 1A):

3.1 Keithley Electrometer - Model 600B.

3.2 Strip Chart Recorder - 1 volt full scale, center zero (e. g. Hewlett-Packard 7100 Model series)

3.3 Filter Holder - 13mm Dia stainless steel, Swinny, Millipore, Cat. No. NC/1 XX30 01200.

3.4 Valve - Hamilton Valve Co., Part No. 2LF1.

3.5 Receiver - Stainless steel beaker, 600 ml, Ace Chemical Co., Cat. No. 10-3430, EDP-NO-82.

3.6 Syringe/Plunger - Luer-Loc Plastipak Syringe, 50cc Becton, Dickinson and Co., Rutherford, N.J. (Fisher Scientific Co., Cat. No. 14-823-20).

3.7 Minisonic Separometer Syringe Drive - Emcee Electronics, Wilmington, Delaware. NOTE: Only the syringe drive, holder, and variable speed control power supply of the Minisonic Separator are required for this test.

3.8 Punch - 1/2" dia. Arch Punch (Gasket cutter) C. S. Osborne Co., Harrison, N.J.

3.9 Tweezers - suitable clean, dry tweezers shall be used at all times when handling the filter specimens.

3.10 Hard Plastic or Teflon Tubing - 1/16" I.D. approximately 12 to 18" long, Eastman Chemical Co.

FIGURE 1A

MINI-STATIC CHARGING TEST

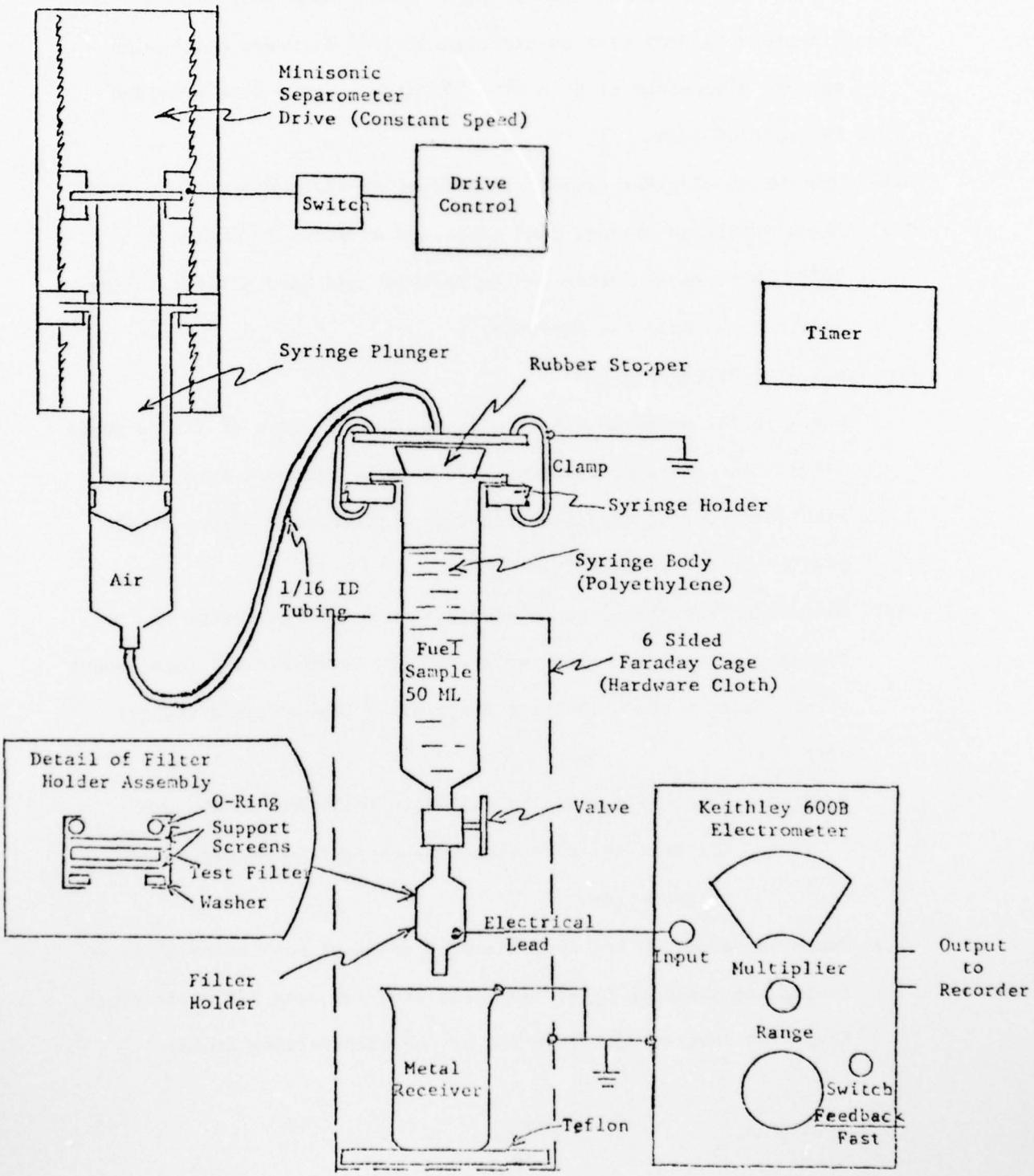

3.11 Rubber stopper to fit snuggly into fuel syringe body.

3.12 Appropriate clamps to hold stopper into syringe body.

3.13 Six-sided Faraday Cage constructed of 1/4" hardware cloth with approx. dimensions of 6" x 6" x 13" high - Entry door provided in front of cage.

3.14 Stop watch or timer capable of indicating elapsed time in seconds.

3.15 Above apparatus arranged and connected as shown in Figure 1.

NOTE: Electrical input lead to Keithley and hard plastic tubing should be as short as possible.

4. Preparation of Filter Media

4.1 Suitable filter media may be selected for any type of filter paper stock. In addition, specimens may also be prepared from new or used coalescer or separator paper type elements - either of the pleated or cylindrical form.

4.2 When using commercial paper elements, cut open cartridge to be tested using knife, scissors, and snips. Remove a 4-5 inch square of the media. Store in large evaporating dish covered tightly with foil.

Caution: Handle all media by the edges only, and do not use for test any part that has been soiled or contacted by the hands.

4.3 Punch out about 20 1/2-inch diameter disks of each material to be tested and place in Petri dish (one dish for each F/S media type). Keep dish covered except in the act of transferring disks.

5. Preparation of Test Apparatus

5.1 Cleaning of Fuel Syringe and Filter Holder. Between each test, thoroughly wash the fuel syringe body and entire holder with chloroform. Dry in a stream of dry nitrogen.

Caution: Let parts equilibrate to room temperature before reusing.

5.2 Filter. Load the filter holder base (lower portion) in the following order: flat Teflon washer, support screen, sample filter media, support screen and Teflon O-ring. Tape threads of top half - to prevent leakage by threads - using about 2-1/2 inches of 1/4-inch Teflon tape. Join halves together finger tight.

5.3 Apparatus

5.3.1 Check that fuel syringe holder and 600B are well grounded. Turn 600B on and allow sufficient time for instrument warm-up. Check batteries of Electrometer.

5.3.2 Adjust Minisonic Separometer drive potentiometer to obtain fuel flow rate of 100 ml/min. (30 seconds/50 ml) during test. Leave drive in UP position.

5.3.3 Apply (occasionally) silicone lubricant to air drive syringe plunger.

5.3.4 Center receiver under filter and connect to ground.

5.4 Syringe

5.4.1 Attach valve to fuel syringe body, turn off. Fill with test fuel to slightly above the 50 ml mark, insert stopper with tubing and place assembled syringe in holder. Clamp stopper to holder.

5.4.2 Attach filter and connect electrometer input to base (lower portion) of filter, avoiding strain on the connection.

5.4.3 OPEN THE VALVE.

6. Test Procedure

6.1 Zero the electrometer on the 0.01 multiplier, then set at 0.1 multiplier and 10^{-6} amp range or other settings if known. Unlock the test button.

6.2 Turn drive direction switch DOWN. Turn drive ON. Start timer when fuel level passes 50 ml mark.

6.3 After approximately 5 seconds set electrometer to best reading range using only the 0.1 or 0.3 multiplier but any current range.

Caution: At this point, remove hands and body from vicinity of filter holder, electrical leads, and Faraday Cage and avoid motion.

6.4 Mark the strip recording when the plunger reaches the 25 to 20 ml mark on the syringe.

6.5 At the end of the travel, turn the drive and timer off.

6.6 Measure the fuel temperature in the receiver.

6.7 Disassemble the syringe and filter holder as soon as possible after recording the data.

6.8 Obtain a repeat measurement by repeating all steps given in sections 5 and 6.

7. Record

7.1 Record the average value of streaming current, in microamperes, between the 25 and 20 ml marks for each run.

Multiplier

Current Range

Time for 50 ml of fuel to flow through the filter

Sample temperature in the receiver

8. Calculation and Report

8.1 Calculate the relative charging tendency of filter and/or fuel for each determination as follows:

$$Q = \frac{i}{v}$$

Where:

Q = Charge Density (microcoulombs/meter^3, $\mu C/m^3$ = μA seconds/m^3)

i = Streaming current (microamperes, μA)

v = Volumetric Flow Rate (meter^3/second, m^3/second)

8.2 Report the average charge density of the two determinations and the average sample temperature.

APPENDIX B

This section contains the data gathered during this program. It also contains a complete set of graphs which illustrate the time dependence of the Self-Generated Voltages for the systems investigated. It should be noted that not all of the data has been included and discussed in the report.

TABLE 1B

The Influence of Load Upon the Measured Wear and Self-Generated Voltages Under Dry Air Blanketing for the HVWO Using the 52100 Steel Metallurgy(1)

Load (g)	Ball Wear Scar Diameter (mm)	Ball Wear Volume (cc)	Track Cross Sectional Area (cm^2)(2)	Cylinder Wear Volume (cc)	Surface Fatigue Demerit Rating	Coefficient of Friction	Self-Generated Voltage (mv)	Apparent Film Resistance (Ohms)
200	0.13	0.08×10^{-7}	0.09	0.11×10^{-5}	1	0.15	+6.3	5×10^{4}
500	0.27	0.41×10^{-7}	0.18	0.24×10^{-5}	1	0.14	+4.9	10^{4}
1000	0.31	0.71×10^{-7}	0.38	0.50×10^{-5}	1	0.12	+4.3	10^{4}
2000	0.33	0.92×10^{-7}	0.41	0.54×10^{-5}	1+	0.14	+0.55	5×10^{2}
4000	0.47	3.77×10^{-7}	1.78	2.35×10^{-5}	3	0.18	-0.30	10

(1) Test Conditions: Ball-on-Cylinder device, loads as noted, 240 rpm, 25°C, 32 minutes.

(2) Ball Wear Volume = 7.73×10^{-3} $(WSD)^4$. Did not subtract the component of Plastic Deformation. Some calculations used throughout.

AD-A058 611 EXXON RESEARCH AND ENGINEERING CO LINDEN NJ PRODUCTS--ETC F/G 20/11
SELF-GENERATED VOLTAGES AND THEIR RELATIONSHIP TO WEAR UNDER BO--ETC(U)
JUL 78 I L GOLDBLATT N00014-75-C-1080
UNCLASSIFIED EXXON/RL.6PH.78 NL

2 OF 2
AD
A058611

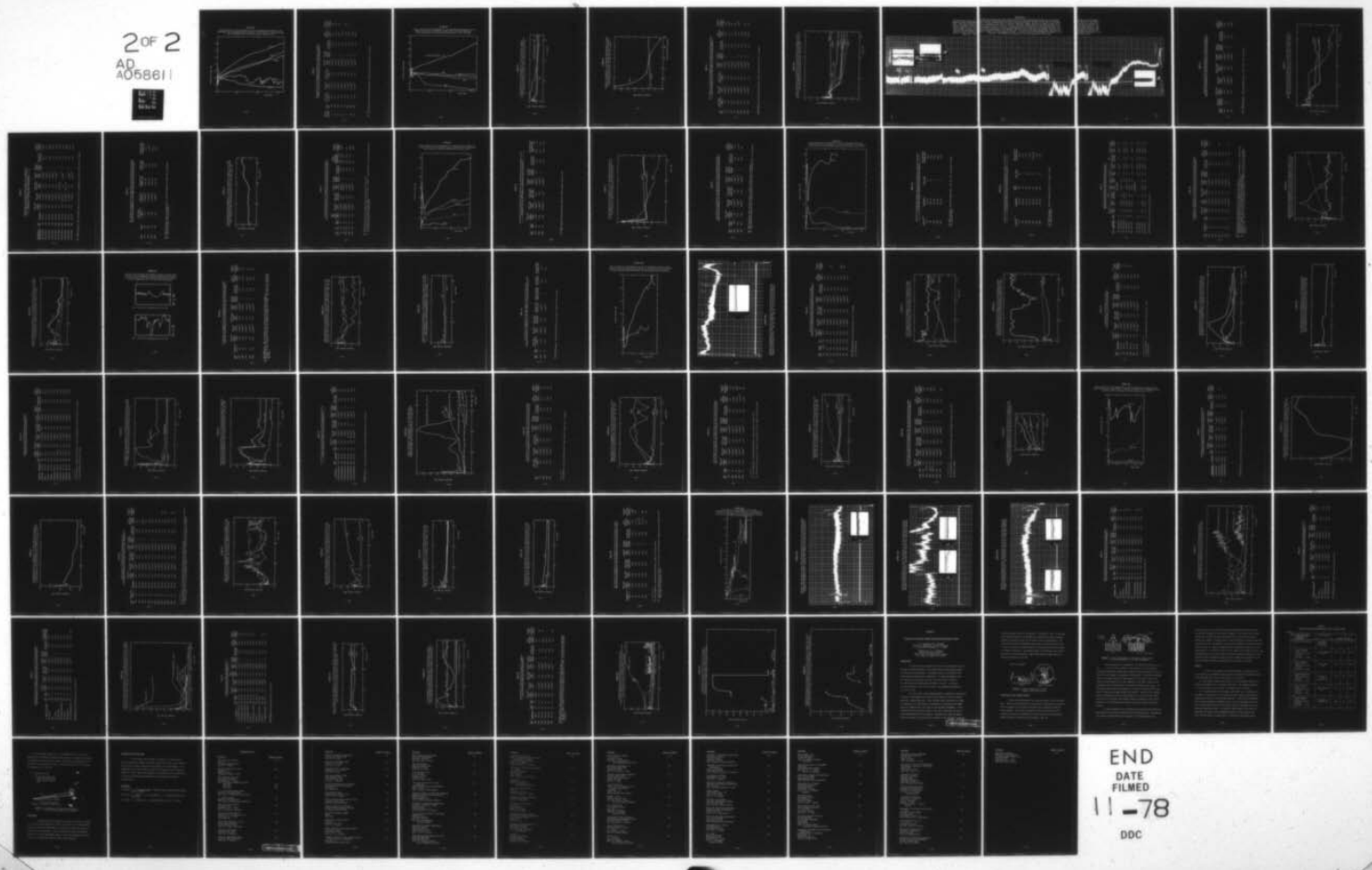

END
DATE FILMED
11-78
DDC

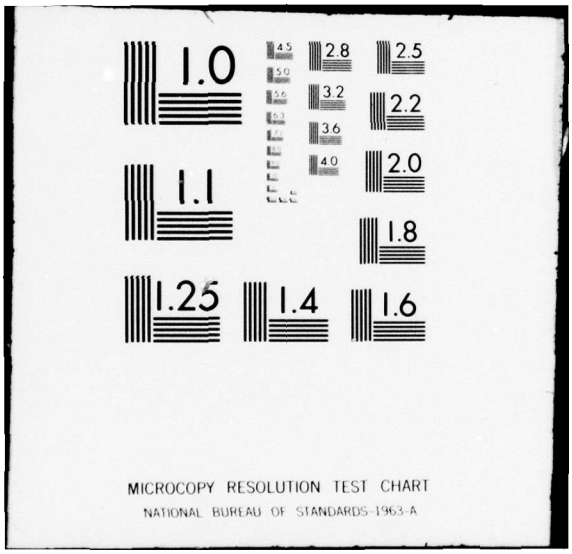
1.0
1.1
1.25
1.4
1.6
1.8
2.0
2.2
2.5
2.8
3.2
3.6
4.0
4.5
5.0
5.6
6.3
MICROCOPY RESOLUTION TEST CHART
NATIONAL BUREAU OF STANDARDS-1963-A

Figure 1B

Traces Showing the Time Dependence of the Self-Generated Voltages for the HVWO Under Dry Air Blanketing as a Function of Load Using the Steel Metallurgy (Test Conditions: Ball-on-Cylinder Device, 240 rpm, 25°C)

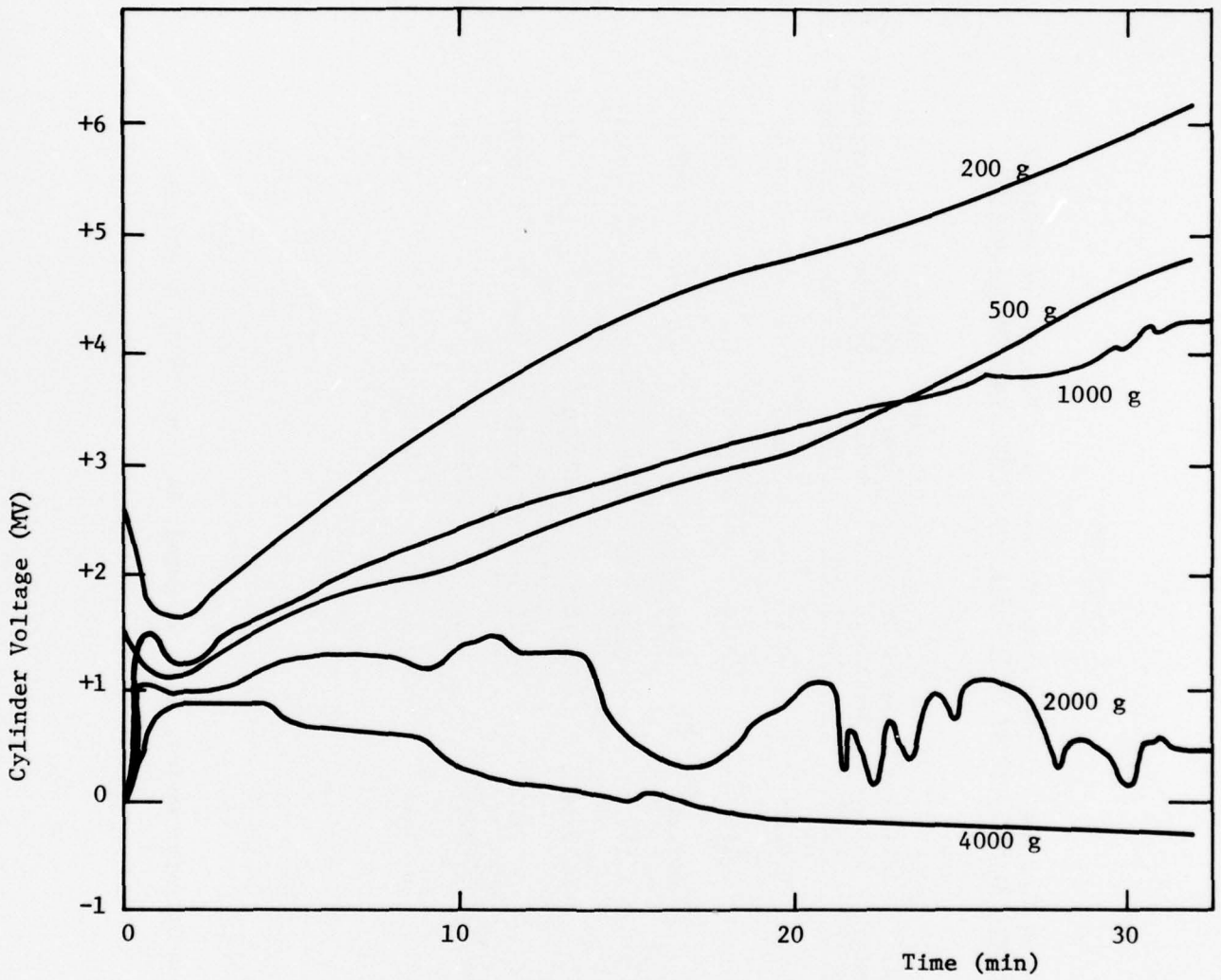

TABLE 2B

Measured Wear and Self-Generated Voltages as a Function of Moisture Content in Air for the HVWO Using the 52100 Steel Metallurgy(1)

Percent Relative Humidity	Load (g)	Ball Wear Scar Diameter (mm)	Ball Wear Volume (cc)	Track Cross Sectional Area (cm^2)	Cylinder Wear Volume (cc)	Surface Fatigue Demerit Rating	Coefficient of Friction	Self-Generated Voltage (mv)	Apparent Film Resistance (Ohms)
4	500	0.27	0.41×10^{-7}	0.17	0.22×10^{-5}	1	0.14	+4.9	10^4
30	500	0.35	1.16×10^{-7}	0.14	0.18×10^{-5}	1	0.13	+0.45	10^3
50	500	0.33	0.92×10^{-7}	0.25	0.33×10^{-5}	1	0.13	+0.15	10^3
66	500	0.35	1.16×10^{-7}	0.21	0.28×10^{-5}	1+	0.13	-0.24	
96	500	0.35	1.16×10^{-7}	0.18	0.24×10^{-5}	1	0.12	-1.59	10^3
4	4000	0.47	3.77×10^{-7}	0.41	0.54×10^{-5}	1+	0.18	-0.30	10
38	4000	0.55	7.07×10^{-7}	3.01	3.97×10^{-5}	1+	0.13	-0.09	
96	4000	0.58	8.75×10^{-7}	3.44	4.54×10^{-5}	1+	0.13	+0.30	

(1) Test Conditions: Ball-on-Cylinder device, loads as noted, 240 rpm, 25°C, 32 minutes.

Figure 2B

Traces Showing the Time Dependence of the Self-Generated Voltages for the HVWO as a Function of Moisture Content Using the Steel Metallurgy (Test Conditions: Ball-on-Cylinder Device, 500 g, 25°C, 240 rpm)

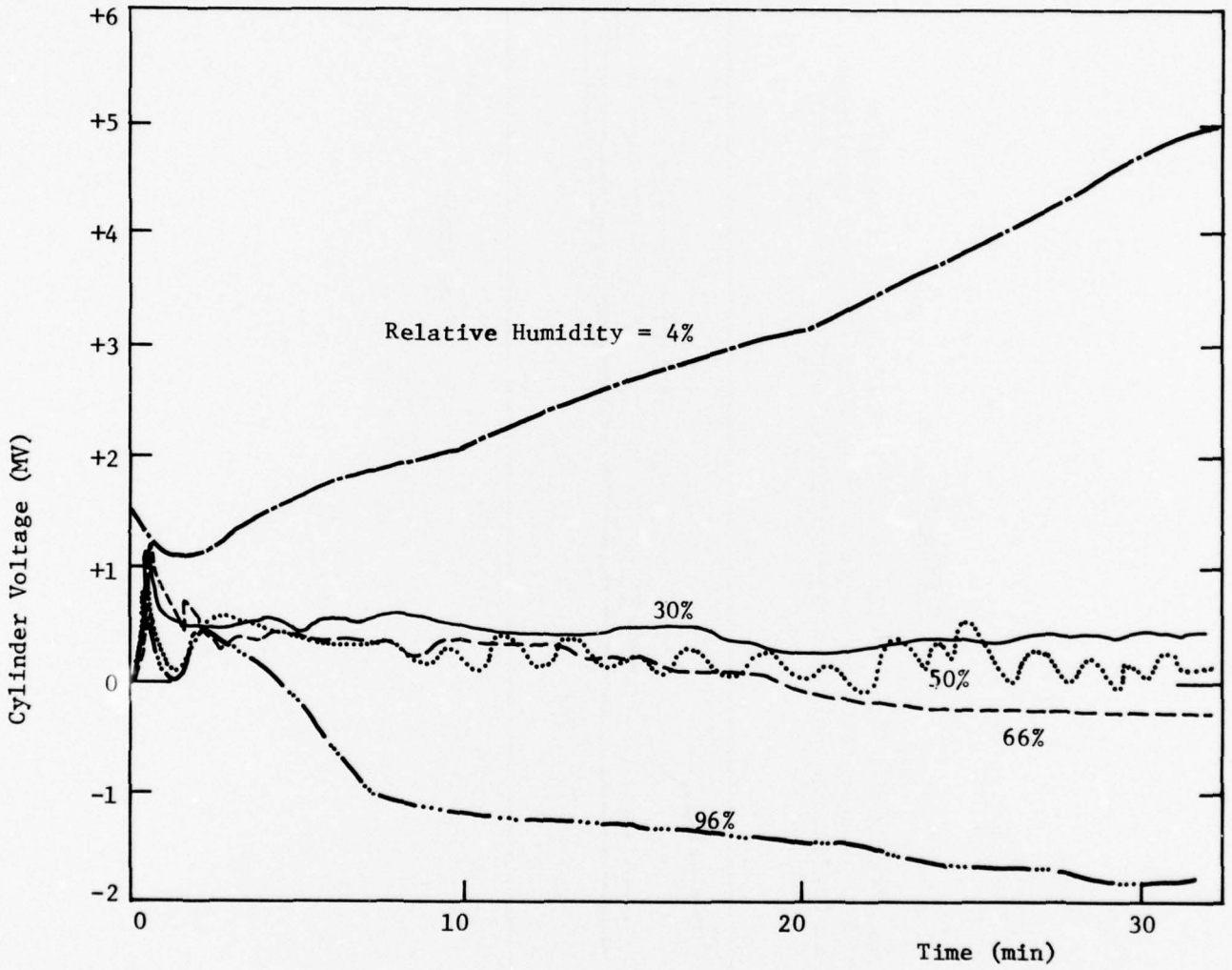

FIGURE 3B

Traces Showing the Time Dependence of the Self-Generated Voltages for the HVWO as a Function of Moisture Level Using the Steel Metallurgy (Test Conditions: Ball-on-Cylinder Device, 4000 g, 240 rpm, 25°C)

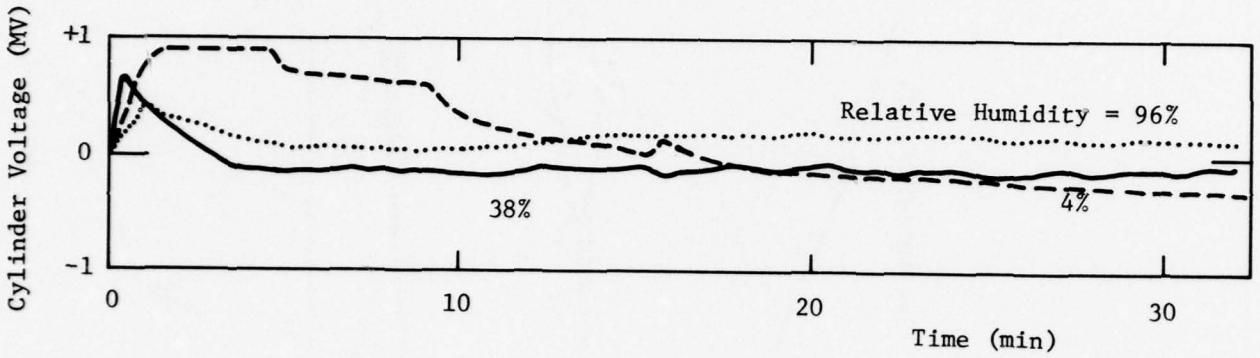

FIGURE 4B

Influence of Humidity in Air Upon the Self-Generated Voltages for the HVWO Using the Steel Metallurgy (Test Conditions: Ball-on-Cylinder Device, 240 rpm, 25°C, 32 minutes)

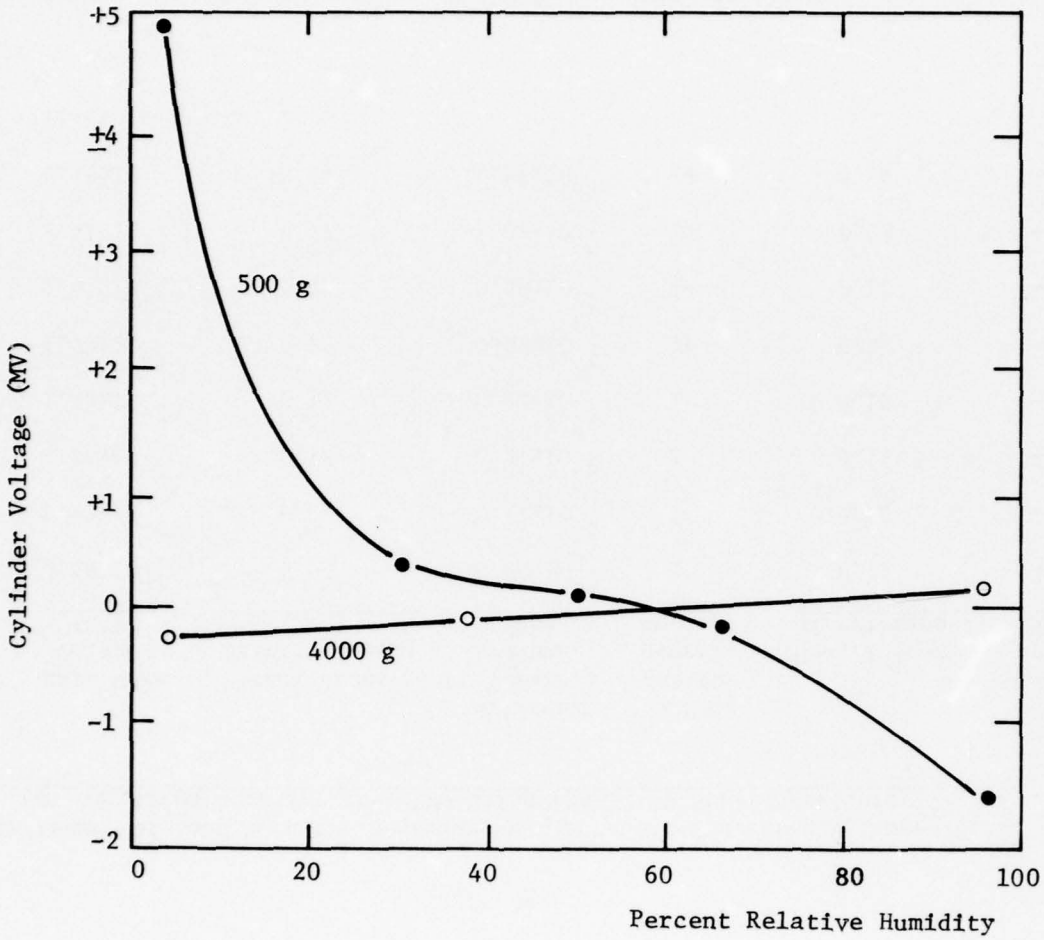

TABLE 3B

The Influence of Load Upon the Measured Wear and Self-Generated Voltages Under Wet Air Atmosphere for the HVWO Using the 52100 Steel Metallurgy(1)

Load (g)	Ball Wear Scar Diameter (mm)	Ball Wear Volume (cc)	Track Cross Sectional Area (cm^2)	Cylinder Wear Volume (cc)	Surface Fatigue Demerit Rating	Coefficient of Friction	Self-Generated Voltage (mv)	Apparent Film Resistance (Ohms)
200	0.28	0.48×10^{-7}	0.05	0.08×10^{-5}	1	0.13	-0.84	5×10^{3}
350	0.33	0.92×10^{-7}	0.09	0.12×10^{-5}	1	0.12	-1.5	5×10^{3}
500	0.35	1.16×10^{-7}	0.18	0.24×10^{-5}	1	0.12	-1.8	10^{4}
700	0.37	1.45×10^{-7}	0.17	0.22×10^{-5}	1	0.13	-2.19	10^{4}
1000	0.40	1.98×10^{-7}	0.25	0.33×10^{-5}	1+	0.12	-1.38	5×10^{3}
1500	0.38	1.61×10^{-7}	0.40	0.53×10^{-5}	1+	0.12	-0.90	
2000	0.42	2.41×10^{-7}	0.77	1.02×10^{-5}	1+	0.13	+0.15	10^{3}
4000	0.53	6.10×10^{-7}	3.44	4.54×10^{-5}	1+	0.14	+0.30	10^{2}

Test Conditions: Ball-on-Cylinder device, loads as noted, 240 rpm, 25°C, 32 minutes.

FIGURE 5B-a

Traces Showing the Time Dependence of the Self-Generated Voltages for the HVWO Under Wet Air Blanketing as a Function of Load Using the Steel Metallurgy (Test Conditions: Ball-on-Cylinder Device, 240 rpm, 25°C)

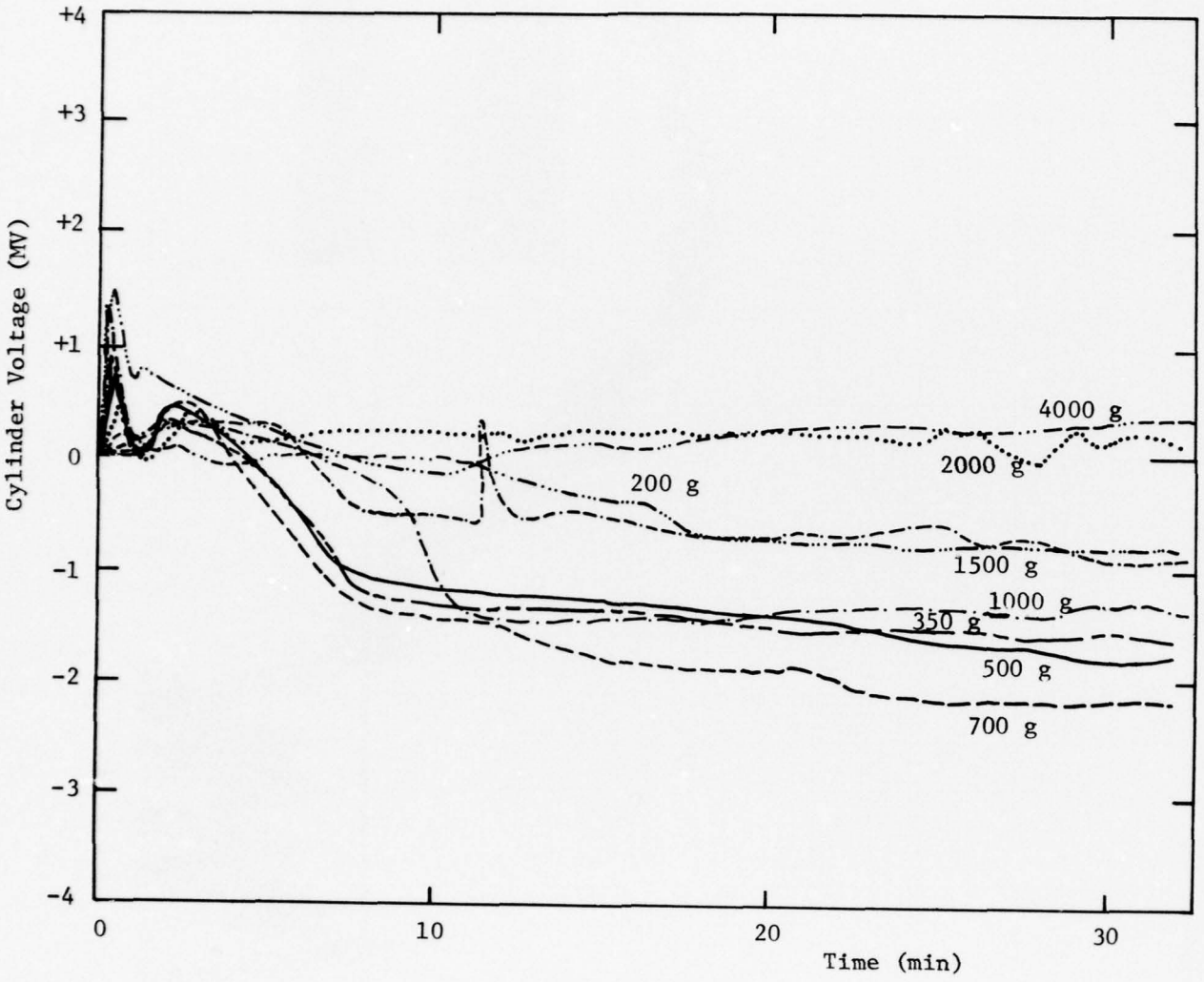

Recorder Trace Showing the A
Showing the Near Instantaneou
Load. (The Upper (Broad Tra
(Contact Potential) and is S
Zero for Which is Set at 10
Factors Which Accompany the
and the Associated Range of
Regions for Which the Oscill
Base Line. The

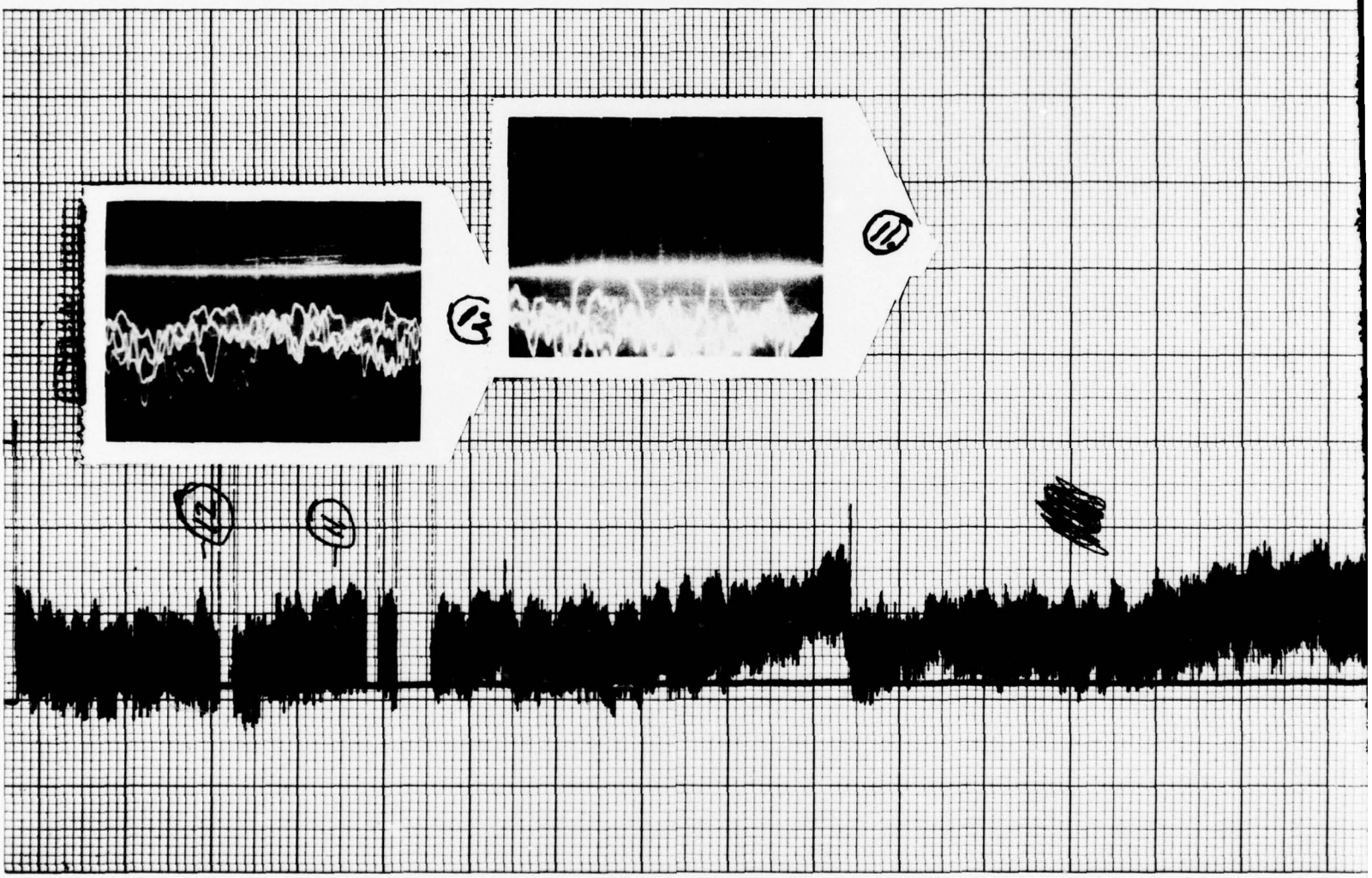

FIGURE 5B-b

order Trace Showing the Actual Time Variation of the Self-Generated Voltage and Oscillograms ing the Near Instantaneous Variations of the Self-Generated Voltage for the Test at the 1000 g d. (The Upper (Broad Trace) is the Self-Generated Voltage, the Zero for Which is Noted as CP ntact Potential) and is Set at 50 Units. The Lower (Narrow Trace) is the Friction Force, the o for Which is Set at 10 Units. The Calibration for the Friction is 10 g/Small Division. The tors Which Accompany the Self-Generated Voltage Trace Indicate the Electrometer Switch Setting d the Associated Range of the Recorder Used. The Letter and Number Designations Identify the ions for Which the Oscillograms Are Given. The Full Line on the Oscillograms Correspond to the Base Line. The Sensitivity Settings for the Oscillograms were 100 mv/cm.)

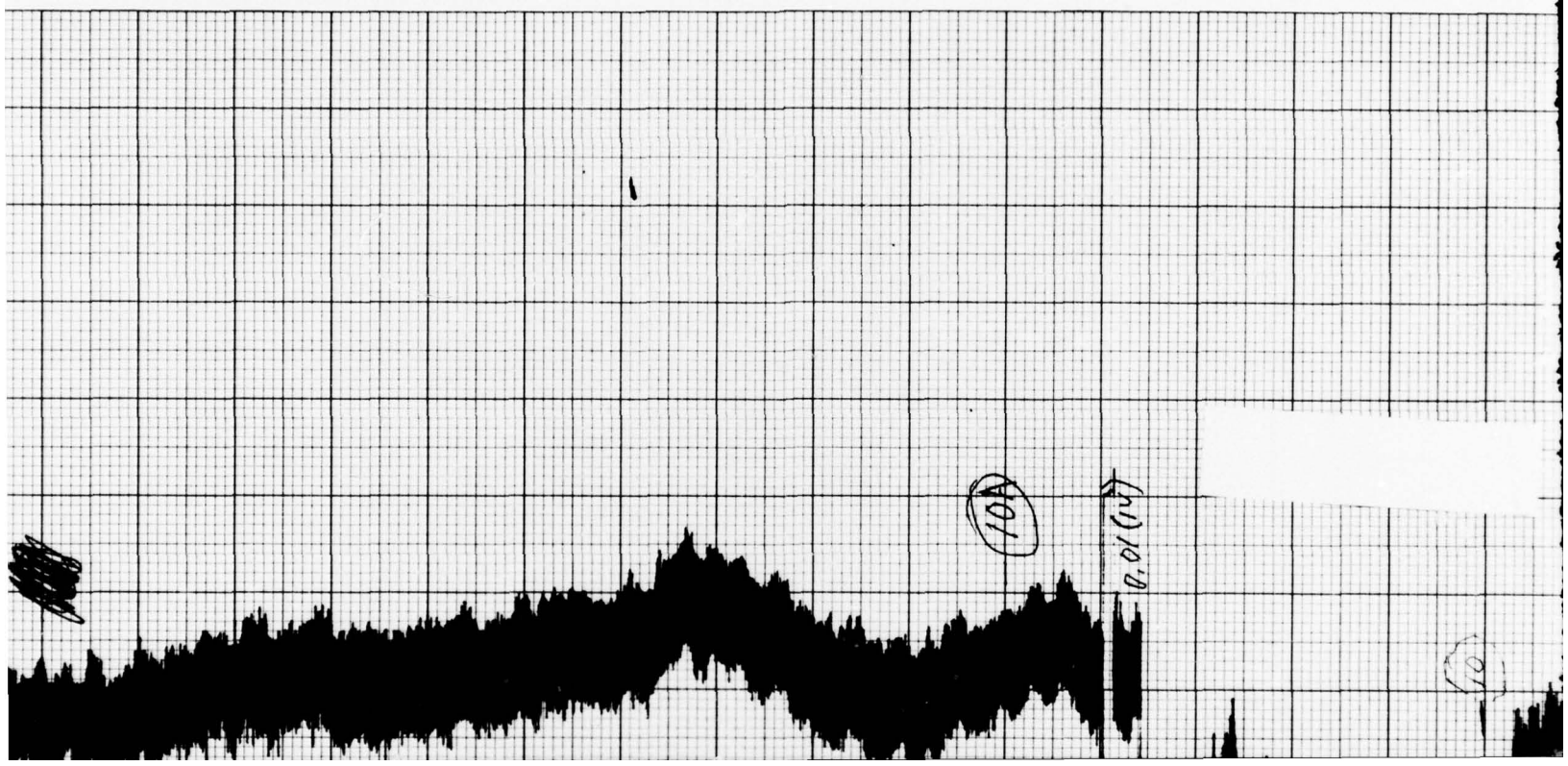

'oltage and Oscillograms
'or the Test at the 1000 g
for Which is Noted as CP
the Friction Force, the
10 g/Small Division. The
.ectrometer Switch Setting
)esignations Identify the
.llograms Correspond to the
:re 100 mv/cm.)

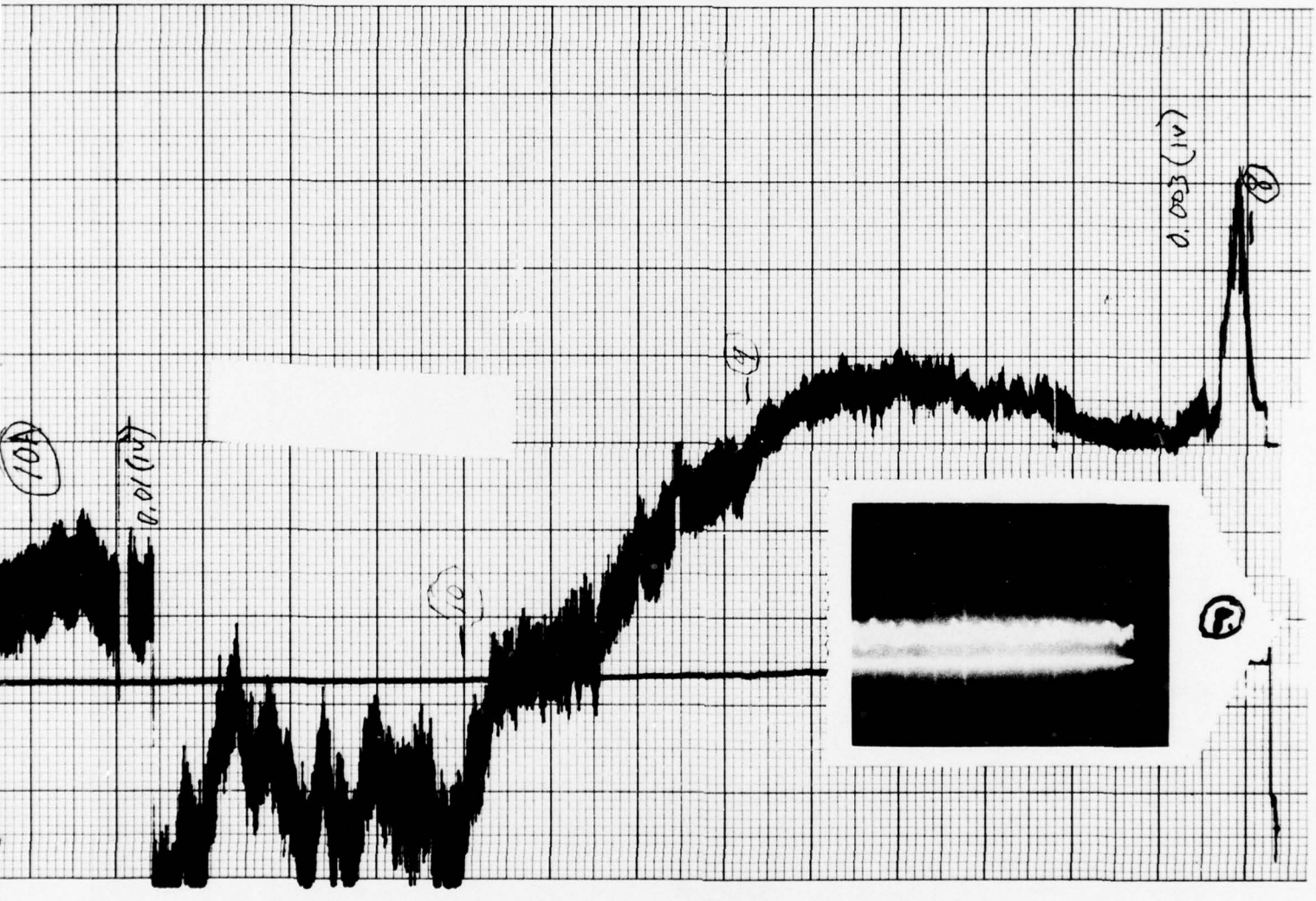

TABLE 4B

Measured Wear and Self-Generated Voltages as a Function of Speed
Under Wet Air Blanketing for the HVWO Using the 52100 Steel Metallurgy(1)

Speed (rpm)	Relative Distance Traveled	Ball Wear Scar Diameter (mm)	Ball Wear Volume (cc)	Track Cross Sectional Area (cm^2)	Cylinder Wear Volume (cc)	Surface Fatigue Demerit Rating	Coefficient of Friction	Self-Generated Voltage (mv)
100	1.0	0.47	3.77×10^{-7}	0.30	0.40×10^{-5}	1	0.15	-3.0
240	1.2	0.40	1.98×10^{-7}	0.25	0.33×10^{-5}	1+	0.12	-1.38
600	3	0.33	0.92×10^{-7}	0.18	0.24×10^{-5}	1	0.12	-0.69

(1) Test Conditions: Ball-on-Cylinder device, 1000 g load, 25°C, 32 minutes.

FIGURE 6B

Traces Showing the Time Dependence of the Self-Generated Voltages for the HVWO Under Wet Air Blanketing as a Function of Speed Using the Steel Metallurgy (Test Conditions: Ball-on-Cylinder Device, 1000 g load, 240 rpm, 25°C)

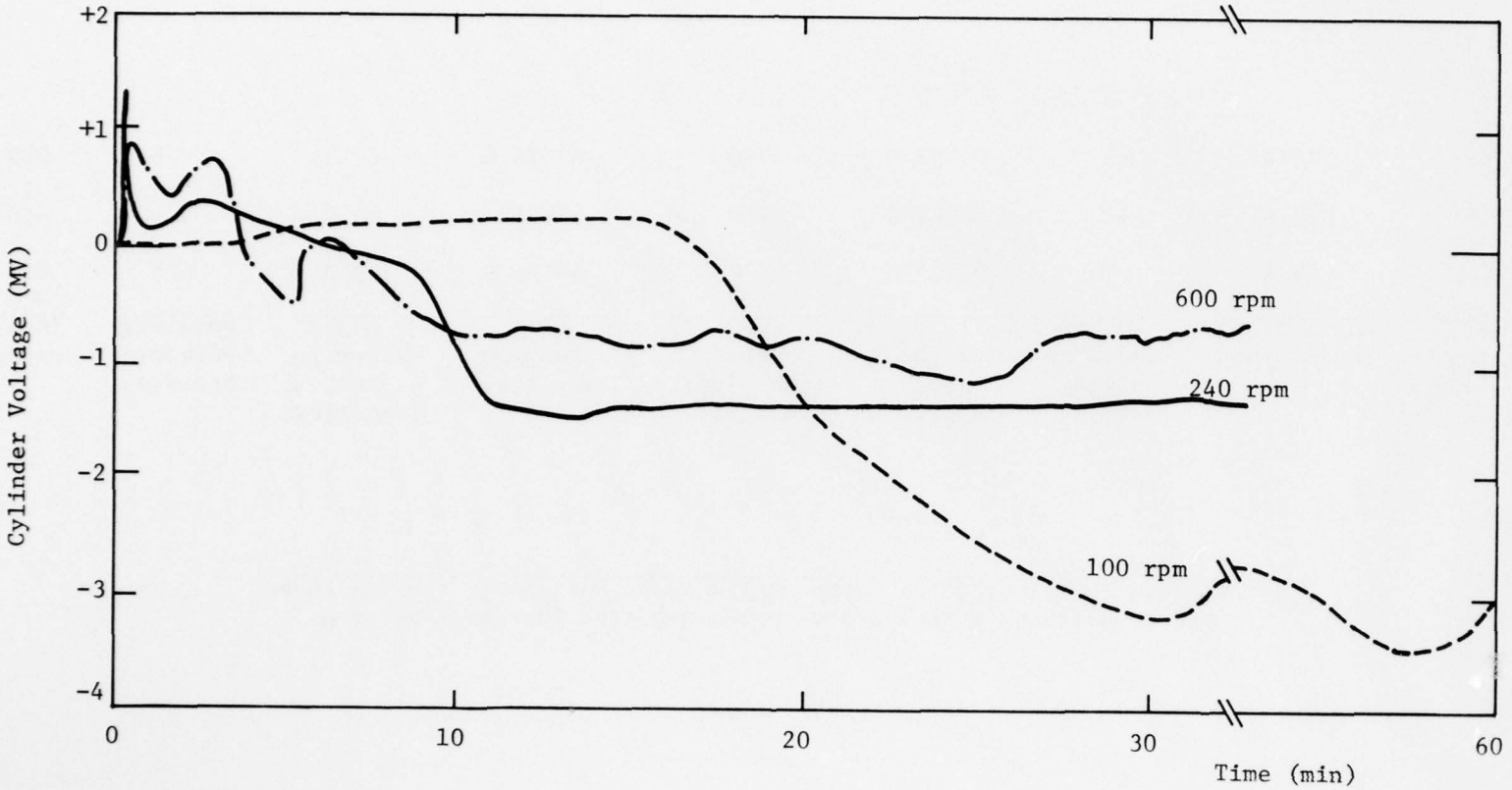

TABLE 5B

Measured Wear and Self-Generated Voltages for the HVWO Using Copper Based Balls Sliding on 52100 Steel Cylinders Under Conditions of Varying Load and Atmosphere

Metallurgy (Ball/Cylinder)	Load (g)	Atmosphere	Ball Wear Scar Diameter (mm)	Ball Wear Volume (cc)	Track Cross Sectional Area (cm^2)	Cylinder Wear Volume (cc)	Surface Fatigue Demerit Rating	Coefficient of Friction	Self-Generated Voltage (mv)
SAE 65/52100	200	Wet Air	0.48	4.10×10^{-7}	0.06	0.89×10^{-5}	1	0.15	+0.02
SAE 65/52100	200	Dry Air	0.50	4.83×10^{-7}	0.09	1.19×10^{-5}	1	0.15	+0.27
Copper/52100	200	Wet Air	0.98	71.30×10^{-7}	0.30	3.9×10^{-5}	3	0.11	+0.02
Copper/52100	200	Dry Air	0.90	50.72×10^{-7}	0.05	0.66×10^{-5}	3	0.12	+0.02
SAE 65/52100	1000	Wet Air	0.57	8.16×10^{-7}	<0.09	$<1.19 \times 10^{-5}$	3	0.15	+0.05
SAE 65/52100	1000	Dry Air	0.52	5.65×10^{-7}	Very Small	--	--	0.13	-0.03
Copper/52100	1000	Wet Air	1.48	370.87×10^{-7}	0.23	3.04×10^{-5}	3	0.13	-0.02
Copper/52100	1000	Dry Air	1.53	423.59×10^{-7}	Very Small	--	3	0.13	+0.02
SAE 65/52100	4000	Wet Air	0.68	16.53×10^{-7}	0.42	5.54×10^{-5}	1	0.17	+0.15
SAE 65/52100	4000	Dry Air	0.75	24.46×10^{-7}	0.49	6.47×10^{-5}	3	0.16	+0.15

(1) Test Conditions: Ball-on-Cylinder device, loads as noted, atmospheres as noted, 240 rpm, 25°C, 32 minutes.

TABLE 6B

The Influence of Speed Upon the Measured Wear and Self-Generated Voltages Under Wet Air Atmosphere for the HVWO Using Copper-on-Steel Metallurgy[1]

Load	Speed	Ball Wear Scar Diameter (mm)	Ball Wear Volume (cc)	Cylinder Wear Volume (cc)	Coefficient of Friction	Self-Generated Voltage (mv)
250	240	0.70	18.56×10^{-7}	Very low	0.11	0.0
250	600	0.68	16.53×10^{-7}	Very low	0.06	+1.2[2]
1000	50	1.00	77.30×10^{-7}	Very low	0.15	+0.01
1000	240	0.87	44.28×10^{-7}	Very low	0.07	-0.03

(1) Test Conditions: Ball-on-Cylinder device, loads and speeds as noted, 25°C, 33 minutes.
(2) The SGV is high at the high speed.

FIGURE 7B

Trace Showing the Time Dependence of the Self-Generated Voltage for the HVWO Under Wet Air Blanketing Using an SAE 65 Bronze Ball on a 52100 Steel Cylinder (Test Conditions: Ball-on-Cylinder Device, 250 g Load, 600 rpm, 25°C)

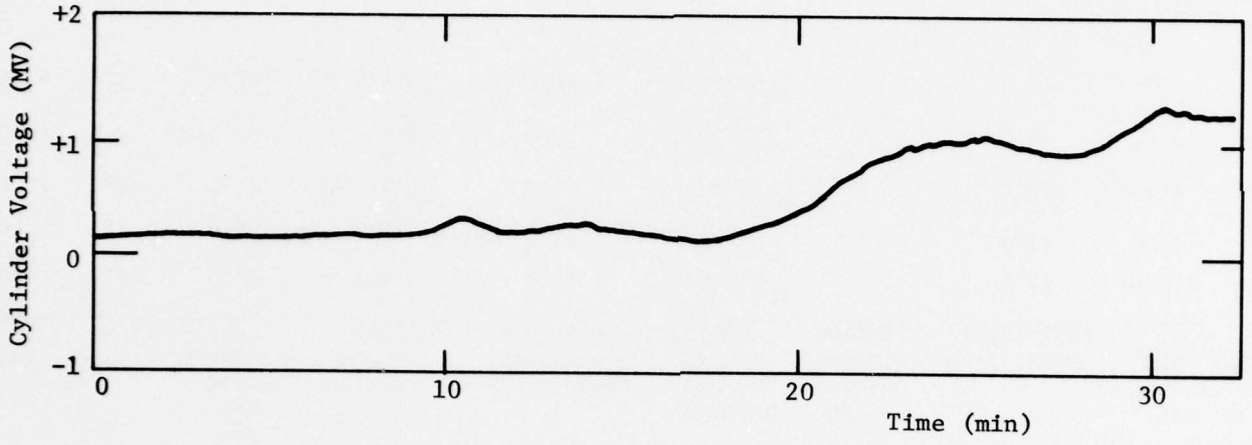

TABLE 7B

The Influence of Load Upon the Measured Wear and Self-Generated Voltages Under Dry Air Atmosphere for the HVWO Using An Aluminum-on-Steel Metallurgy(1)

Load (g)	CLA (μ)	Time (min)	Ball Wear Scar Diameter (mm)	Ball Wear Volume (cc)	Track Cross Sectional Area (cm^2)	Cylinder Wear Volume (cc)	Surface Fatigue Demerit Rating	Coefficient of Friction	Self-Generated Voltage (mv) Time (min) 16	32	Apparent Film Resistance (Ohms)
200	0.13	32	0.30	0.63×10^{-7}	0.07	0.09×10^{-5}	1	0.15	+10.8	+14.1	5×10^{6}
500	0.23	32	0.40	1.98×10^{-7}	0.17	0.22×10^{-5}	1	0.12	+2.1	+2.5	
1000[2]	0.13	32	0.37	1.45×10^{-7}	0.09	0.12×10^{-5}	1	0.13	+4.9	+6.0	10^{5}
2000	0.13	32	0.44	2.90×10^{-7}	0.14	0.18×10^{-5}	1	0.15	+3.8	+4.8	5×10^{3}
4000	0.16	16	0.50	4.83×10^{-7}	0.35	0.46×10^{-5}	1	0.17	+0.7	--	5×10^{2}

(1) Test Conditions: Ball-on-Cylinder Device, loads as noted, 240 rpm, 25°C.

(2) A 16 min test gave a Ball Wear Scar Diameter of 0.37 mm, or 1.45×10^{-7} cc Ball Wear and a Track Cross Sectional area of 0.14 cm^2 or 0.18×10^{-5} cc Cylinder Wear.

FIGURE 8B

Traces Showing the Time Dependence of the Self-Generated Voltages for the HVWO Under Dry Air Blanketing Using an Aluminum-on-Steel Metallurgy (Test Conditions: Ball-on-Cylinder Device, 240 rpm, 25°C)

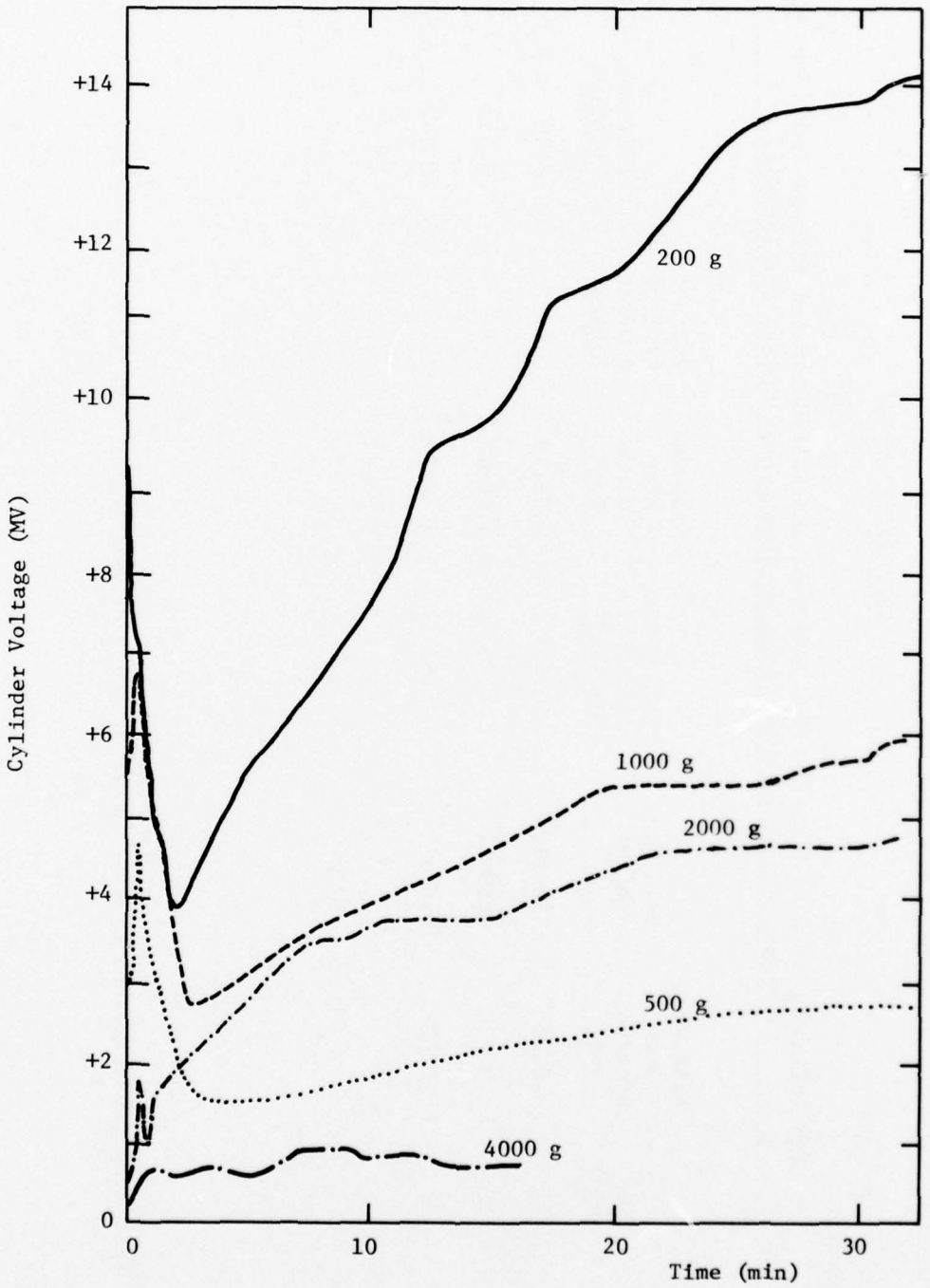

TABLE 8B

The Influence of Load Upon the Measured Wear and Self-Generated Voltage Under Wet Air Atmosphere for the HVWO Using an Aluminum-on-Steel Metallurgy(1)

Load (g)	Time (min)	Ball Wear Scar Diameter (mm)	Ball Wear Volume (cc)	Track Cross Sectional Area (cm^2)	Cylinder Wear Volume (cc)	Surface Fatigue Demerit Rating	Coefficient of Friction	Self-Generated Voltage (mv) 16	32
200	32	0.38	1.61×10^{-7}	0.44	0.58×10^{-5}	1+	0.15	+0.24	-1.0
1000	32	0.50	4.83×10^{-7}	1.06	1.40×10^{-5}	3	0.12	+1.2	+1.3
2000	32	0.60	10.02×10^{-7}	1.67	2.20×10^{-5}	2	0.14	+0.72	+1.25

(1) Test Condition: Ball-on-Cylinder Device, loads as noted, 240 rpm, 25°C.

FIGURE 9B

Traces Showing the Time Dependence of the Self-Generated Voltages for the HVWO Under Wet Air Blanketing Using an Aluminum-on-Steel Metallurgy (Test Conditions: Ball-on-Cylinder Device, 240 rpm, 25°C)

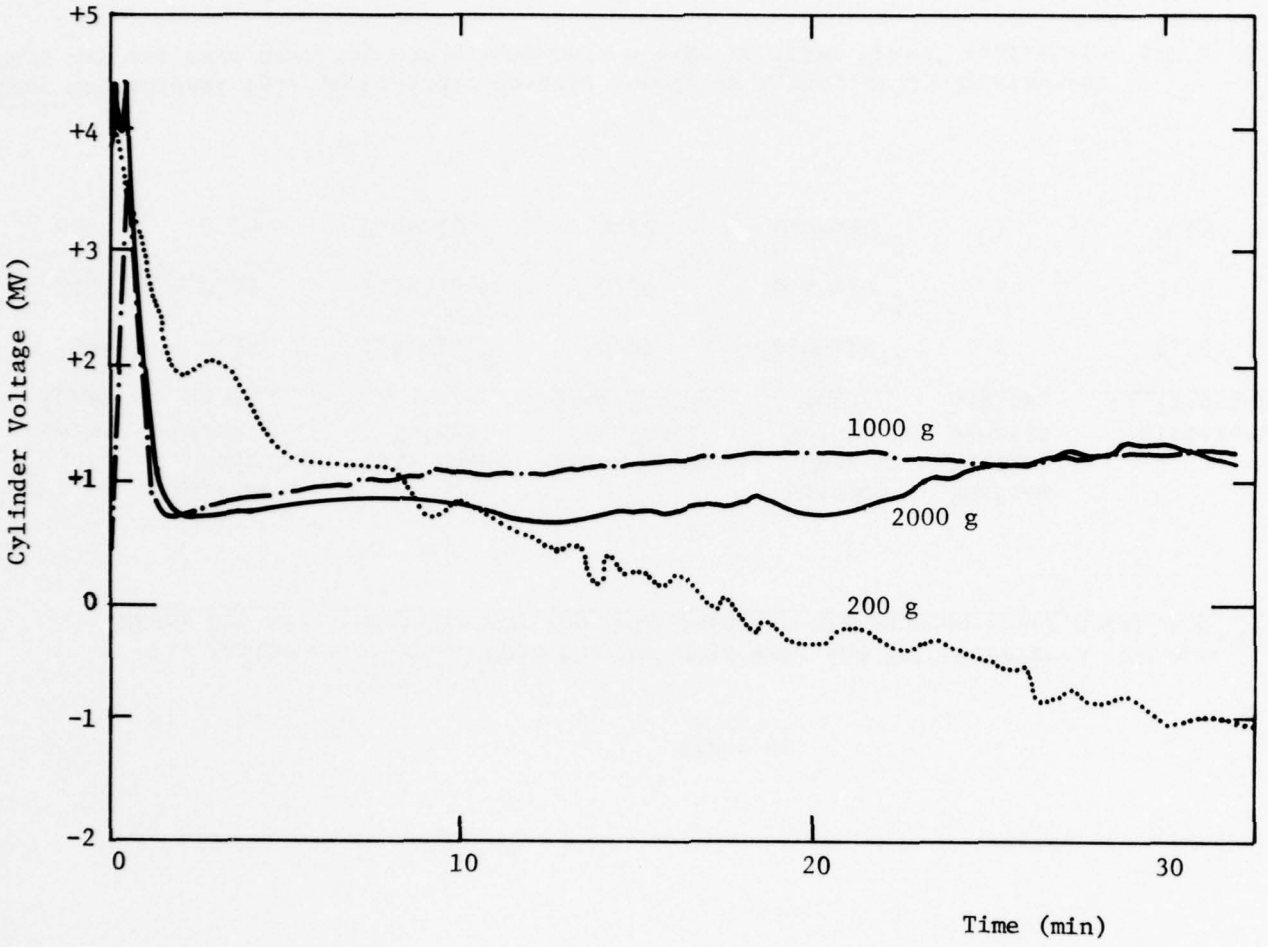

TABLE 9B

The Influence of Speed Upon the Measured Wear and Self-Generated Voltages Under Dry Air Atmosphere for the HVWO Using An Aluminum-on-Steel Metallurgy[1]

Load (g)	Speed (rpm)	Ball Wear Scar Diameter (mm)	Ball Wear Volume (cc)	Track Cross Sectional Area (cm^2)	Cylinder Wear Volume (cc)	Surface Fatigue Demerit Rating	Coefficient of Friction	Self-Generated Voltage (mv)
1000	50[2]	0.38	1.61×10^{-7}	0.07	0.09×10^{-5}	1	0.16	+ 0.2
1000	240	0.35	1.16×10^{-7}	0.30	0.40×10^{-5}	1	0.16	+ 2.6
1000	600	0.28	0.48×10^{-7}	0.18	0.24×10^{-5}	1	0.16	+12

(1) Test Conditions: Ball-on-Cylinder device, speeds as noted, 25°C, 32 minutes.
(2) Test may not have been run for a long enough time to allow "near" equilibrium SGV's to be attained.

Figure 10B

Traces Showing the Time Dependence of the Self-Generated Voltages for the HVWO Under Dry Air Blanketing as a Function of Speed for the Aluminum-on-Steel Metallurgy (Test Conditions: Ball-on-Cylinder Device, 100 g, 25°C)

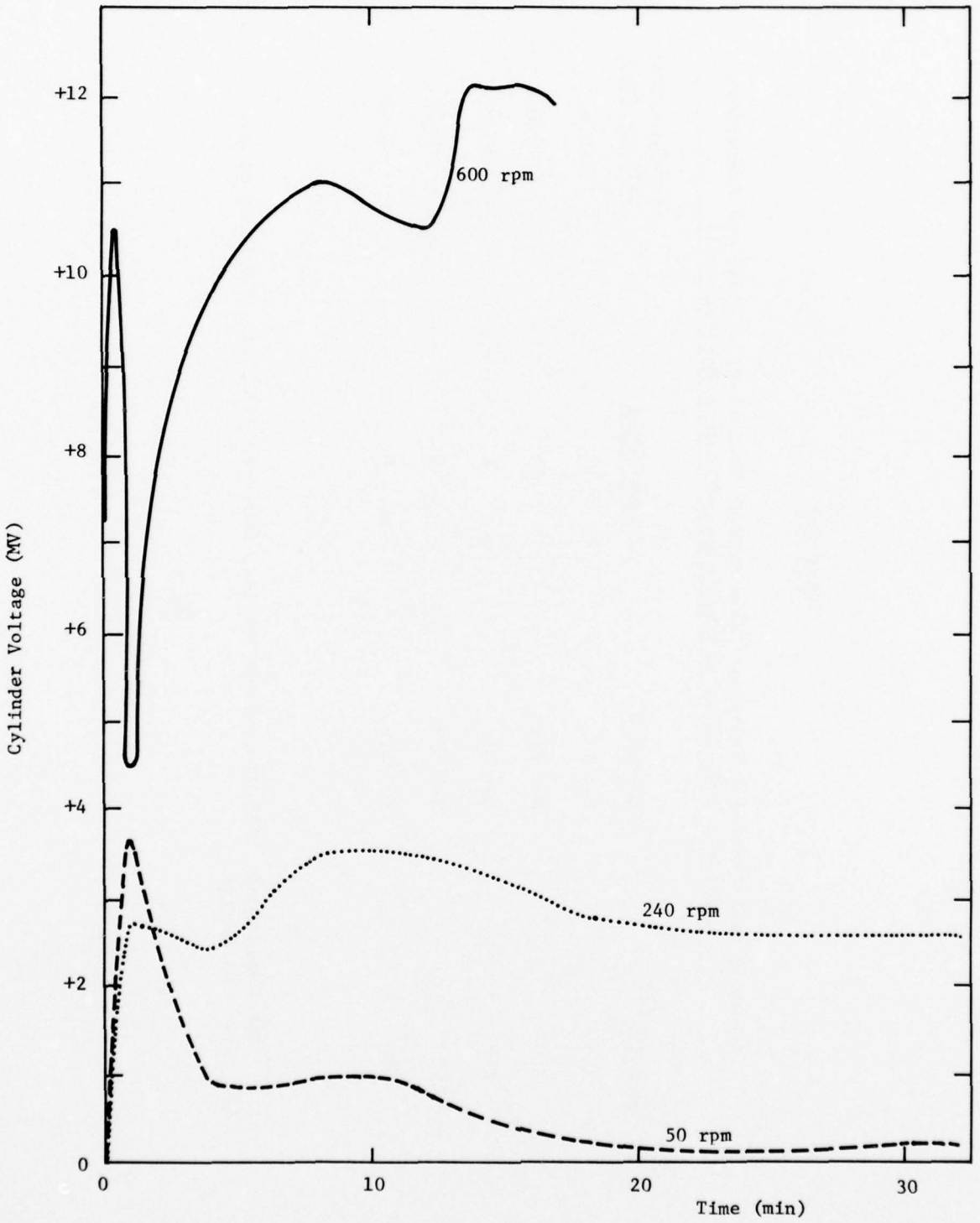

TABLE 10B

Measured Self-Generated Voltages Under Several Conditions of Load and Atmosphere for the HVWO Using an Aluminum-on-Aluminum Metallurgy(1)

Load (g)(2)	Atmosphere	Time (min)	Self-Generated Voltage (mv)
250	Dry Air	18	+0.01
250	Wet Air	19	+0.01
650	Wet Air	6	+0.01
1000	Wet Air	2	+0.01
1250	Wet Air	6	-0.04

(1) Test Conditions: Ball-on-Cylinder device, 240 rpm, 25°C, all others as noted.
(2) Wear was severe.

TABLE 11B

Measured Self-Generated Voltages Under Several Conditions of Load and Atmosphere for the HVWO Using a Steel-on-Aluminum Metallurgy(1)

Load (g)(2)	Atmosphere	Speed (rpm)	Time (min)	Self-Generated Voltage (mv)
250	Dry Air	240	16	-0.01
650	Dry Air	240	7	-0.03
1000	Dry Air	240	30	-0.10
250	Wet Air	240	16	-0.03
650	Wet Air	240	10	-0.05-0.08
2000	Wet Air	1000	8	-0.06
2000	Wet Air	240	16	-0.05

(1) Test Conditions: Ball-on-Cylinder device, 25°C, others as noted.
(2) Wear was severe.

TABLE 12B

Measured Wear and Self-Generated Voltages Under Both Inerted and Oxygenated Atmospheres Using the HVWO and the 52100 Steel Metallurgy(1)

			Argon					Air				
Load (g)	Metallurgy (Ball/Cylinder)	Time (min)	Ball Wear Scar Diameter (mm)	Ball Wear Volume (cc)	Track Cross Sectional Area (cm^2)	Cylinder Wear Volume (cc)	Self-Generated Voltage (mv)	Ball Wear Scar Diameter (mm)	Ball Wear Volume (cc)	Track Cross Sectional Area (cm^2)	Cylinder Wear Volume (cc)	Self-Generated Voltage (mv)
						Dry Condition						
200	Aluminum/Steel	32	--	--	--	--	--	0.30	0.63×10^{-7}	0.10	0.13×10^{-5}	+14.1
250	Aluminum/Steel	32	0.40	1.98×10^{-7}	0.18	0.23×10^{-5}	-0.19	--	--	--	--	--
500	Aluminum/Steel	32	0.55	7.07×10^{-7}	very small	--	-0.08	0.40	1.98×10^{-7}	0.17	0.22×10^{-5}	+ 2.5
500	Steel/Steel	36	0.23	0.22×10^{-7}	0.23	0.30×10^{-5}	+0.06	0.27	0.40×10^{-7}	0.18	0.24×10^{-5}	+ 4.9
500	Steel/Steel	360	0.23	0.22×10^{-7}	0.16	0.21×10^{-5}	+0.18	--	--	--	--	--
2000	Steel/Steel	36	0.32	0.81×10^{-7}	0.50	0.66×10^{-5}	0.00	0.33	0.92×10^{-7}	0.41	0.54×10^{-5}	+ 0.55
						Wet Condition						
200	Steel/Steel	32	--	--	--	--	--	0.28	0.48×10^{-7}	0.05	0.08×10^{-5}	- 0.84
350	Steel/Steel	32	--	--	--	--	--	0.33	0.92×10^{-7}	0.09	0.12×10^{-7}	- 1.5
500	Steel/Steel	32	0.25	0.30×10^{-7}	0.15	0.20×10^{-5}	+0.05	0.35	1.16×10^{-7}	0.18	0.24×10^{-5}	- 1.8
2000	Steel/Steel	32	0.30	0.63×10^{-7}	0.69	0.91×10^{-5}	+0.03	0.42	2.41×10^{-7}	0.77	1.02×10^{-7}	+ 0.15

(1) Test Conditions: Ball-on-Cylinder device, 240 rpm, 25°C.

TABLE 13B

The Influence of Temperature Upon the Measured Wear and Self-Generated Voltages Under Dry Air Blanketing for the HVWO Using the 52100 Steel Metallurgy(1)

Load (g)	Temperature (°C)	Time (min)	Ball Wear Scar Diameter (mm)	Ball Wear Volume (cc)	Track Cross Sectional Area (cm^2)	Cylinder Wear Volume (cc)	Surface Fatigue Demerit Rating	Coefficient of Friction	Self-Generated Voltage (mv)(3)	Apparent Film Resistance (Ohms)
1000	25	32	0.31	0.71×10^{-7}	0.38	0.50×10^{-5}	1	0.12	+4.3	10^4
1000	52	32	0.28	0.48×10^{-7}	0.72	0.95×10	1	0.14	+1.11	
1000	79	32	0.43	2.64×10^{-7}	0.33	0.44×10^{-5}	2	0.14	+0.78	
4000	25	32	0.47	3.77×10^{-7}	1.78	2.35×10^{-5}	3	0.18	-0.30	10
4000	52	16	0.38	1.61×10^{-7}	0.88	1.16×10^{-5}	1(2)	0.14	+0.39	
4000	52	32	0.47	3.77×10^{-7}	1.37	1.81×10^{-5}	3	0.15	-0.21	
4000	79	32	0.71	19.64×10^{-7}	7.75	10.23×10^{-5}	3	0.15	-0.19	10

(1) Test Conditions: Ball-on-Cylinder device, loads as noted, 240 rpm.
(2) Plasticization of the cylinder track was observed at the termination of this shortened test. Longer testing resulted in a severely worn track and a negative self generated voltage.
(3) The zero for the SGV's in the steel-on-steel system is temperature dependent and follows the relationship SGV (MV) = $0.209 - 6.9 \times 10^{-3}$ T (°C) over the temperature range 25°C - 160°C. SGV's have been temperature corrected.

FIGURE 11B

Traces Showing the Time Dependence of the Self-Generated Voltages for the HVWO Under Dry Air Blanketing as a Function of Temperature Using the Steel Metallurgy (Test Conditions: Ball-on-Cylinder Device, 1000 g, 240 rpm)

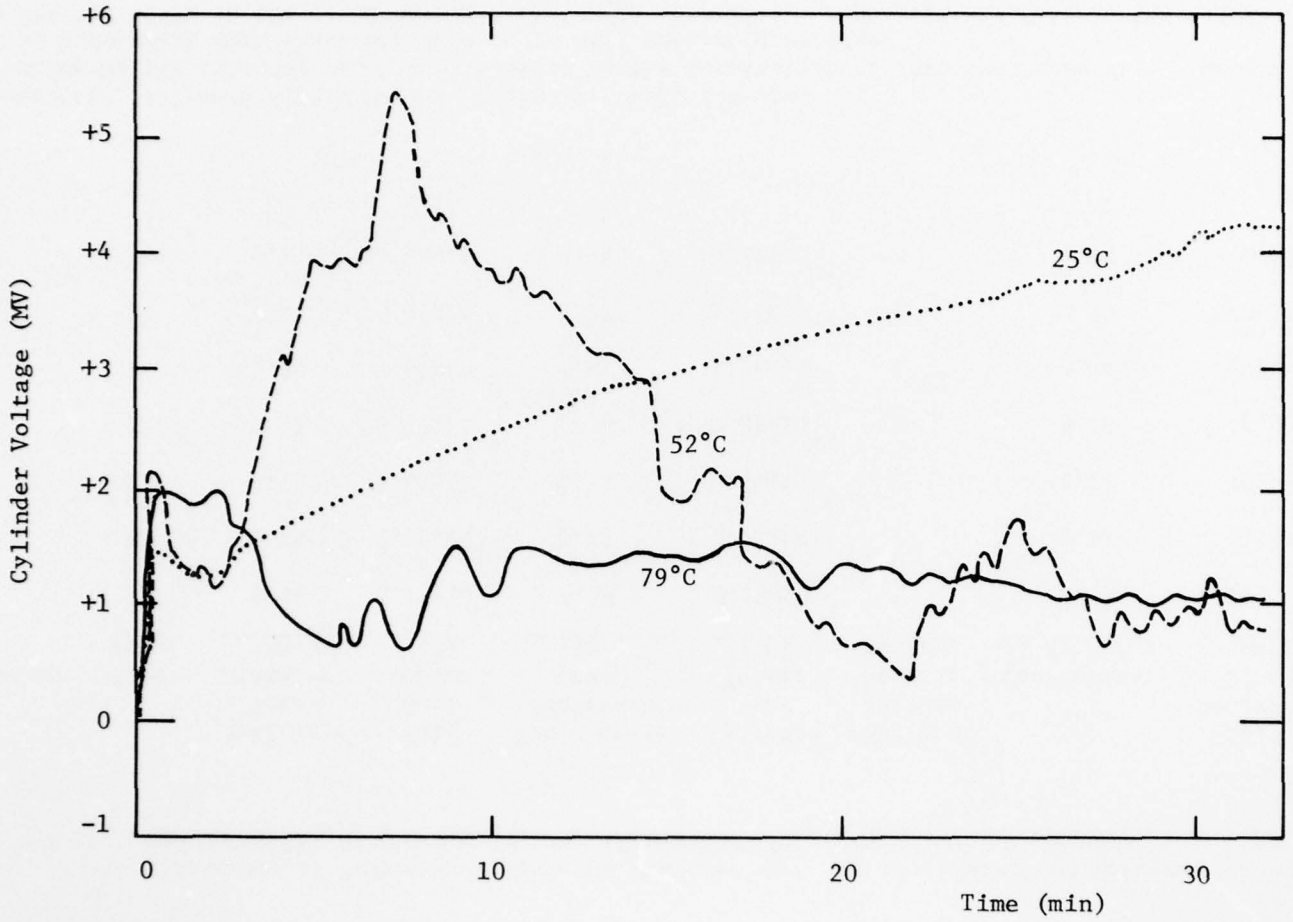

FIGURE 12B

Traces Showing the Time Dependence of the Self-Generated Voltages for the HVWO Under Dry Air Blanketing as a Function of Temperature Using the Steel Metallurgy (Test Conditions: Ball-on-Cylinder Device, 4000 g, 240 rpm)

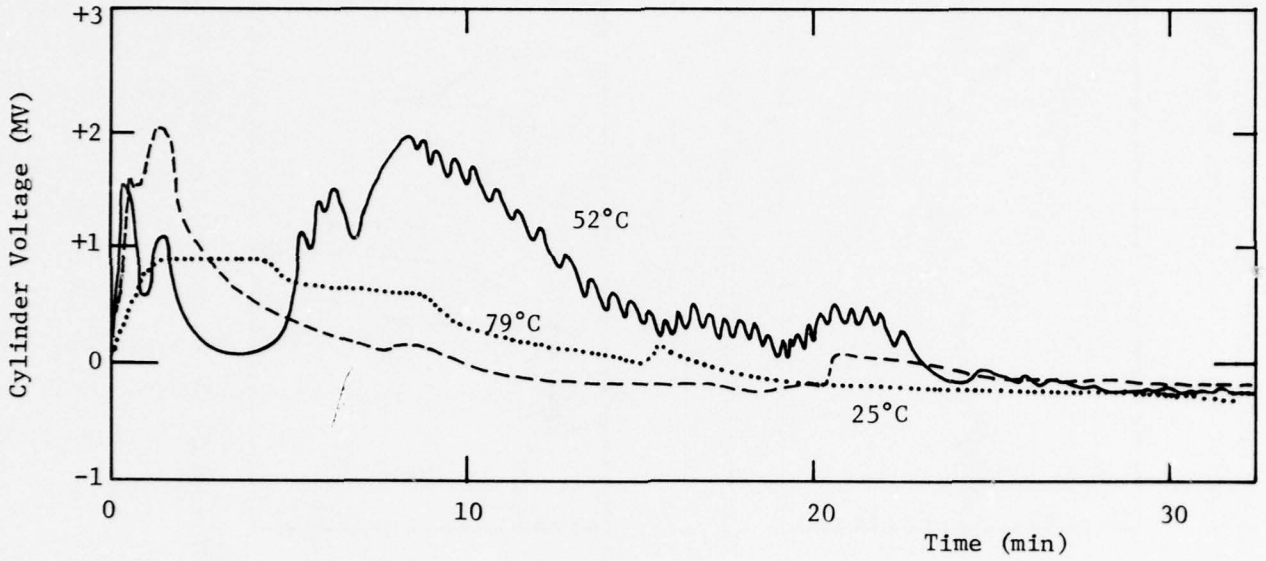

FIGURE 13B

Talysurf Traces Showing the Change in Surface Profiles Before and After the Self-Generated Voltages Undergoes a Transition in Polarity (Test Conditions: Ball-on-Cylinder Device, 4000 g, Dry Air Blanketing, 52°C, 240 rpm, Steel Metallurgy)

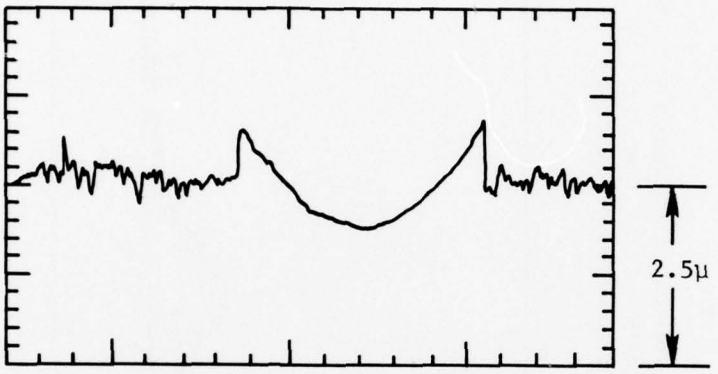

SGV = +0.39 MV at Termination After 16 min.

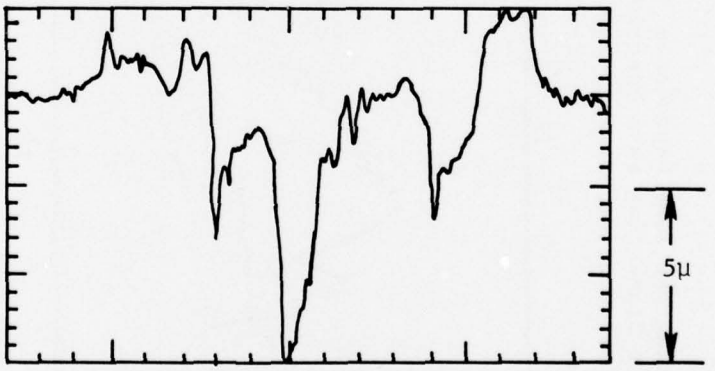

SGV = -0.21 MV at Termination After 32 min.

TABLE 14B

The Influence of Temperature Upon the Measured Wear and Self-Generated Voltages Under Wet Air Blanketing for the HVWO Using the 52100 Steel Metallurgy(1)

Load (g)	Temperature (°C)	Ball Wear Scar Diameter (mm)	Ball Wear Volume (cc)	Track Cross Sectional Area (cm^2)	Cylinder Wear Volume (cc)	Surface Fatigue Demerit Rating	Coefficient of Friction	Self-Generated Voltage (mv)(2)	Apparent Film Resistance (Ohms)
1000	25	0.36	1.30×10^{-7}	0.35	0.46×10^{-5}	1	0.12	-1.20	10^4
1000	52	0.30	0.63×10^{-7}	0.78	1.03×10^{-5}	1	0.15	+0.78	10^2
1000	79	0.50	4.83×10^{-7}	0.81	1.07×10^{-5}	2	0.17	+0.42	10
4000	25	0.53	6.10×10^{-7}	3.44	4.54×10^{-5}	1^+	0.14	+0.30	10^2
4000	79	0.95	62.96×10^{-7}	8.70	11.48×10^{-5}	3	0.37	-0.14	10

(1) Test Conditions: Ball-on-Cylinder device, Loads as noted, 240 rpm, 32 minutes.
(2) The zero for the SGV's in the steel-on-steel system is temperature dependent and follows the relationship SGV (MV) = $0.209 - 6.96 \times 10^{-3}$ T (°C) over the temperature range 25°C - 160°C. SGV's have been temperature corrected.

FIGURE 14B

Traces Showing the Time Dependence of the Self-Generated Voltages for the HVWO Under Wet Air Blanketing as a Function of Temperature Using the Steel Metallurgy (Test Conditions: Ball-on-Cylinder Device, 1000 g load, 240 rpm)

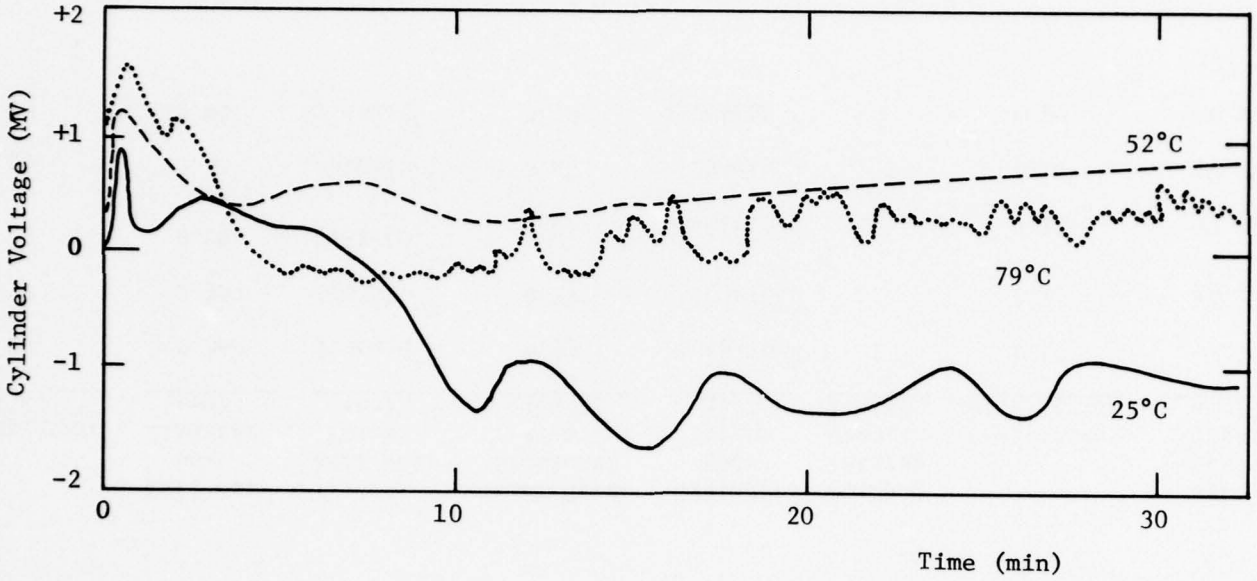

FIGURE 15B

Traces Showing the Time Dependence of the Self-Generated Voltages for the HVWO Under Wet Air Blanketing as a Function of Temperature Using the Steel Metallurgy (Test Conditions: Ball-on-Cylinder Device, 4000 g, 240 rpm)

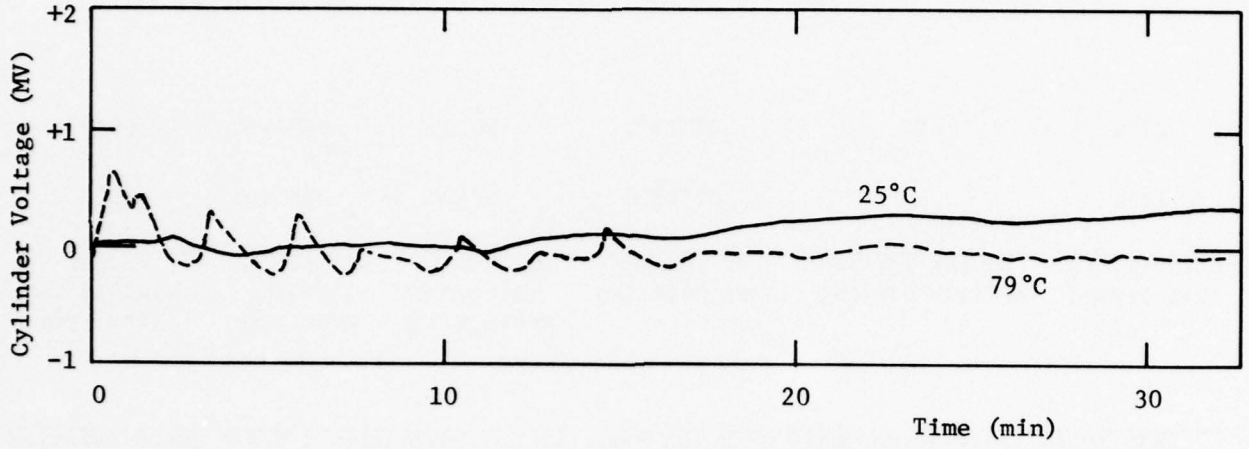

TABLE 15B

The Influence of Temperature Upon the Measured Wear and Self-Generated Voltages Under Dry Air Blanketing for the HVWO Using an Aluminum-on-Steel Metallurgy(1)

Load (g)	Temp (°C)	Ball Wear Scar Diameter (cm^2)	Ball Wear Volume (cc)	Track Cross Sectional Area (cm^2)	Cylinder Wear Volume (cc)	Surface Fatigue Demerit Rating	Coefficient of Friction	Self-Generated Voltage (mv)
1000	25	0.33	0.92×10^{-7}	0.08	0.11×10^{-5}	1	0.11	+ 4.3
1000	79	0.33	0.42×10^{-7}	0.08	0.11×10^{-5}	1	0.12	+11.1

(1) Test Conditions: Ball-on-Cylinder device, 240 rpm, 32 minutes, others as noted.

FIGURE 16B-a

Traces Showing the Time Dependence of the Self-Generated Voltages for the HVWO Under Dry Air Blanketing as a Function of Temperature Using an Aluminum-on-Steel Metallurgy (Test Conditions: Ball-on-Cylinder Device, 240 rpm)

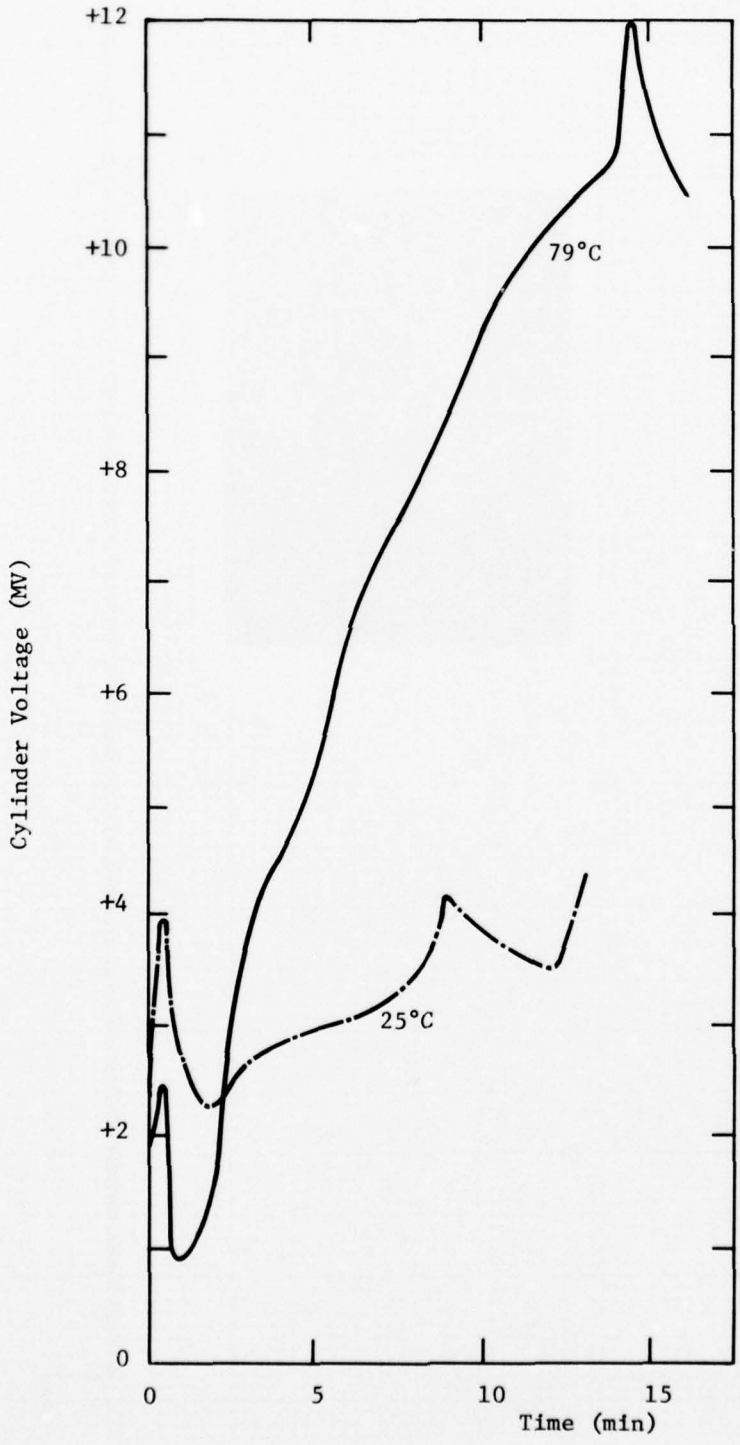

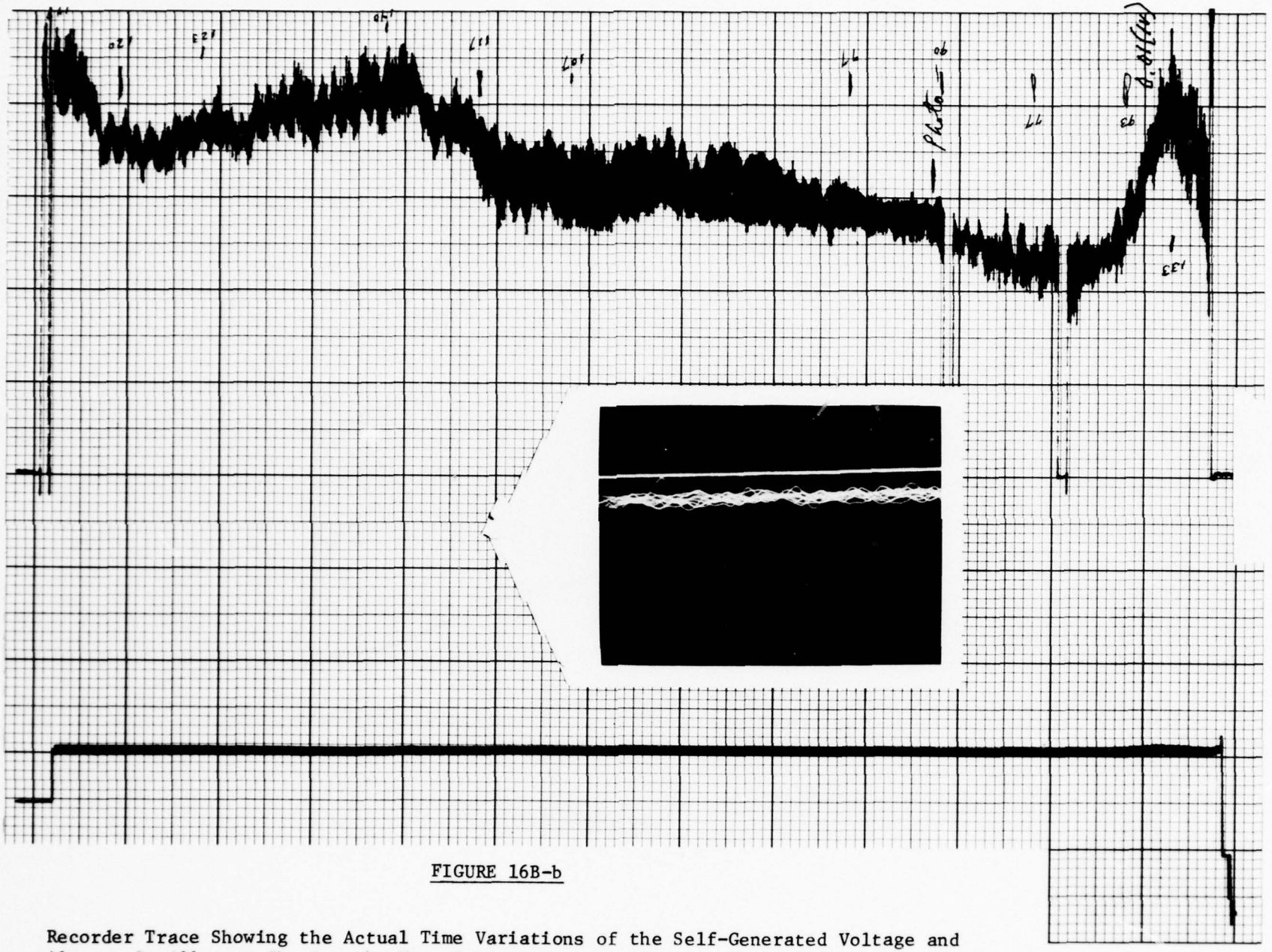

FIGURE 16B-b

Recorder Trace Showing the Actual Time Variations of the Self-Generated Voltage and Also an Oscillogram Showing the Near Instantaneous Variation of the Self-Generated Voltage for the Test at 25°C. (See Fig. 5B-b, Page 92, for Additional Discussion)

TABLE 16B

Measured Wear and Self-Generated Voltages for the IVWO
Under Wet Air Blanketing Using an Aluminum-on-Steel Metallurgy(1)

Load (g)	Speed (rpm)	CLA (μ)	Ball Wear Scar Diameter (mm)	Ball Wear Volume (cc)	Track Cross Sectional Area (cm^2)	Cylinder Wear Volume (cc)	Coefficient of Friction	Self-Generated Voltage (mv)	Relative Film Resistance (Ohms)
250	50(2)	0.14	0.37	1.45×10^{-7}	0.13	0.17×10^{-5}	0.14	+2.7	
250	240	0.14	0.37	1.45×10^{-7}	0.37	0.49×10^{-5}	0.11	+1.5	
250	600	0.14	0.37	1.45×10^{-7}	1.01	1.33×10^{-5}	0.10	+2.9	10^5
500	50	0.18	0.47	3.77×10^{-7}	0.45	0.59×10^{-5}	0.09	+1.4	
500	240	0.18	0.42	2.41×10^{-7}	1.05	1.39×10^{-5}	0.14	+1.2	
500	240	0.23	0.48	4.10×10^{-7}	0.98	1.29×10^{-5}	0.12	+0.45	5×10^2
500	240	0.25	0.51	5.23×10^{-7}	0.69	0.91×10^{-5}	0.12	+0.36	10^2
500	600	0.18	0.35	1.16×10^{-7}	1.55	2.05×10^{-5}	0.12	+6.0	

(1) Test Conditions: Ball-on-Cylinder Device, 25°C, 32 minutes.

(2) 60 minute test.

FIGURE 17B

Traces Showing the Time Dependence of the Self-Generated Voltages for the IVWO Under Wet Air Blanketing Using an Aluminum-on-Steel Metallurgy (Test Conditions: Ball-on-Cylinder Device, 250 g, 25°C)

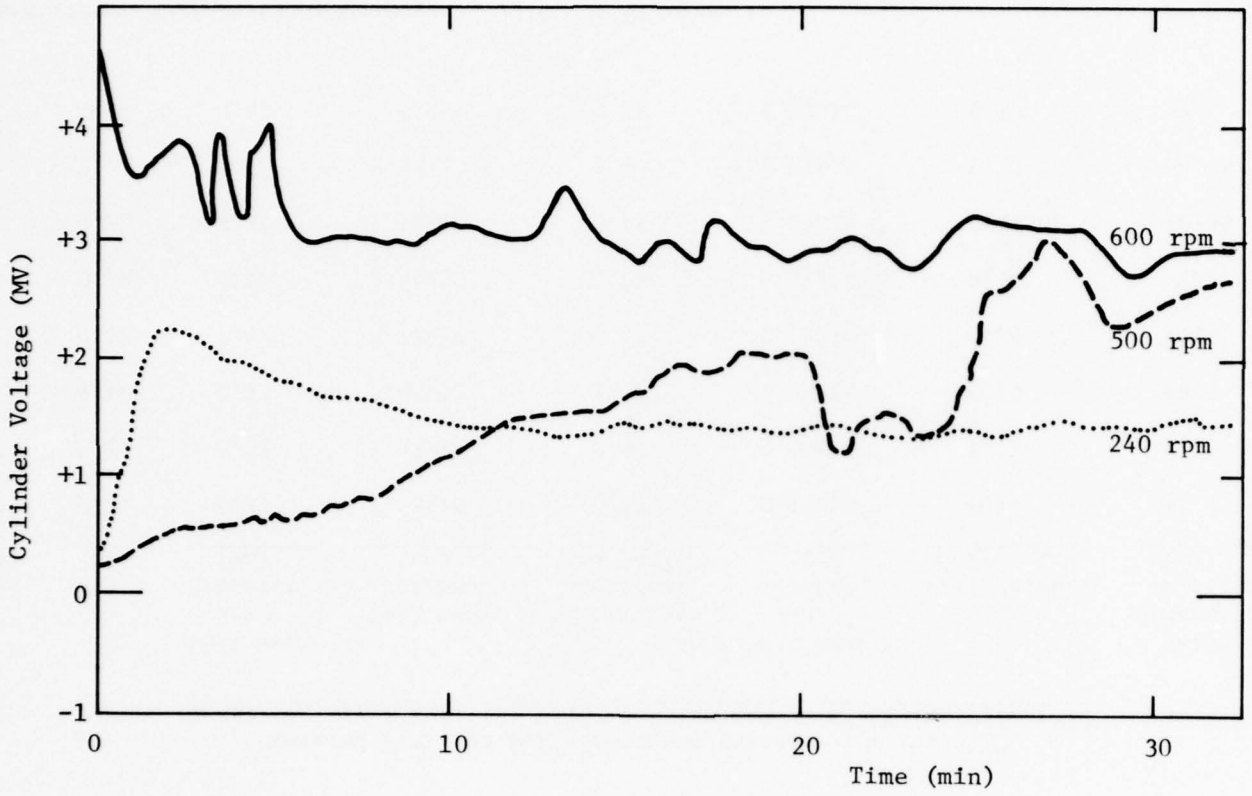

FIGURE 18B

Traces Showing the Time Dependence of the Self-Generated Voltages for the IVWO Under Wet Air Blanketing Using an Aluminum-on-Steel Metallurgy (Test Conditions: Ball-on-Cylinder Device, 500 g, 25°C)

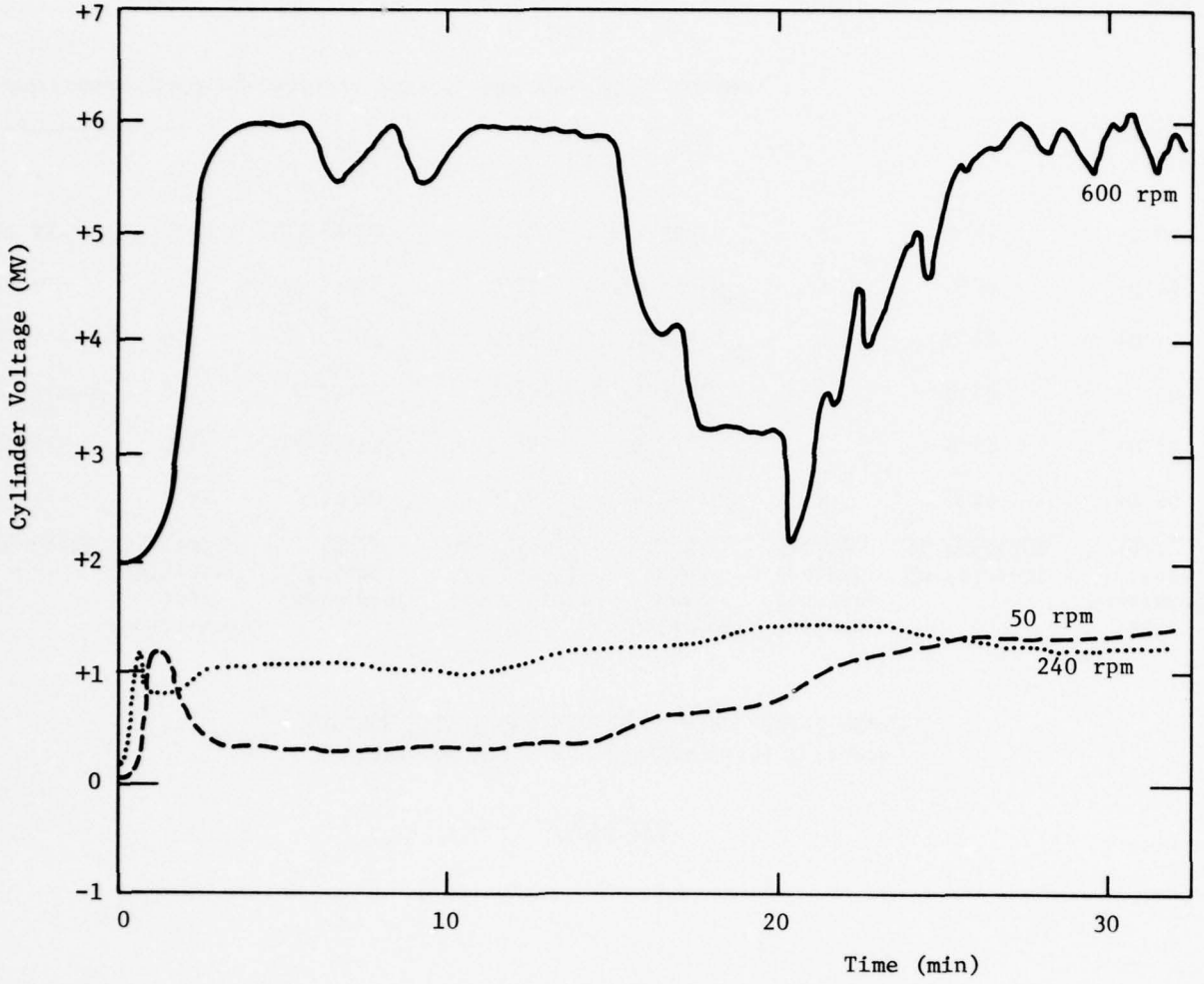

TABLE 17B

Measured Wear and Self-Generated Voltages
for the LVWO Using the 52100 Steel Metallurgy(1)

Load (g)	Atmosphere	Ball Wear Scar Diameter (mm)	Ball Wear Volume (cc)	Track Cross Sectional Area (cm^2)	Cylinder Wear Volume (cc)	Surface Fatigue Demerit Rating	Coefficient of Friction	Self-Generated Voltage (cc)	Relative Film Resistance (Ohms)
500	Dry Air	0.45	3.17×10^{-7}	0.06	0.08×10^{-5}	1	0.17	+0.50	10^3
500	Wet Air	0.61	10.70×10^{-7}	0.25	0.33×10^{-5}	1	0.17	+0.20	10^2
1000	Dry Air(2)	0.53	6.10×10^{-7}	0.23	0.30×10^{-5}	1	0.19	+0.18	10
1000	Wet Air	0.75	24.46×10^{-7}	0.72	0.95×10^{-5}	3	0.22	+0.15	10
2000	Dry Air	0.77	27.17×10^{-7}	0.34	0.45×10^{-5}	3	0.39	-0.05	
2000	Wet Air	1.43	323.32×10^{-7}	1.24	163.68×10^{-5}	3	0.43	+0.06	

(1) Test Conditions: Ball-on-Cylinder device, 240 rpm, 25°C, 32 min.

(2) 60 min test.

FIGURE 19B

Traces Showing the Time Dependence of the Self-Generated Voltages for the LVWO Under Dry Air Blanketing as a Function of Load Using the Steel Metallurgy (Test Conditions: Ball-on-Cylinder Device, 240 rpm, 25°C)

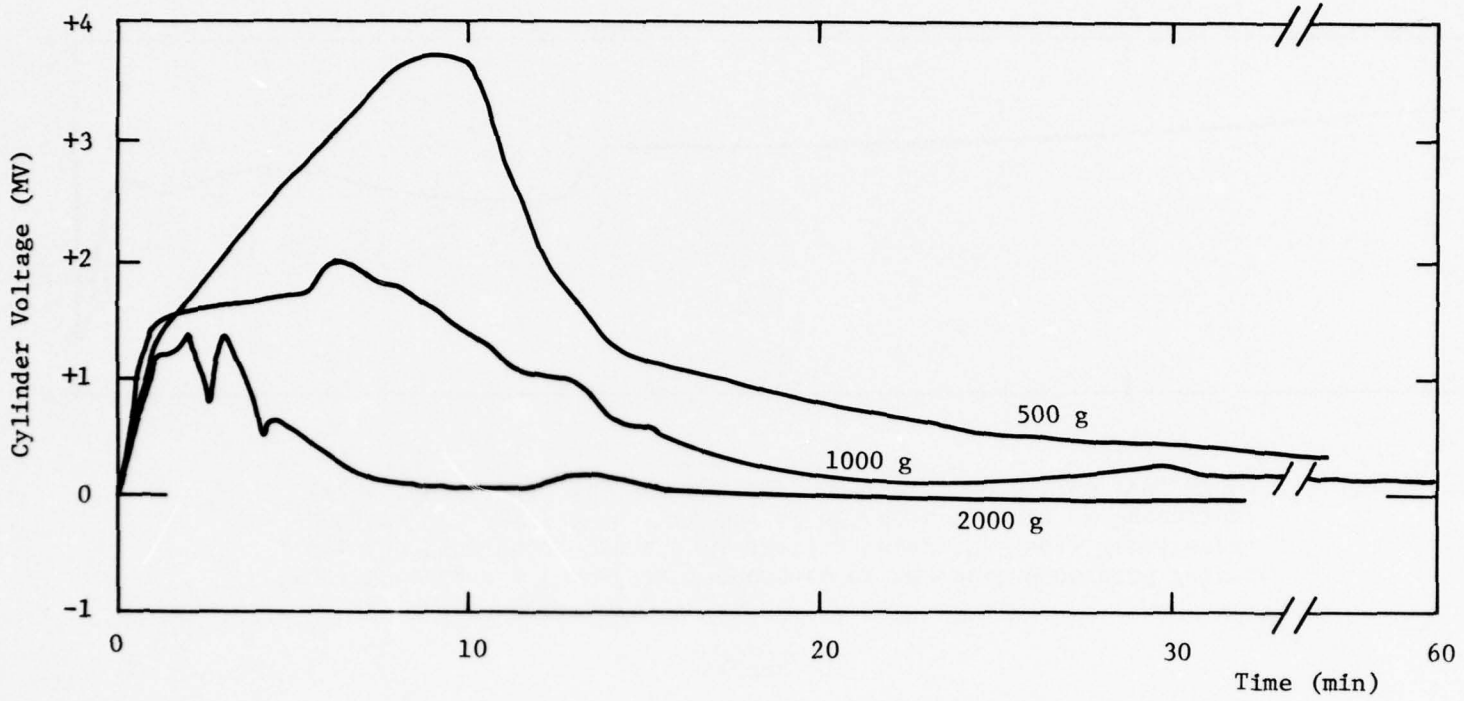

FIGURE 20B

Trace Showing the Long Time Dependence of the Self-Generated Voltage for the LVWO Under Dry Air Blanketing Using the Steel Metallurgy. Note the Transition in Polarity After About 6 Hours of Operation (Test Conditions: Ball-on-Cylinder Device, 1000 g, 240 rpm, 25°C)

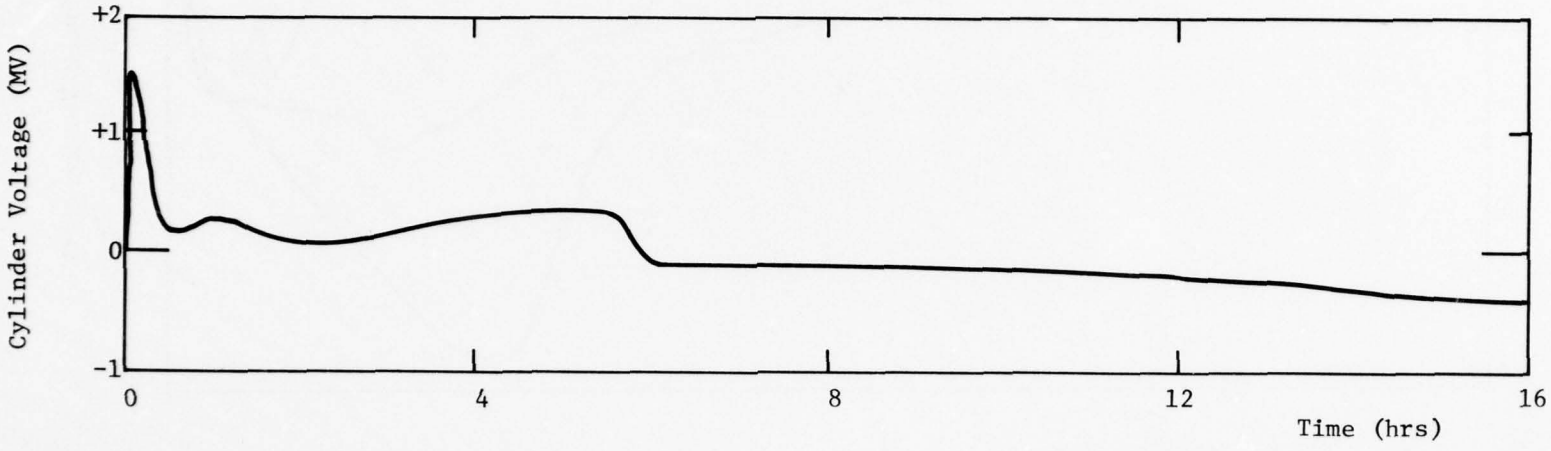

TABLE 18B

Measured Wear and Self-Generated Voltages for Paraffinic Hydrocarbons Using the 52100 Steel Metallurgy(1)

Lubricant	Atmosphere	Load (g)	Cylinder Surface Roughness (μ)	Ball Wear Scar Diameter (mm)	Ball Wear Volume (cc)	Track Cross Sectional Area (cm^2)	Cylinder Wear Volume (cc)	Surface Fatigue Demerit Rating	Coefficient of Friction	Self-Generated Voltage (mv)
Hexadecane	Wet Air	250	0.23	0.75	24.46×10^{-7}	0.03	0.04×10^{-5}	1+	0.22	+0.09
Decane	Dry Air	500	0.18	0.83	36.69×10^{-7}	0.04	0.05×10^{-5}	2	0.18	+0.21
Dodecane	Dry Air	500	0.18	0.72	20.77×10^{-7}	0.14	0.18×10^{-5}	1+	0.17	+0.20
Dodecane	Dry Air	500	0.33	0.78	28.61×10^{-7}	0.09	0.12×10^{-5}	1	0.20	+0.12
Tetradecane	Dry Air	500	0.18	0.63	12.18×10^{-7}	0.09	0.12×10^{-5}	1	0.16	+0.24
Hexadecane	Dry Air	500	0.18 (2)	0.48	4.10×10^{-7}	0.20	0.26×10^{-5}	3	0.17	+1.65
Hexadecane	Wet Air	500	0.18 (2)	0.87	44.28×10^{-7}	0.43	0.57×10^{-5}	3	0.19	+0.09
Hexadecane	Dry Air	500	0.23 (2)	0.53	1.10×10^{-7}	0.12	0.16×10^{-5}	3	0.13	+0.80
Hexadecane	Wet Air	500	0.23 (2)	0.88	46.36×10^{-7}	0.80	1.06×10^{-5}	3	0.15	+0.15
Hexadecane	Dry Air	500	0.33 (2)	0.62	11.42×10^{-7}	0.11	0.15×10^{-5}	1	0.14	-0.06

(1) Test Conditions: Ball-on-Cylinder device, Loads and Atmospheres as Noted, 240 rpm, 25°C, 32 minutes.

(2) Surface Roughness Effects may be noted.

FIGURE 21B

Traces Showing the Time Dependence of the Self-Generated Voltages for a Series of Paraffinic Hydrocarbons Under Dry Air Blanketing Using the Steel Metallurgy (Test Conditions: Ball-on-Cylinder Device, 500 g, 240 rpm, 25°C)

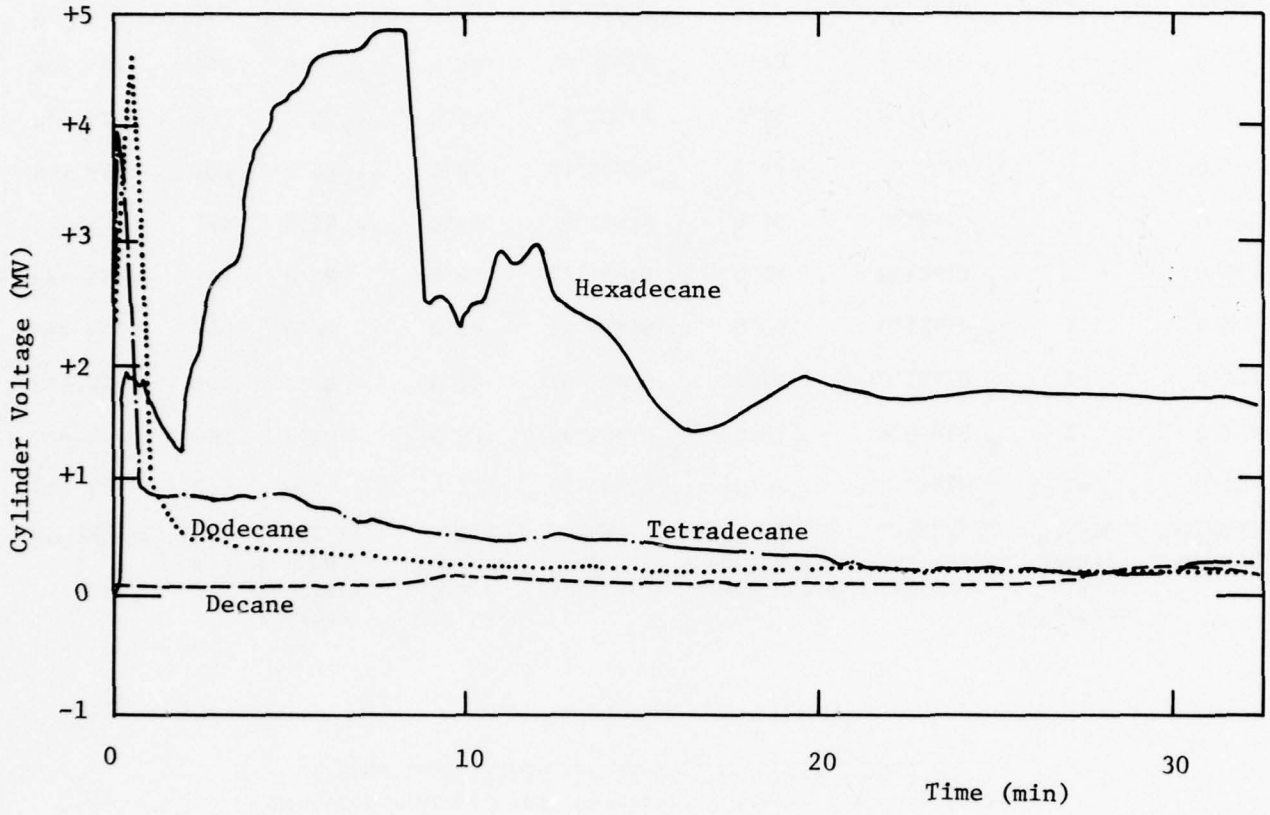

FIGURE 22B

Traces Showing the Time Dependence of the Self-Generated Voltages for Hexadecane Under Dry Air Blanketing as a Function of Surface Roughness Using the Steel Metallurgy (Test Conditions: Ball-on-Cylinder Device, 500 g, 240 rpm, 25°C)

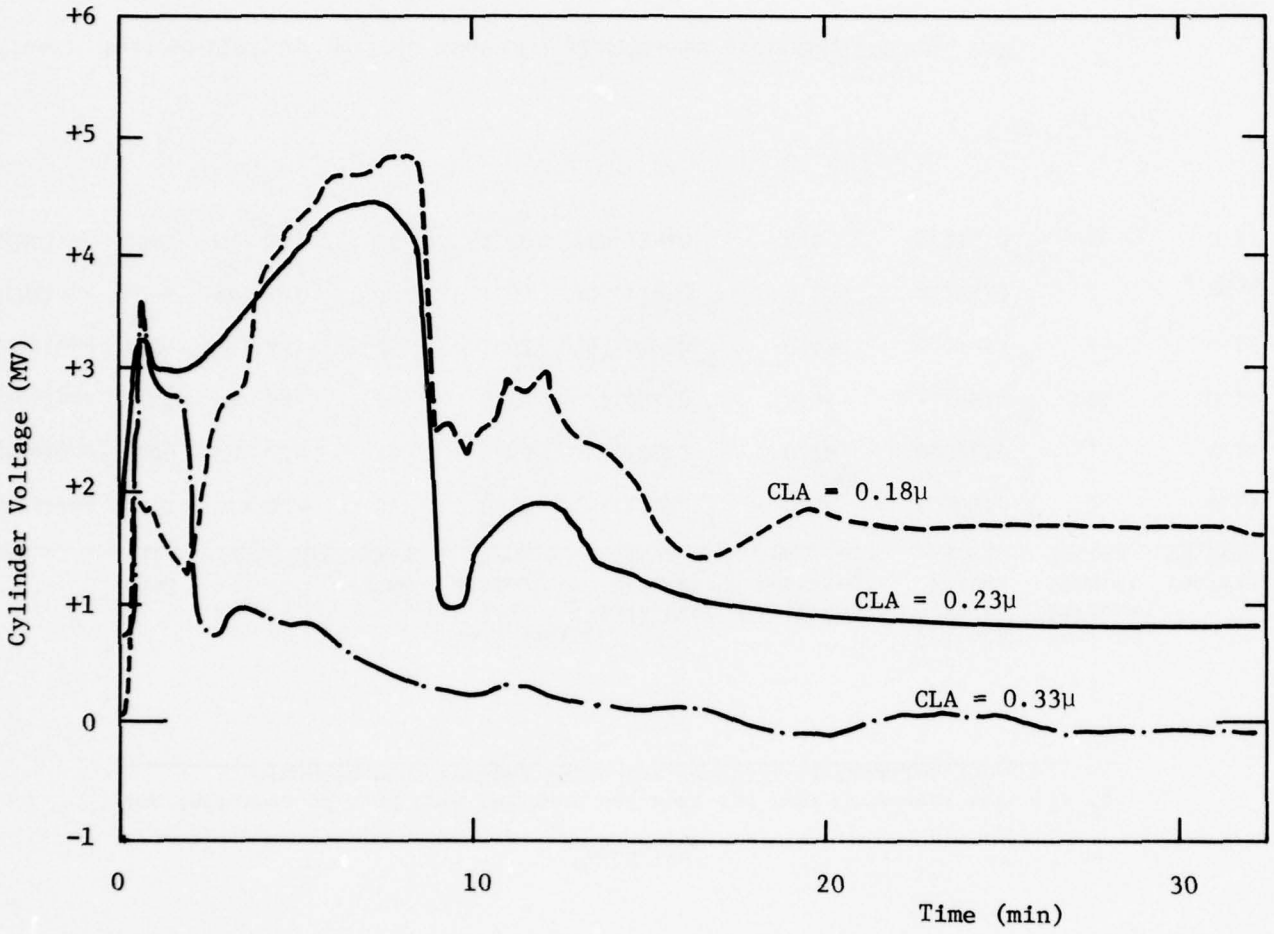

TABLE 19B

The Influence of Load Upon the Measured Wear and Self-Generated Voltages for Aromatic Hydrocarbons Using the 52100 Steel Metallurgy(1)

Lubricant	Load (g)	Atmosphere	Time (min)	Ball Wear Scar Diameter (mm)	Ball Wear Volume (cc)	Track Cross Sectional Area (cm^2)	Cylinder Wear Volume (cc)	Surface Fatigue Demerit Rating	Coefficient of Friction	Self-Generated Voltage (cc)
1-Methylnaphthalene	500	Dry Air	32	0.35	1.16×10^{-7}	0.38	0.50×10^{-5}	1	0.15	+3.0
1-Methylnaphthalene	500	Wet Air	32	0.53	6.10×10^{-7}	0.28	0.37×10^{-5}	1	0.14	+2.9
1-Methylnaphthalene	1000	Wet Air	60	0.56	7.60×10^{-7}	0.86	1.14×10^{-5}	1+	0.15	0.51
1-Chloronaphthalene	1000	Wet Air	36	1.02	83.67×10^{-7}	0.45	0.59×10^{-5}	1	0.13	+0.6
1-Chloronaphthalene	1000	Wet Air	60	1.08	105.17×10^{-7}	0.2	0.26×10^{-5}	1	0.10	+1.02
1-Chloronaphthalene	4000	Wet Air	64	1.20	160.29×10^{-7}	4.6	6.07×10^{-5}	3	0.17	0.0

(1) Test Conditions: Ball-on-Cylinder device, Loads and Atmospheres as noted, 240 rpm, 25°C.

FIGURE 23B

Traces Showing the Time Dependence of the Self-Generated Voltages for Aromatic Hydrocarbons Using the Steel Metallurgy (Test Conditions: Ball-on-Cylinder Device, 240 rpm, 25°C)

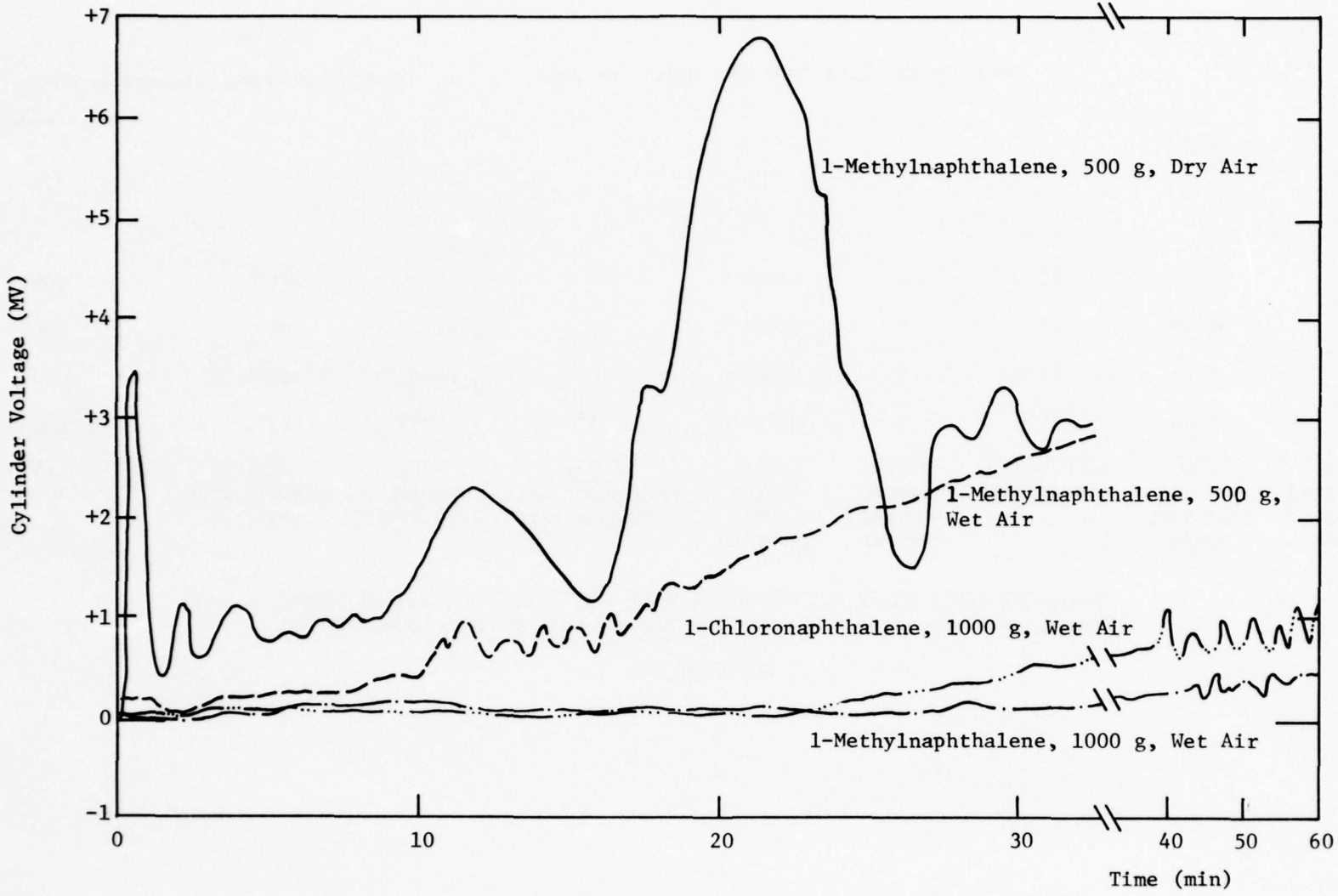

TABLE 20B

The Influence of Load Upon The Measured Wear and Self-Generated Voltages Under Dry Air Atmosphere for The HVLRO Using the 52100 Steel Metallurgy

Load (g)	Ball Wear Scar Diameter (mm)	Ball Wear Volume (cc)	Track Cross Sectional Area (cm^2)	Cylinder Wear Volume (cc)	Surface Fatigue Demerit Rating	Coefficient of Friction	Self-Generated Voltage (mv)	Apparent Film Resistance (Ohms)
500	0.22	0.18×10^{-7}	0.18	0.24×10^{-4}	1	0.12	+2.6	10^4
1000	0.25	0.30×10^{-7}	0.30	0.40×10^{-5}	1	0.13	+2.3	10^4
2000	0.38	1.61×10^{-7}	0.87	1.15×10^{-5}	3	0.18	-0.06	10^2
4000	0.48	4.10×10^{-7}	2.13	2.82×10^{-5}	3	0.19	-0.24	10^2

Test Conditions: Ball-on-Cylinder device, Loads as Noted, 240 rpm, 25°C, 32 minutes.

FIGURE 24B

Traces Showing the Time Dependence of the Self-Generated Voltages for the HVLRO Under Dry Air Blanketing as a Function of Load Using the Steel Metallurgy (Test Conditions: Ball-on-Cylinder Device, 240 rpm, 25°C)

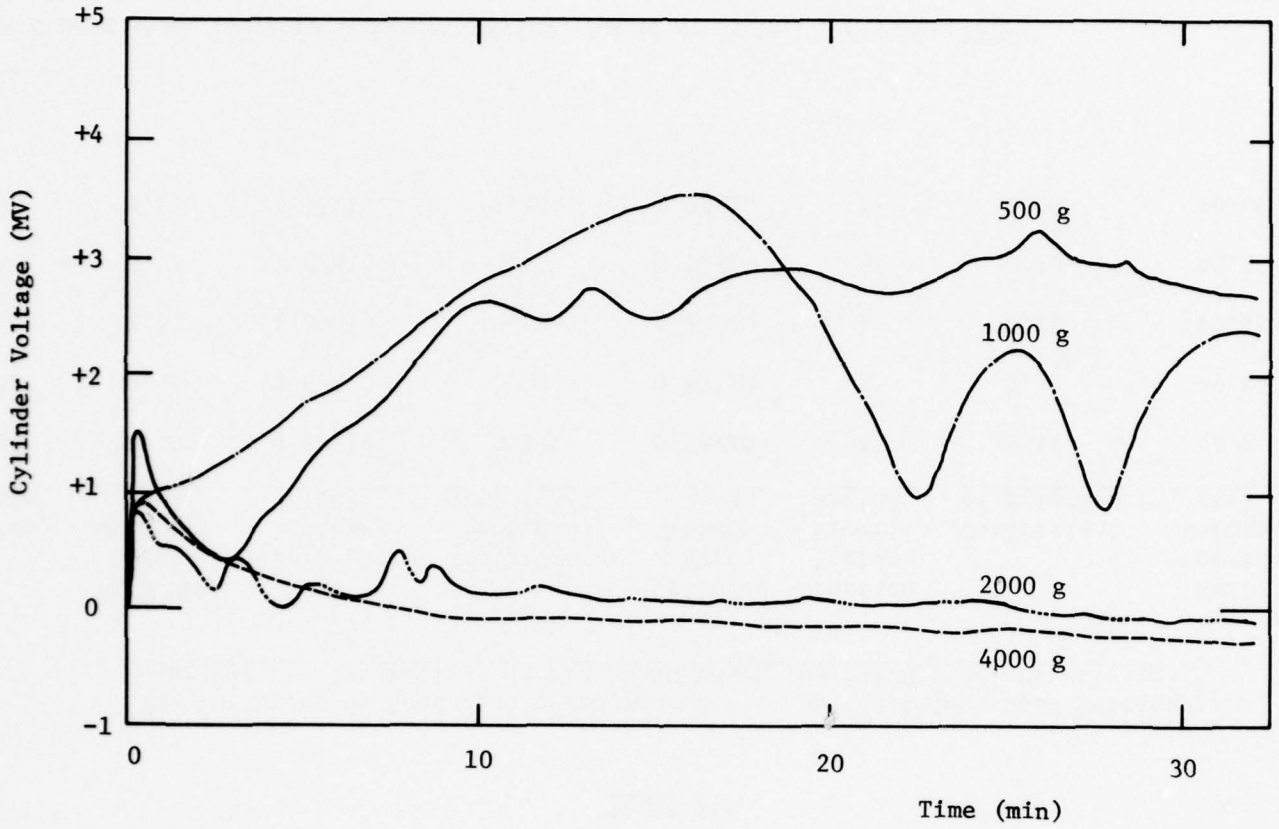

TABLE 21B

The Influence of Load Upon the Measured Wear and Self-Generated Voltages Under Wet Air Blanketing for the HVLRO Using the 52100 Steel Metallurgy(1)

Load (g)	Time (min)	Ball Wear Scar Diameter (mm)	Ball Wear Volume (cc)	Track Cross Sectional Area (cm^2)	Cylinder Wear Volume (cc)	Surface Fatigue Demerit Rating	Coefficient of Friction	Self-Generated Voltage (mv)	Relative Film Resistance (Ohms)
500	32	0.30	0.63×10^{-7}	0.10	0.13×10^{-5}	1	0.14	+2.8	10^4
1000	32	0.30	0.63×10^{-7}	0.52	$0.69.10^{-5}$	1	0.13	+0.66	10^3
2000	32	0.39	1.80×10^{-7}	0.68	0.90×10^{-5}	1	0.15	+0.46	5×10^2
2000	960	0.55	7.07×10^{-7}	3.65	4.82×10^{-5}	3	0.15	+0.24 (2)	10^2
4000	32	0.46	3.46×10^{-7}	1.49	1.97×10^{-5}	1+	0.15	+0.09	10^2

(1) Test Conditions: Ball-on-Cylinder device, Loads as Noted, 240 rpm, 25°C.

(2) After long test period, no transition in polarity of SGV as might be noted with HVWO.

FIGURE 25B

Traces Showing the Time Dependence of the Self-Generated Voltages for the HVLRO Under Wet Air Blanketing as a Function of Load Using the Steel Metallurgy (Test Conditions: Ball-on-Cylinder Device, 240 rpm, 25°C)

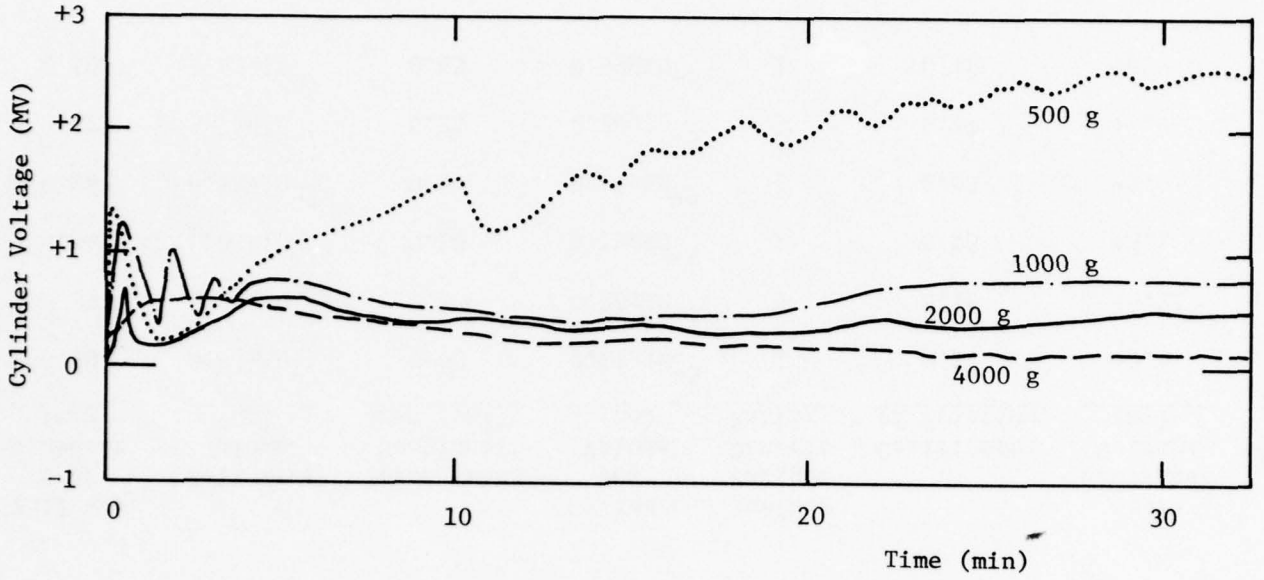

TABLE 22B

The Influence of Load Upon the Measured Wear and Self-Generated Voltages Under Dry Air Blanketing for the HVLRO Using the Aluminum-on-Steel Metallurgy(1)

Load	RPM	Ball Wear Scar Diameter (mm)	Ball Wear Volume (cc)	Track Cross Sectional Area (cm^2)	Cylinder Wear Volume (cc)	Surface Fatigue Demerit Rating	Coefficient of Friction	Self-Generated Voltage (mv)	Relative Film Resistance (Ohms)
500	240	0.30	0.63×10^{-7}	0.08	0.11×10^{-5}	1	0.12	+3.6	10^5
1000	50 (2)	0.33	0.92×10^{-7}	0.20	0.26×10^{-5}	1	0.16	+0.21	10^2
1000	240 (2)	0.34	1.03×10^{-7}	0.10	0.13×10^{-5}	1	0.13	+3.1	5×10^4
1000	600 (2)	0.28	0.48×10^{-7}	0.08	0.11×10^{-5}	1	0.08	+8.4	10^6
2000	240	0.47	3.77×10^{-7}	0.23	0.30×10^{-5}	1	0.17	+1.9	
4000	240	0.50	4.83×10^{-7}	0.45	0.59×10^{-5}	1	0.18	+0.7	10^3

(1) Test Conditions: Ball-on-Cylinder device, Loads and Speeds as noted, 16 min, 25°C.

(2) Effect of Speed.

FIGURE 26B

Traces Showing the Time Dependence of the Self-Generated Voltages for the HVLRO Under Dry Air Blanketing as a Function of Load for an Aluminum-on-Steel Metallurgy (Test Conditions: Ball-on-Cylinder Device, 240 rpm, 25°C)

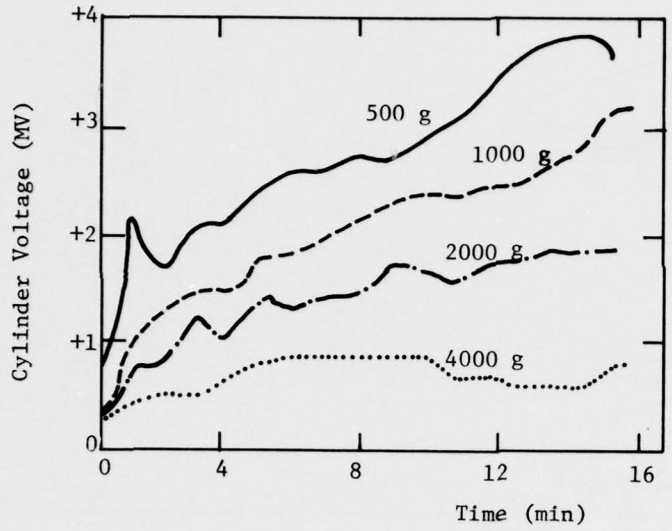

FIGURE 27B

Traces Showing the Time Dependence of the Self-Generated Voltages for the HVLRO Under Dry Air Blanketing as a Function of Speed for an Aluminum-on-steel Metallurgy (Test Conditions: Ball-on-Cylinder Device, 25°C)

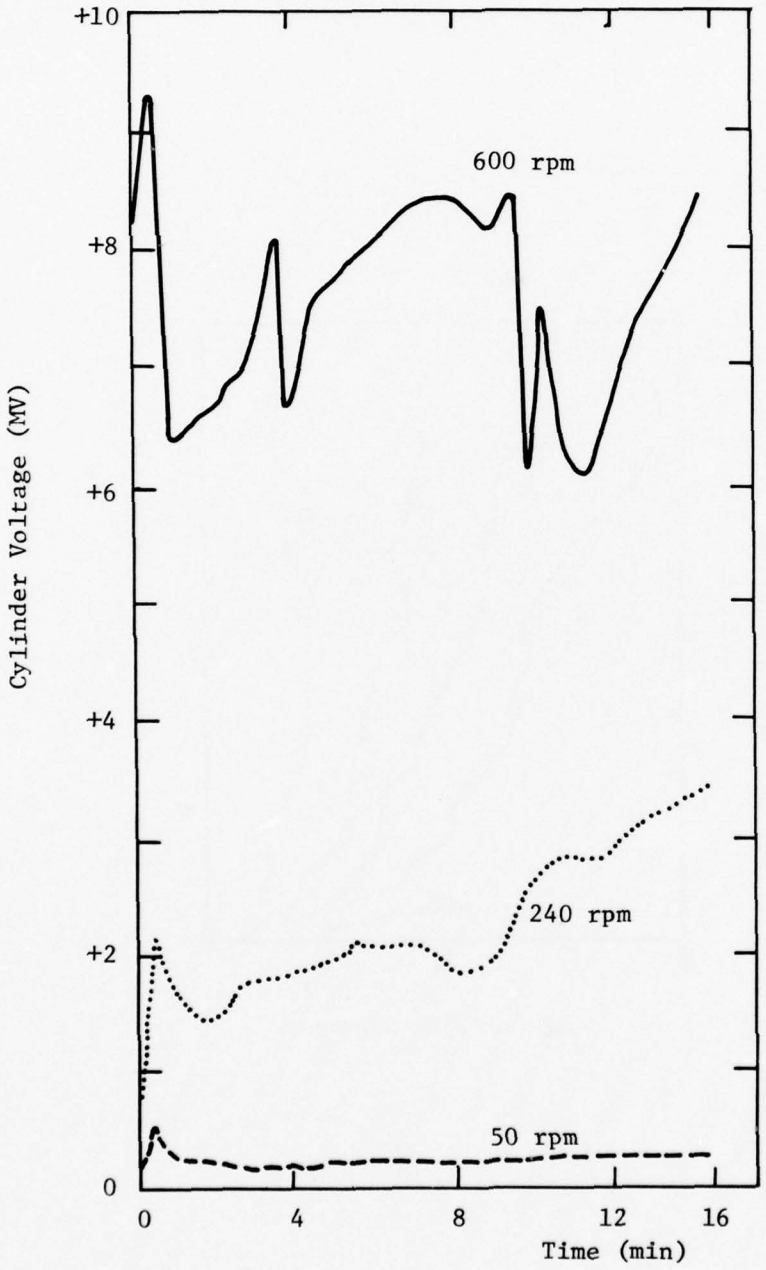

TABLE 23B

Measured Wear and Self-Generated Voltages for the HVLRO Using Several Aluminum-on-Aluminum and Steel-on-Aluminum Metallurgies(1)

Metal Couple (Ball/Cylinder)	Atmosphere	Time (min)	Ball Wear Scar Diameter (mm)	Ball Wear Volume (cc)	Track Cross Sectional Area (cm^2)	Cylinder Wear Volume (cc)	Surface Fatigue Demerit Rating	Coefficient of Friction	Self-Generated Voltage (mv)	Relative Film Resistance (Ohms)
Steel/Aluminum	Dry Air	30	0.28	0.48×10^{-7}	1.70	2.24×10^{-5}	2	0.11	-2.4	
Steel/Aluminum	Wet Air	30	0.27	0.41×10^{-7}	0.03	0.04×10^{-5}	1	0.12	-390	10^7
Aluminum/Aluminum	Dry Air	32	0.53	6.10×10^{-7}	17.5	23.1×10^{-5}	2	0.18	-0.01	
Aluminum/Aluminum	Wet Air	1	0.30	0.63×10^{-7}	1.95	2.57×10^{-5}	3	0.18	+0.01	

(1) Test Conditions: Ball-on-Cylinder device, 1000g, 240 rpm, 25°C, Metallurgies as noted.

FIGURE 28B

Trace Showing the Time Dependence of the Self-Generaged Voltage for the HVLRO Under Dry Air Blanketing Using an Aluminum-on-Steel Metallurgy (Test Condition: Ball-on-Cylinder Device, 1000 g, 240 rpm, 25°C)

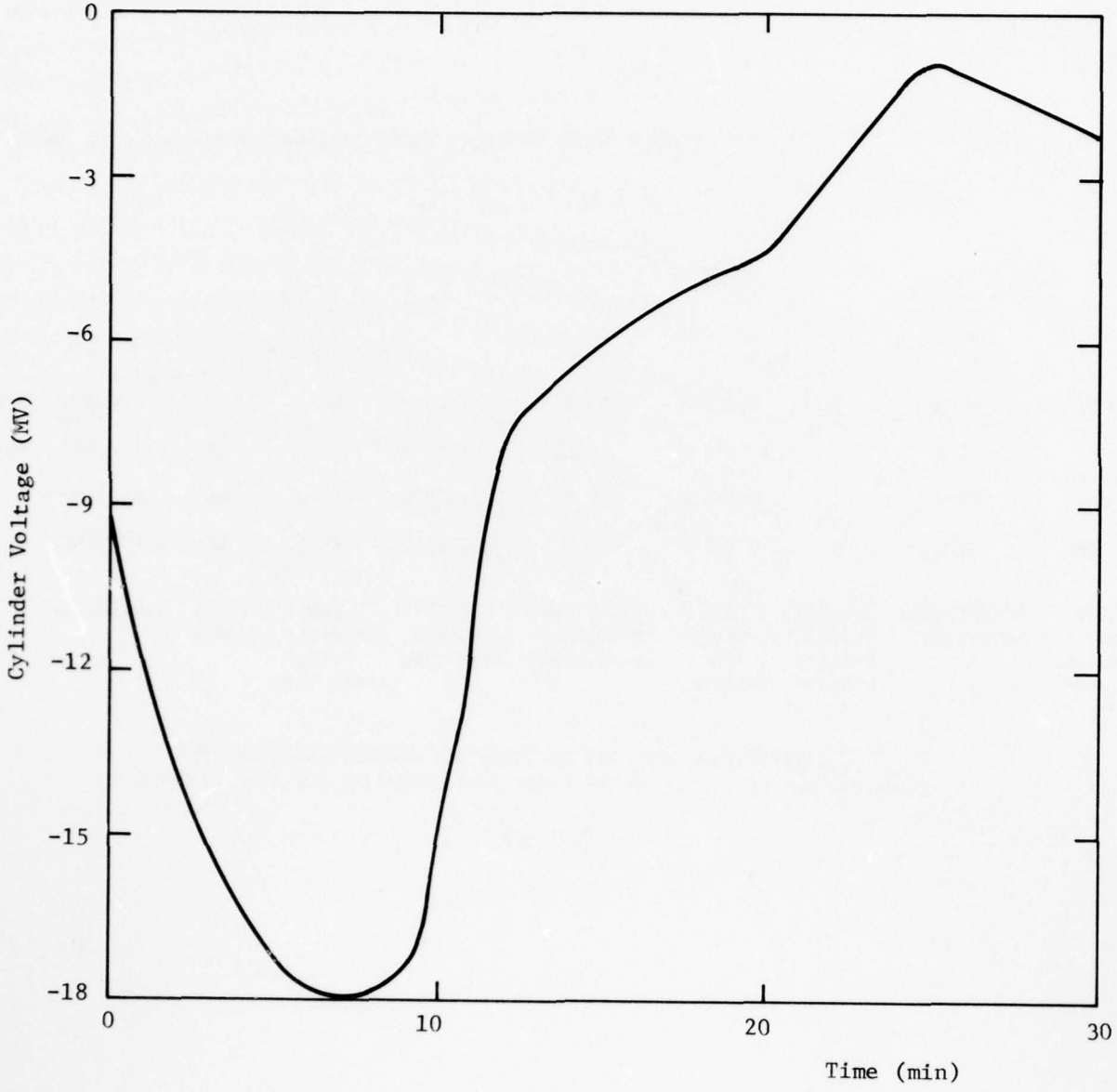

FIGURE 29B

Trace Showing the Time Dependence of the Self-Generated Voltage for the HVLRO Under Wet Air Blanketing for an Aluminum-on-Steel Metallurgy (Test Conditions: Ball-on-Cylinder Device, 1000 g, 240 rpm, 25°C)

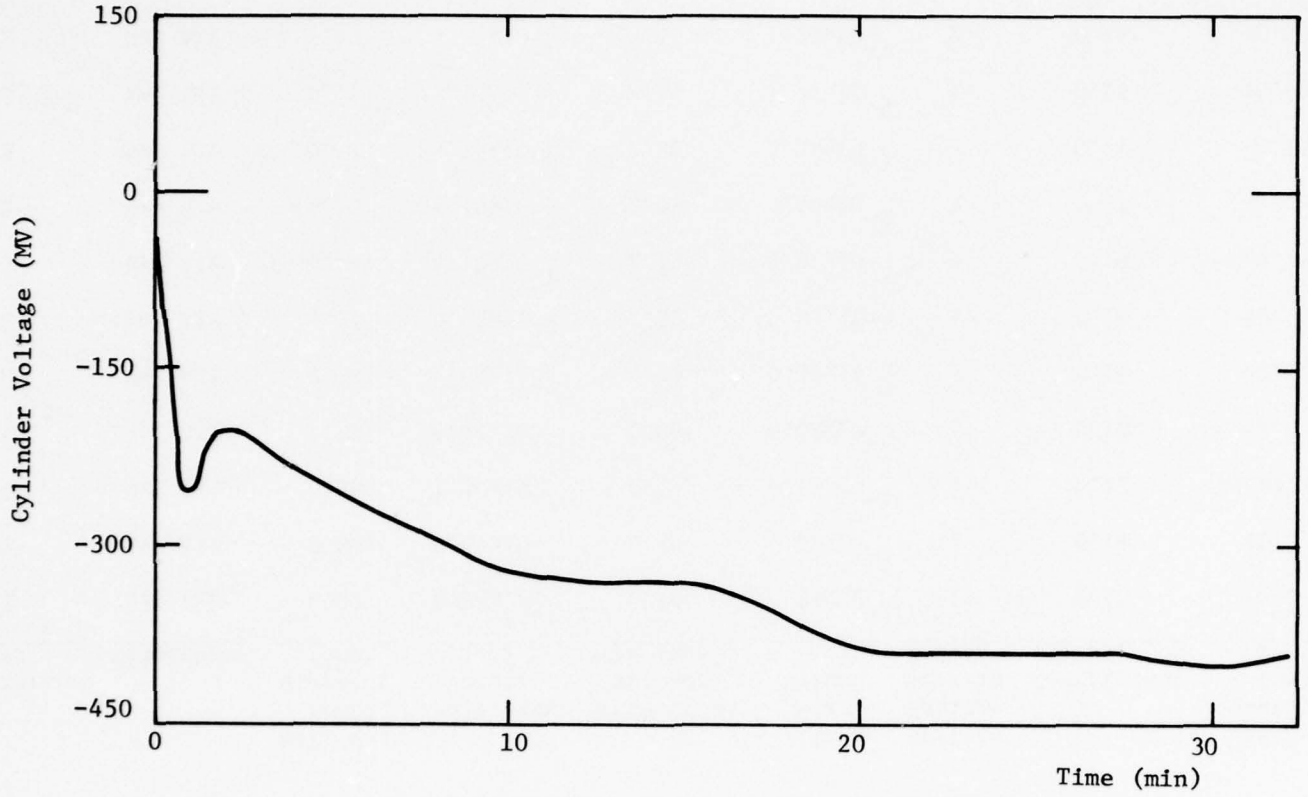

TABLE 24B

The Influence of Temperature Upon the Measured Wear and Self-Generated Voltage for the HVLRO Using the Steel Metallurgy(1)

Load (g)	Temperature (°C)	Atmosphere	Ball Wear Scar Diameter (mm)	Ball Wear Volume (cc)	Track Cross Sectional Area (cm^2)	Cylinder Wear Volume (cc)	Surface Fatigue Demerit Rating	Coefficient of Friction	Self-Generated Voltage (mv)(2)	Relative Film Resistance (Ohms)
500	25	Dry Air	0.22	0.18×10^{-7}	0.18	0.24×10^{-5}	1	0.16	+2.6	
500	52	Dry Air	0.30	0.63×10^{-7}	0.45	0.60×10^{-5}	2	0.14	+1.2	
500	79	Dry Air	0.36	1.30×10^{-7}	0.1	0.13×10^{-5}	1+	0.12	erratic	
500	25	Wet Air	0.27	0.41×10^{-7}	0.06	0.08×10^{-5}	1	0.15	+2.8	
500	52	Wet Air	0.34	1.03×10^{-7}	0.29	0.38×10^{-5}	2	0.18	+0.41	
500	79	Wet Air	0.31	0.92×10^{-7}	1.53	2.02×10^{-5}	1+	0.14	+0.42	
4000	25	Dry Air	0.48	4.10×10^{-7}	2.13	2.82×10^{-5}	3	0.19	-0.24	
4000	52	Dry Air	0.53	6.10×10^{-7}	2.65	3.50×10^{-5}	3	0.17	-0.18	
4000	79	Dry Air	0.58	8.75×10^{-7}	2.31	3.05×10^{-5}	3	0.19	-0.15	10
4000	25	Wet Air	0.46	3.46×10^{-7}	1.49	1.97×10^{-5}	1+	0.15	+0.09	10^2
4000	32	Wet Air	0.48	4.10×10^{-7}	0.91	1.20×10^{-5}	2	0.16	-0.09	
4000	52	Wet Air	0.45	3.17×10^{-7}	3.01	3.97×10^{-5}	2	0.18	-0.23	10
4000	79	Wet Air	0.50	4.83×10^{-7}	4.85	6.40×10^{-5}	2	0.19	-0.24	10

(1) Test Conditions: Ball-on-Cylinder device, loads as noted, 240 rpm, 32 min.
(2) The zero for the SGV's in the steel-on-steel system is temperature dependent and follows the relationship SGV (MV) = $0.209 - 6.96 \times 10^{-3}$ T (°C) over the temperature range 25°C - 160°C. SGV's have been temperature corrected.

FIGURE 30B

Traces Showing the Time Dependence of the Self-Generated Voltages for the HVLRO Under Dry Air Blanketing as a Function of Temperature Using the Steel Metallurgy (Test Conditions: Ball-on-Cylinder Device, 500 g, 240 rpm)

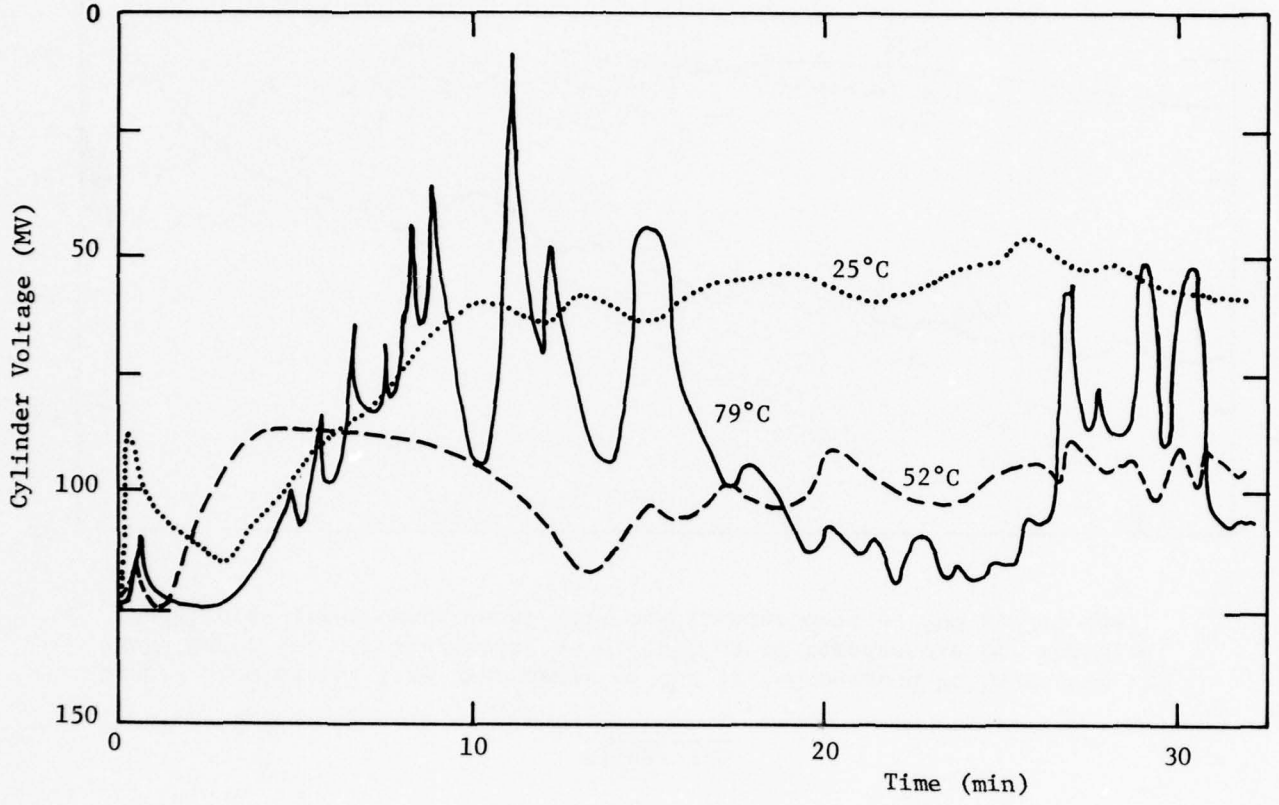

FIGURE 31B

Traces Showing the Time Dependence of the Self-Generated Voltages for the HVLRO Under Wet Air Blanketing as a Function of Temperature for the Steel Metallurgy (Test Conditions: Ball-on-Cylinder Device, 500 g, 240 rpm)

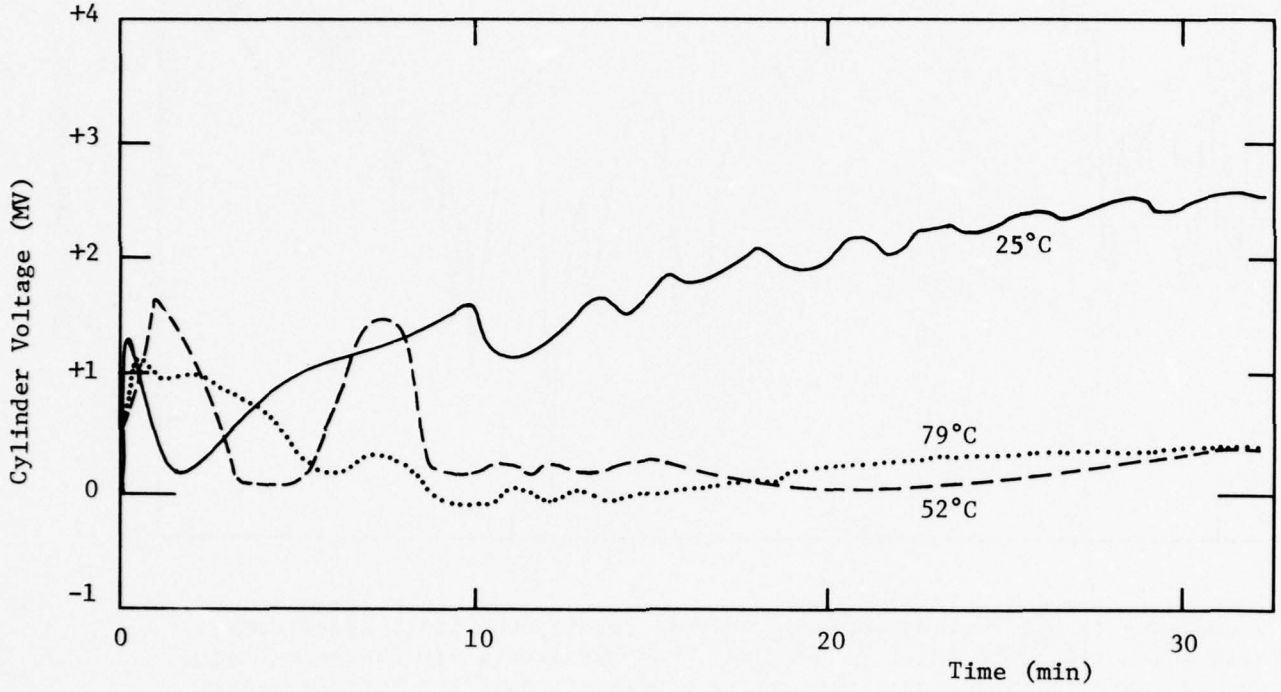

FIGURE 32B

Traces Showing the Time Dependence of the Self-Generated Voltages for the HVLRO Under Dry Air Blanketing as a Function of Temperature for the Steel Metallurgy (Test Conditions: Ball-on-Cylinder Device, 4000 g, 240 rpm)

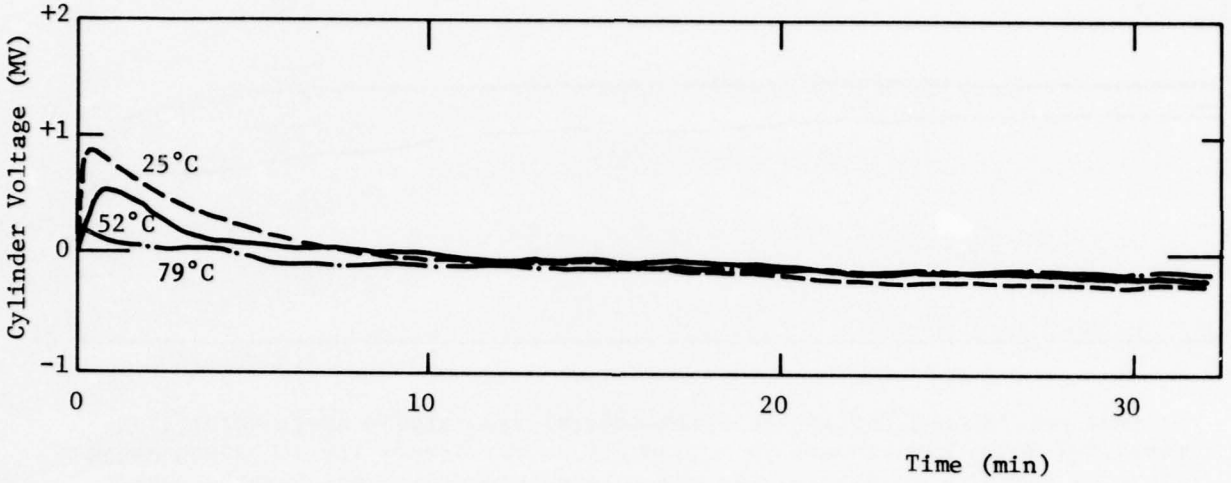

FIGURE 33B

Traces Showing the Time Dependence of the Self-Generated Voltages for the HVLRO Under Wet Air Blanketing as a Function of Temperature Using the Steel Metallurgy (Test Conditions: Ball-on-Cylinder Device, 4000 g, 240 rpm)

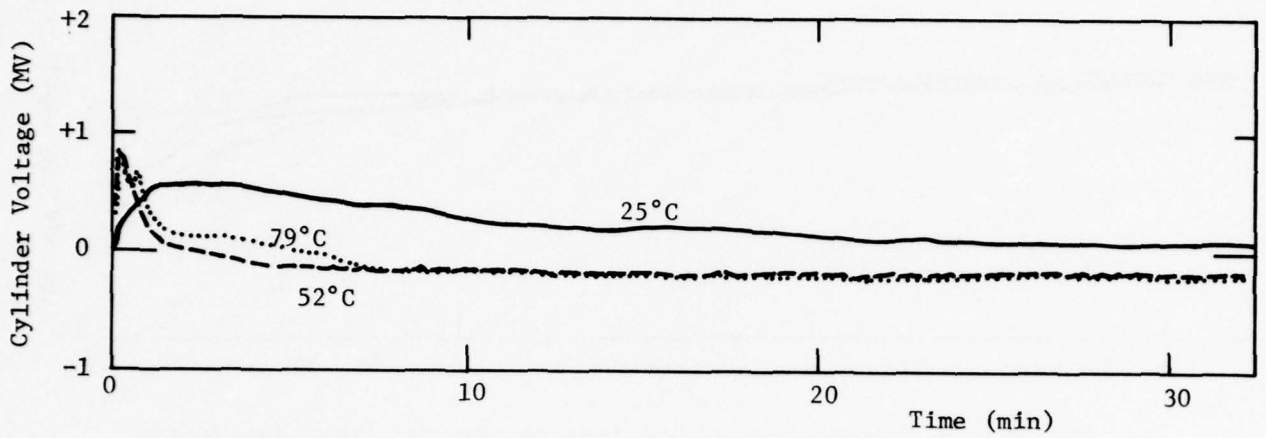

TABLE 25B

The Influence of Temperature Upon the Measured Wear and Self-Generated Voltage Under Dry Air Blanketing for the HVLRO Using an Aluminum-on-Steel Metallurgy(1)

Temperature (°C)	Ball Wear Scar Diameter (mm)	Ball Wear Volume (cc)	Track Cross Sectional Area (cm^2)	Cylinder Wear Volume (cc)	Surface Fatigue Demerit Rating	Coefficient of Friction	Self-Generated Voltage (mv)	Relative Film Resistance (Ohms)
25	0.34	1.03	0.07	0.09	1	0.13	+ 3.1	$5x10^4$
52	0.57	8.16	0.05	0.07	1	0.11	+ 0.36	10^2
79	0.43	2.64	0.08	0.11	1+	0.10	+13.5 (2)	
96	0.35	1.16	0.27	0.36	2	0.09	+17.1 (2)	$>10^5$
121	0.37	1.45	0.12	0.16	1	0.09	+ 5.4	10^3

(1) Test Conditions: Ball-on-Cylinder device, 1000 g, 240 rpm, 16 min.

(2) There were considerable fluctuations in the Traces of Self-Generated Voltages with time (Figure B) and hence these are approximate values.

FIGURE 34B-a

Traces Showing the Time Dependence of the Self-Generated Voltages for the HVLRO Under Dry Air Blanketing as a Function of Temperature for an Aluminum-on-Steel Metallurgy (Test Conditions: Ball-on-Cylinder Device, 1000 g, 240 rpm)

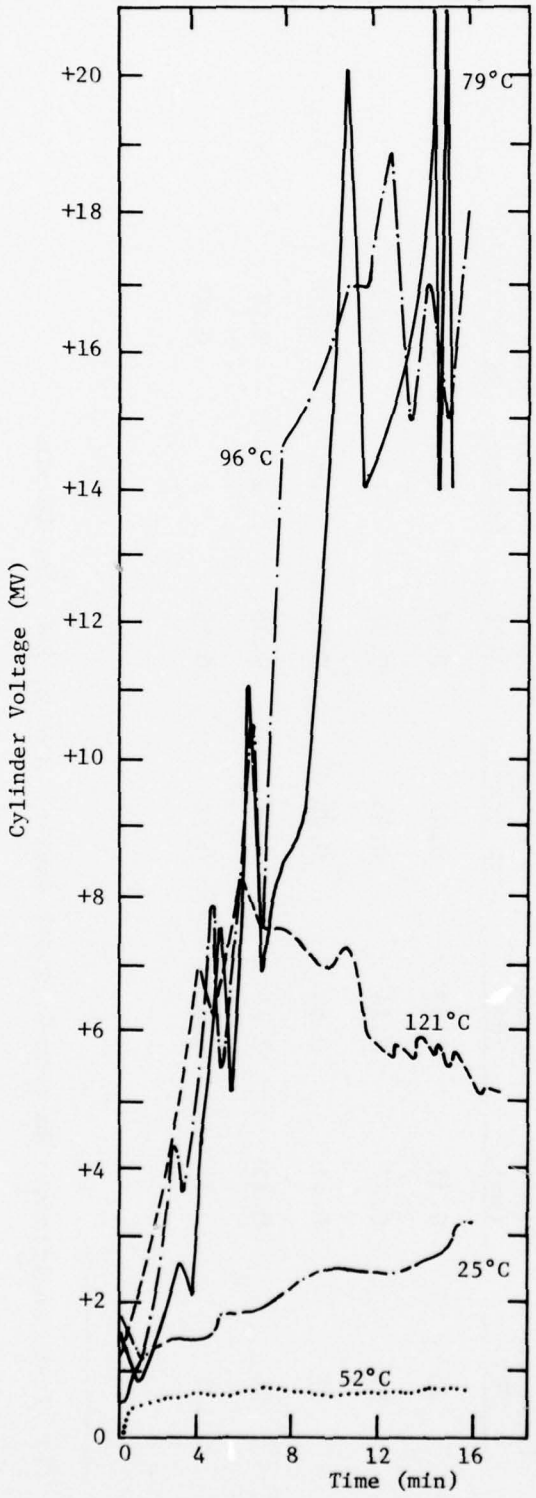

FIGURE 34B-b

Recorder Trace Showing the Actual Time Dependent Variation of the Self-Generated Voltage and Also an Oscillogram Showing the Near Instantaneous Variation of the Self-Generated Voltage for the Test at 52°C. (See Fig. 5B-b, Page 92, for Additional Discussion)

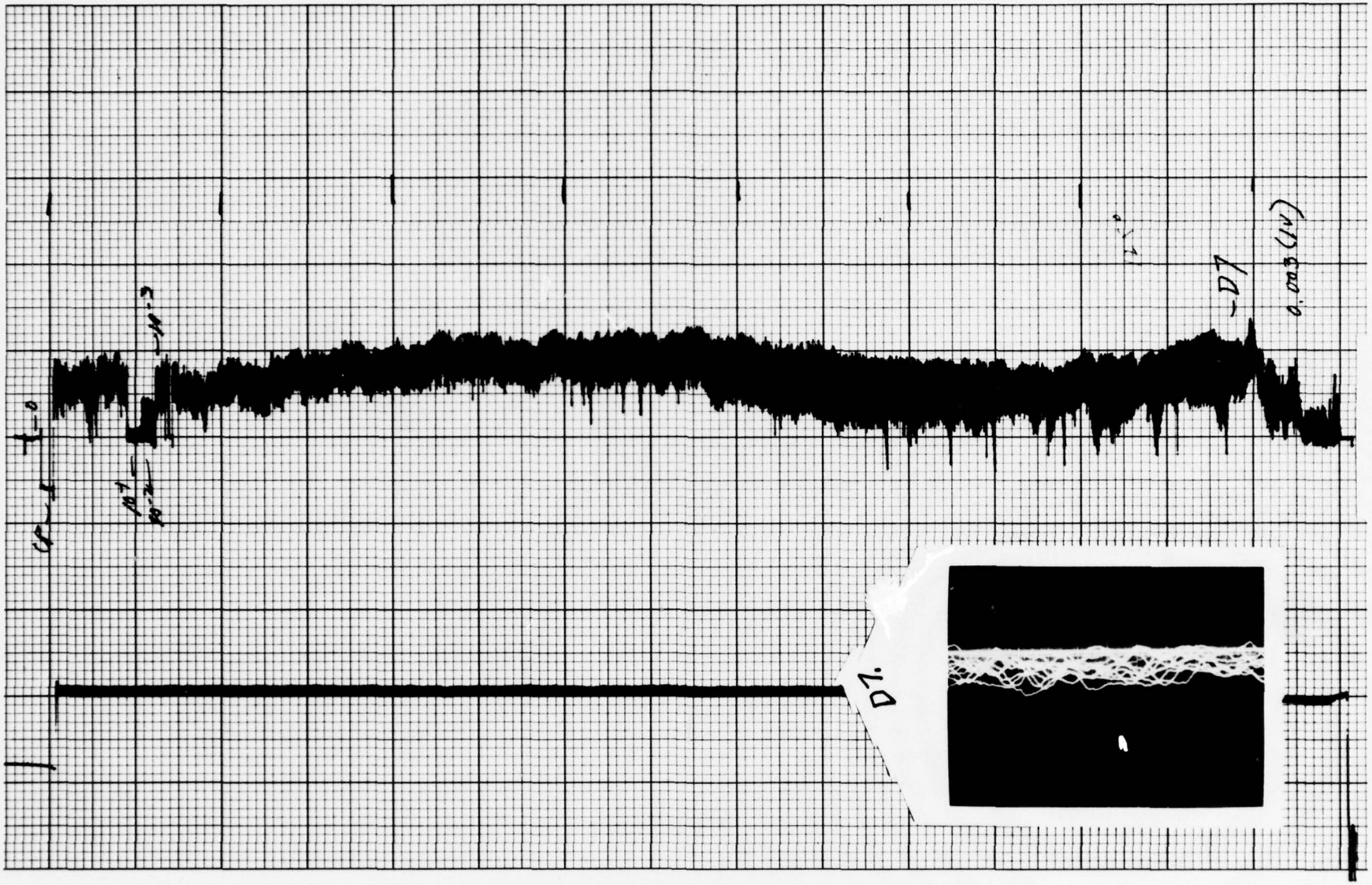

FIGURE 34B-c

Recorder Trace Showing the Actual Time Variation of the Self-Generated Voltage and Also Oscillograms Showing the Near Instantaneous Variations of the Self-Generated Voltages for the Test at 79°C. (See Fig. 5B-b, Page 92, for Additional Discussion)

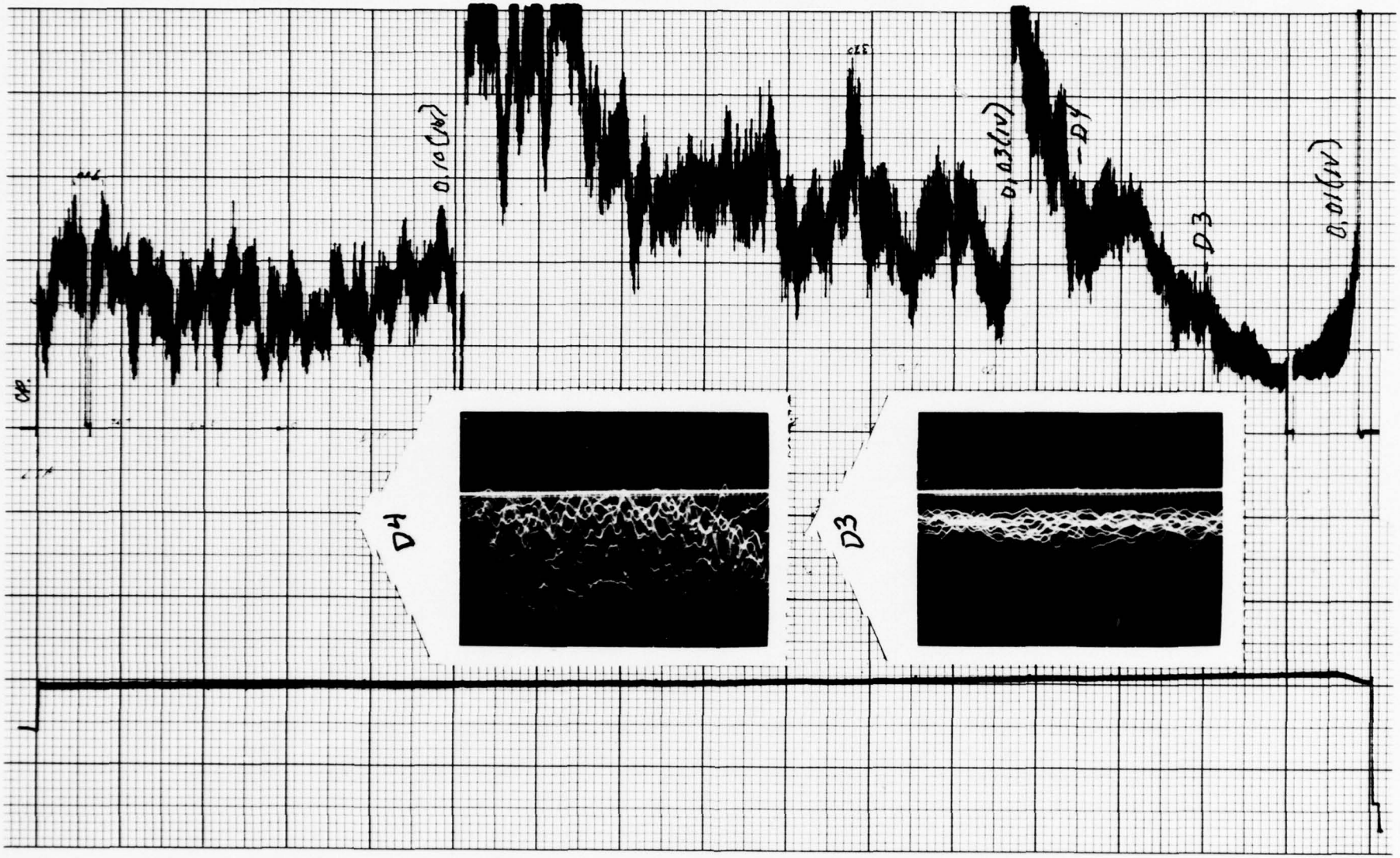

FIGURE 34B-d

Recorder Traces Showing the Actual Time VAriation of the Self-Generated Voltage and Also Oscillograms Showing the Near Instantaneous Variations of the Self-Generated Voltages for the Test at 121°C. (See Fig. 5B-b, Page 92, for Additional Discussion)

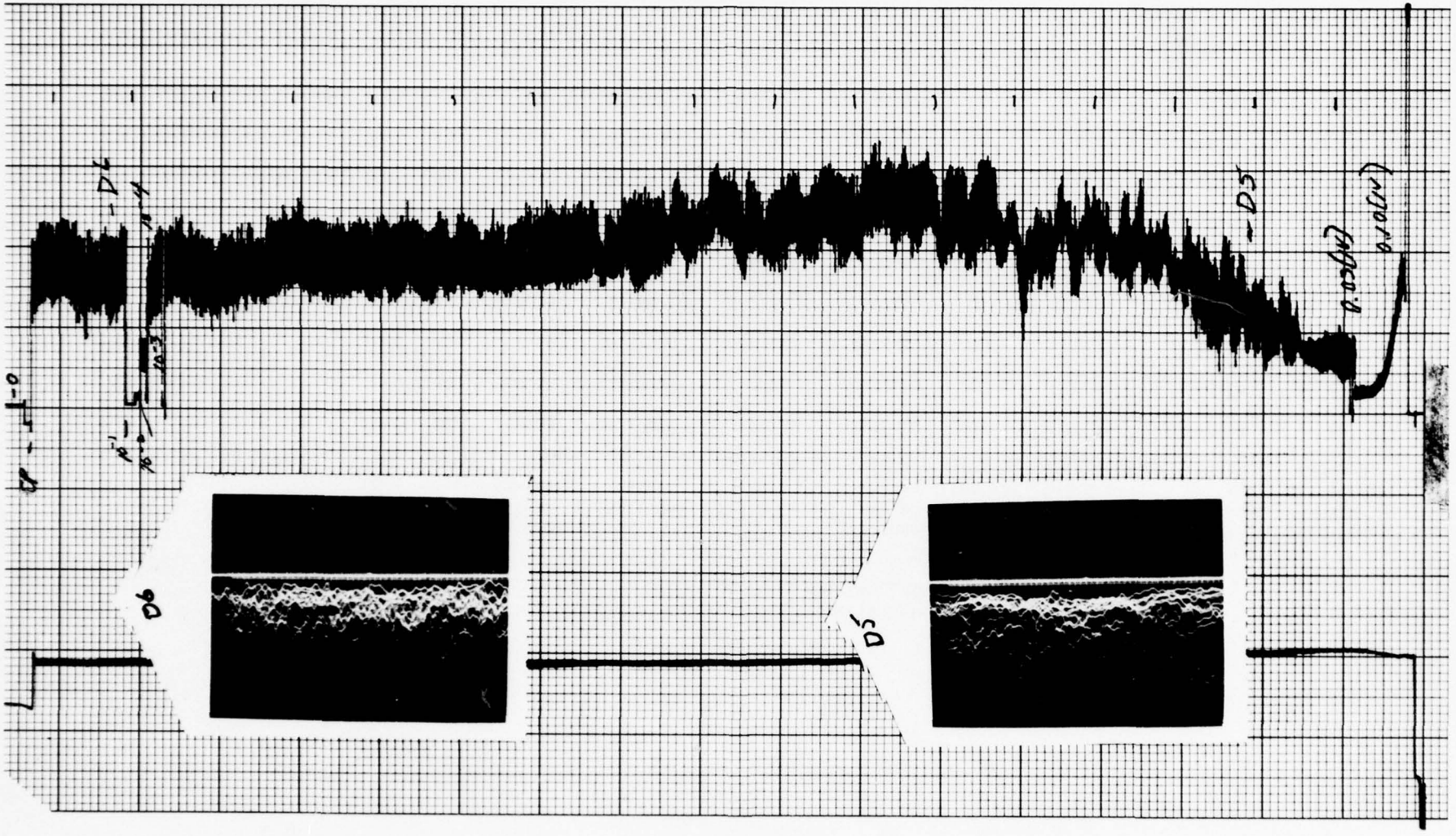

TABLE 26B

Measured Wear and Self-Generated Voltages for Aromatic Hydrocarbons Mixed with the LVWO Under Dry Air Blanketing Using the Steel Metallurgy(1)

Additive in LVWO	Load (g)	Time (min)	Ball Wear Scar Diameter (mm)	Ball Wear Volume (cc)	Track Cross Sectional Area (cm^2)	Cylinder Wear Volume (cc)	Surface Fatigue Demerit Rating	Coefficient of Friction	Self-Generated Voltage (cc)	Relative Film Resistance (Ohms)
None	1000	32	0.53	6.10×10^{-7}	0.23	0.30×10^{-5}	1	0.19	+0.18	10
20% Toluene	1000	32	0.63	12.18×10^{-7}	0.25	0.33×10^{-5}	3	0.20	+0.15	10
20% Mesitylene	1000	32	0.60	10.02×10^{-7}	0.17	0.22×10^{-5}	1	0.19	+0.40	50
20% 1-Methylnaphthalene	1000	32	0.35	1.16×10^{-7}	0.13	0.17×10^{-5}	2	0.18	+3.0	10^3
20% 1-Chloronaphthalene	1000	32	0.57	8.16×10^{-7}	0.32	0.42×10^{-5}	1	0.17	+4.0	10^3
None	2000	32	0.77	27.17×10^{-7}	0.34	0.45×10^{-5}	3	0.39	-0.05	
20% 1-Methylnaphthalene	2000	32	0.50	4.83×10^{-7}	0.84	1.11×10^{-5}	3	0.21	-0.15	10
20% 1-Chloronaphthalene	2000	45	0.68	16.53×10^{-7}	1.39	1.83×10^{-5}	3	0.19	+0.8	10^2
20% 1-Chloronaphthalene	4000	45	0.80	31.66×10^{-7}	1.75	2.31×10^{-5}	3	0.15	+0.45	10^3

Test Conditions: Ball-on Cylinder Device, 240 rpm, 25°C

FIGURE 35B

Traces Showing the Time Dependence of the Self-Generated Voltages for Aromatic Hydrocarbons - LVWO Mixtures Under Dry Air Blanketing Using the Steel Metallurgy (Test Conditions: Ball-on-Cylinder Device, 240 rpm, 25°C)

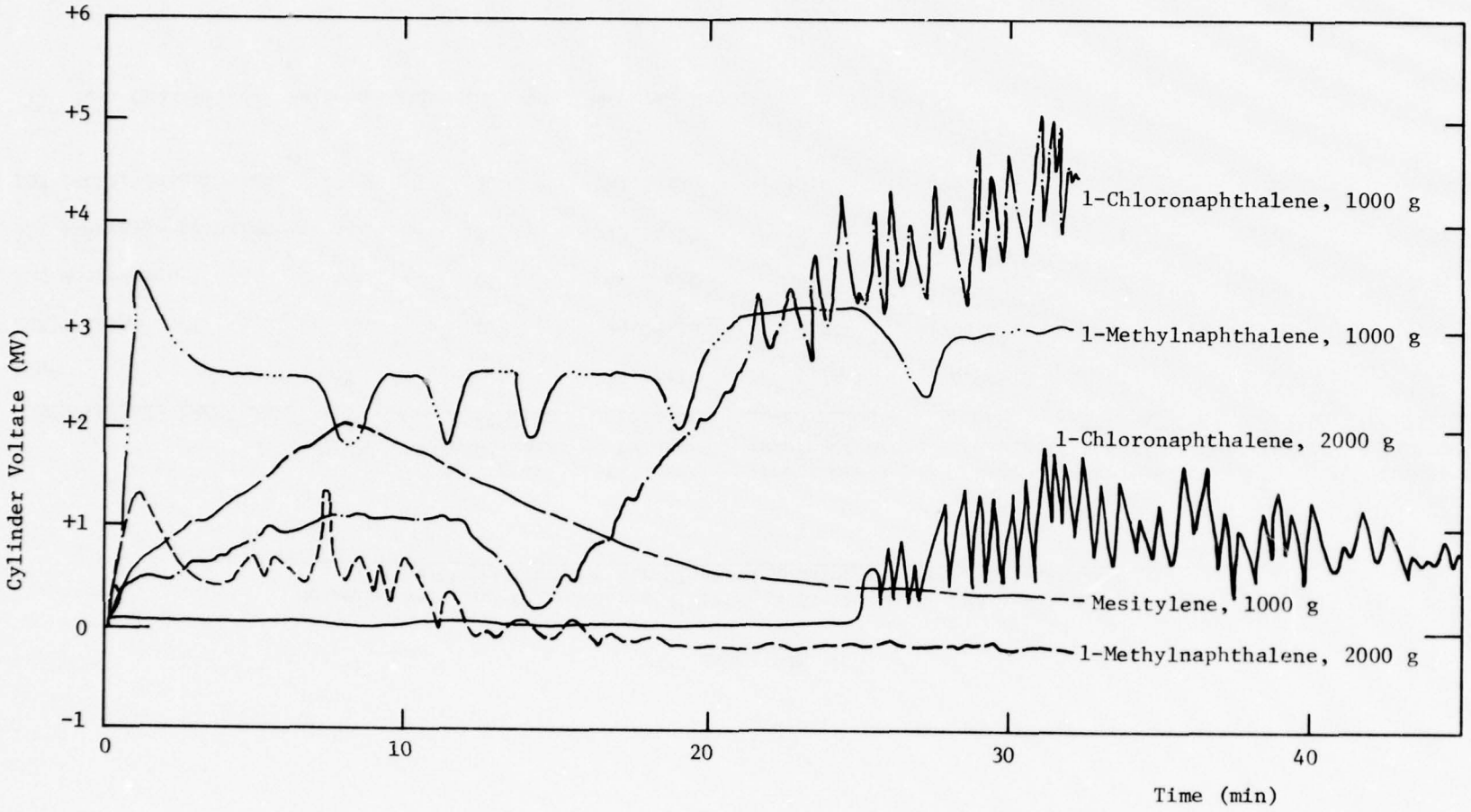

TABLE 27B

Measured Wear and Self-Generated Voltages for Aromatic Hydrocarbons Mixed With the LVWO Under Wet Air Blanketing Using the Steel Metallurgy(1)

Additive in Bayol 35	Time (min)	Ball Wear Scar Diameter (mm)	Ball Wear Volume (cc)	Track Cross Sectional Area (cm^2)	Cylinder Wear Volume (cc)	Surface Fatigue Demerit Rating	Coefficient of Friction	Self-Generated Voltage (mv)
None	32	0.75	24.46×10^{-7}	0.72	0.95×10^{-5}	3	0.22	+0.15
20% Toluene	15	0.87	44.28×10^{-7}	>0.24	$>0.32 \times 10^{-5}$	3	0.23	0.0
20% Mesitylene	15	0.87	44.28×10^{-7}	0.60	0.79×10^{-5}	2	0.21	+0.01
20% 1-Methylnaphthalene	32	0.67	15.58×10^{-7}	0.45	0.59×10^{-5}	1	0.20	+0.18
20% 1-Chloronaphthalene	32	1.33	241.87×10^{-7}	>0.45	$>0.59 \times 10^{-5}$	3	0.20	+0.02

(1) Test Conditions: Ball-on-Cylinder Device, 240 rpm, 25°C.

TABLE 28B

Measured Wear and Self-Generated Voltages for Aromatic Hydrocarbons Mixed With the LVWO Under Dry Air Blanketing Using an Aluminum-on-Steel Metallurgy(1)

Additive in LVWO	Load (g)	Time (min)	Ball Wear Scar Diameter (mm)	Ball Wear Volume (cc)	Track Cross Sectional Area (cm^2)	Cylinder Wear Volume (cc)	Surface Fatigue Demerit Rating	Coefficient of Friction	Self-Generated Voltage (mv) 16 min	32 min
20% Toluene	500	16	0.35	1.16×10^{-7}	0.08	0.11×10^{-5}	1	0.20	+5.8	
None	1000	16	0.42	2.41×10^{-7}	0.20	0.26×10^{-5}	3	0.19	+0.45	
20% Toluene	1000	16	0.43	2.64×10^{-7}	0.10	0.13×10^{-5}	1+	0.19	+0.48	
20% Mesitylene	1000	16	0.42	2.41×10^{-7}	0.22	0.29×10^{-5}	3	0.17	+0.45	
20% 1-Methylnaphthalene	1000	16	0.42	2.41×10^{-7}	0.13	0.17×10^{-5}	1	0.17	+2.6	
20% Toluene	2000	16	0150	4.83×10^{-7}	0.23	0.30×10^{-5}	3	0.21	+0.45	
20% Mesitylene	2000	16	0.45	3.17×10^{-7}	0.24	0.32×10^{-5}	1	0.20	+0.66	
20% 1-Chloronaphthalene	4000	32	0.67	15.58×10^{-7}	1.30	1.74×10^{-5}	3	0.18	+0.24	+0.12

Test Conditions: Ball-on-Cylinder Device, 240 rpm, 25°C

FIGURE 36B

Traces Showing the Time Dependence of the Self-Generated Voltages for Aromatic Hydrocarbon - LVWO Mixtures Under Dry Air Atmosphere Blanketing Using an Aluminum-on-Steel Metallurgy (Test Conditions: Ball-on-Cylinder Device, 240 rpm, 25°C)

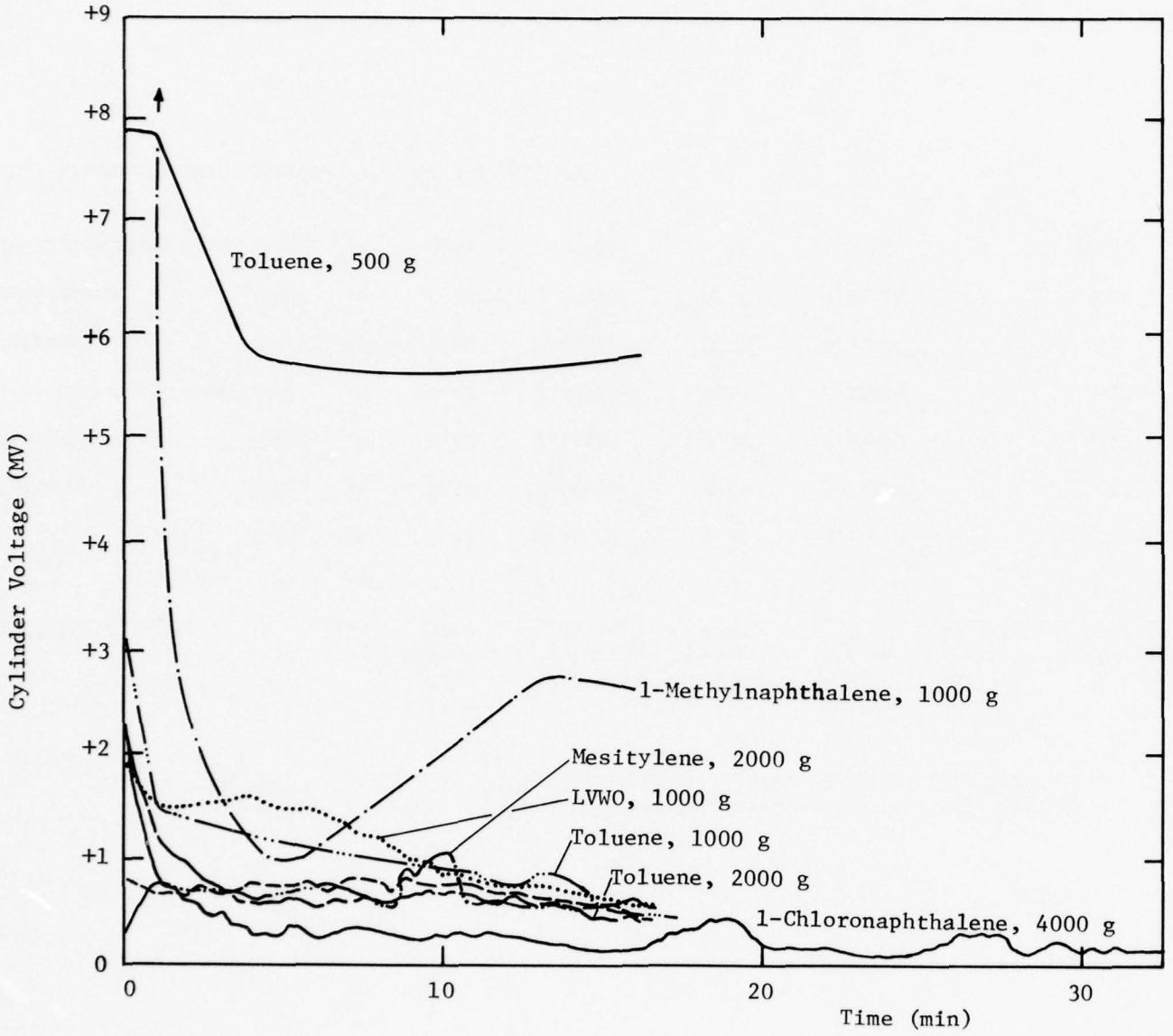

TABLE 29B

Measured Wear and Self-Generated Voltages for Ester Base Stocks Using the Steel Metallurgy(1)

Lubricant	Load (g)	Atmosphere	Ball Wear Scar Diameter (mm)	Ball Wear Volume (cc)	Track Cross Sectional Area (cm^2)	Cylinder Wear Volume (cc)	Surface Fatigue Demerit Rating	Coefficient of Friction	Self-Generated Voltage (mv)	Apparent Film Resistance (Ohms)
Di-2-Ethylhexyl Sebacate	500	Wet Air	0.24	0.26×10^{-7}	0.11	0.15×10^{-5}	1+	0.10	+0.69	10^4
Di-2-Ethylhexyl Sebacate	1000	Wet Air	0.25	0.30×10^{-7}	0.18	0.24×10^{-5}	1	0.11	+0.57	10^3
Di-2-Ethylhexyl Sebacate	2000	Wet Air	0.28	0.48×10^{-7}	0.19	0.25×10^{-5}	1	0.12	+0.24	10^3
Di-2-Ethylhexyl Adipate	2000	Wet Air	0.33	0.92×10^{-7}	0.54	0.71×10^{-5}	3	0.12	+0.06	10^3
Hercolube J	2000	Wet Air	0.32	0.81×10^{-7}	0.37	0.49×10^{-5}	3	0.11	+1.41	10^3
Di-2-Ethylhexyl Adipate	2000	Dry Air	0.31	0.71×10^{-7}	0.95	1.25×10^{-5}	1	0.12	+0.20	10^3
Hercolube J	2000	Dry Air	0.30	0.63×10^{-7}	0.38	0.50×10^{-5}	3	0.12	+1.50	
Di-2-Ethylhexyl Adipate	2000	Argon	0.37	1.45×10^{-7}	1.10	1.45×10^{-5}	3	0.13	+0.03	
Hercolube J	2000	Argon	0.38	0.90×10^{-7}	0.30	0.40×10^{-5}	1	0.12	+0.03	10
Di-2-Ethylhexyl Azelate	4000	Wet Air	0.37	1.45×10^{-7}	1.93	2.55×10^{-5}	1+	0.14	+0.24	10^2

Test Conditions: Ball-on-Cylinder Device, 240 rpm, 25°C.

FIGURE 37B

Traces Showing the Time Dependence of the Self-Generated Voltages for Di-2-Ethylhexyl Sebacate Under Wet Air Blanketing as a Function of Load Using the Steel Metallurgy (Test Conditions: Ball-on-Cylinder Device, 240 rpm, 25°C)

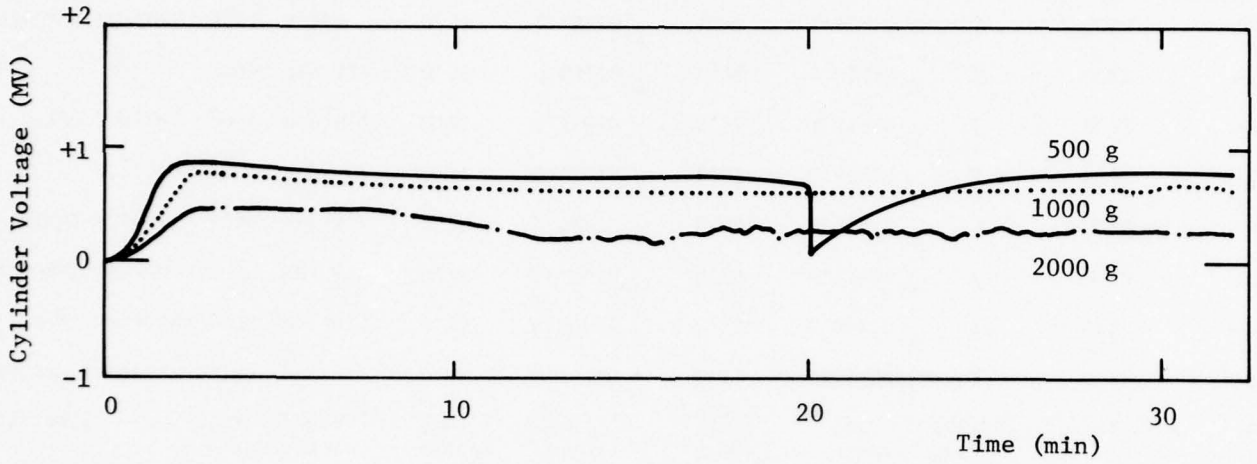

FIGURE 38B

Traces Showing the Time Dependence of the Self-Generated Voltages for Di-2-Ethylhexyl Adipate and Hercolube J Using the Steel Metallurgy (Test Conditions: Ball-on-Cylinder Device, 2000 g, 240 rpm, 25°C)

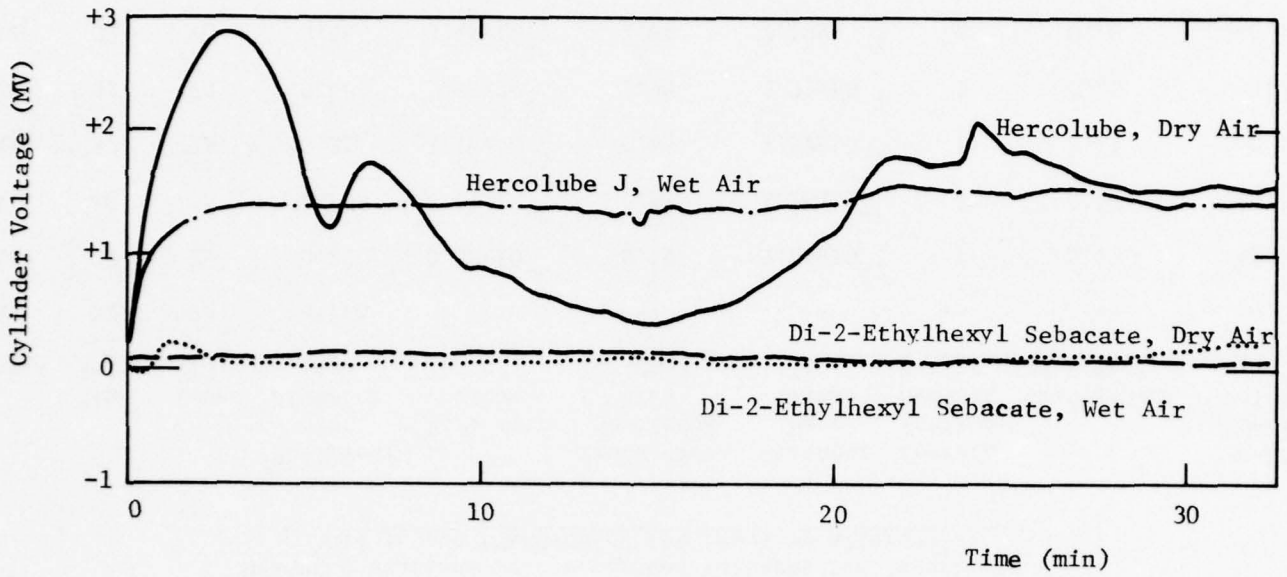

TABLE 30B

Measured Wear and Self-Generated Voltages for Isostearic Acid in the HVLRO Using the Steel Metallurgy[1]

Load (g)	Atmosphere	Time (min)	Temp. (°C)	Ball Wear Scar Diameter (mm)	Ball Wear Volume (cc)	Track Cross Sectional Area (cm^2)	Cylinder Wear Volume (cc)	Surface Fatigue Demerit Rating	Coefficient of Friction	Self-Generated Voltage (mv)[2]	Apparent Film Resistance (Ohms)
2000	Argon	32	79	Failed	--	--	--	--	--	~0.0	
2000	Wet Air	32	25	0.25	0.30×10^{-5}	0.19	0.25×10^{-7}	1	0.13	+3.7	10^5
4000	Wet Air	48	25	0.38	1.61×10^{-5}	0.88	1.16×10^{-7}	2	0.17	+0.15	10
4000	Dry Air	32	25	0.35	1.16×10^{-5}	0.85	1.12×10^{-7}	1+	0.15	+0.40	
4000	Wet Air	32	70	0.40	1.98×10^{-5}	2.98	3.93×10^{-7}	1	0.18	-0.21	
4000	Dry Air	32	70	0.46	3.46×10^{-5}	1.66	2.19×1^{-7}	3	0.18	-0.12	10^2

(1) Test Conditions: Ball-on-Cylinder Device, 1% Isostearic Acid, 240 rpm.
(2) The zero for the SGV's in the steel-on-steel system is temperature dependent and follows the relationship SGV (MV) = $0.209 - 6.96 \times 10^{-3}$ T (°C) over the temperature range 25°C - 160°C. SGV's have been temperature corrected.

FIGURE 39B

Traces Showing the Time Dependence of the Self-Generated Voltages for 1% Isostearic Acid in the HVLRO Using the Steel Metallurgy (Test Conditions: Ball-on-Cylinder Device, 240 rpm)

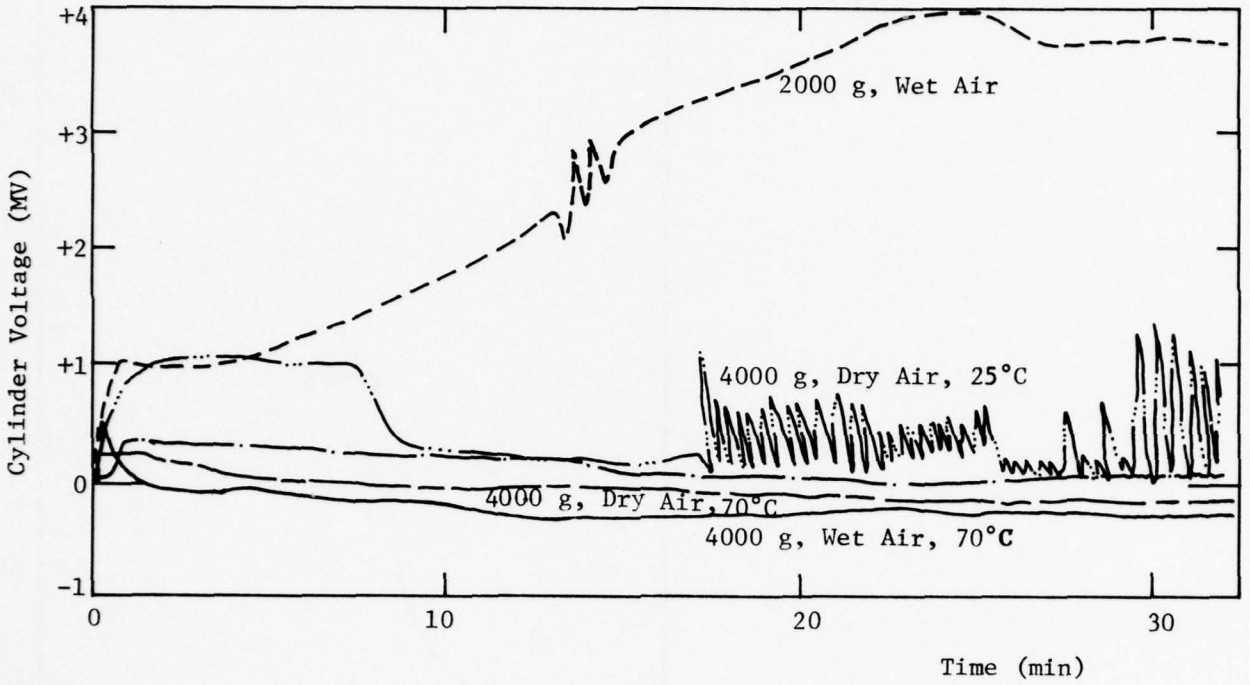

FIGURE 40B

Self-Generated Voltages as Mesured for 3% Tricresyl Phosphate in LVWO Under Various Blanketing Atmospheres (Test Conditions: Ball-on-Cylinder Device, 500 g, 240 rpm)

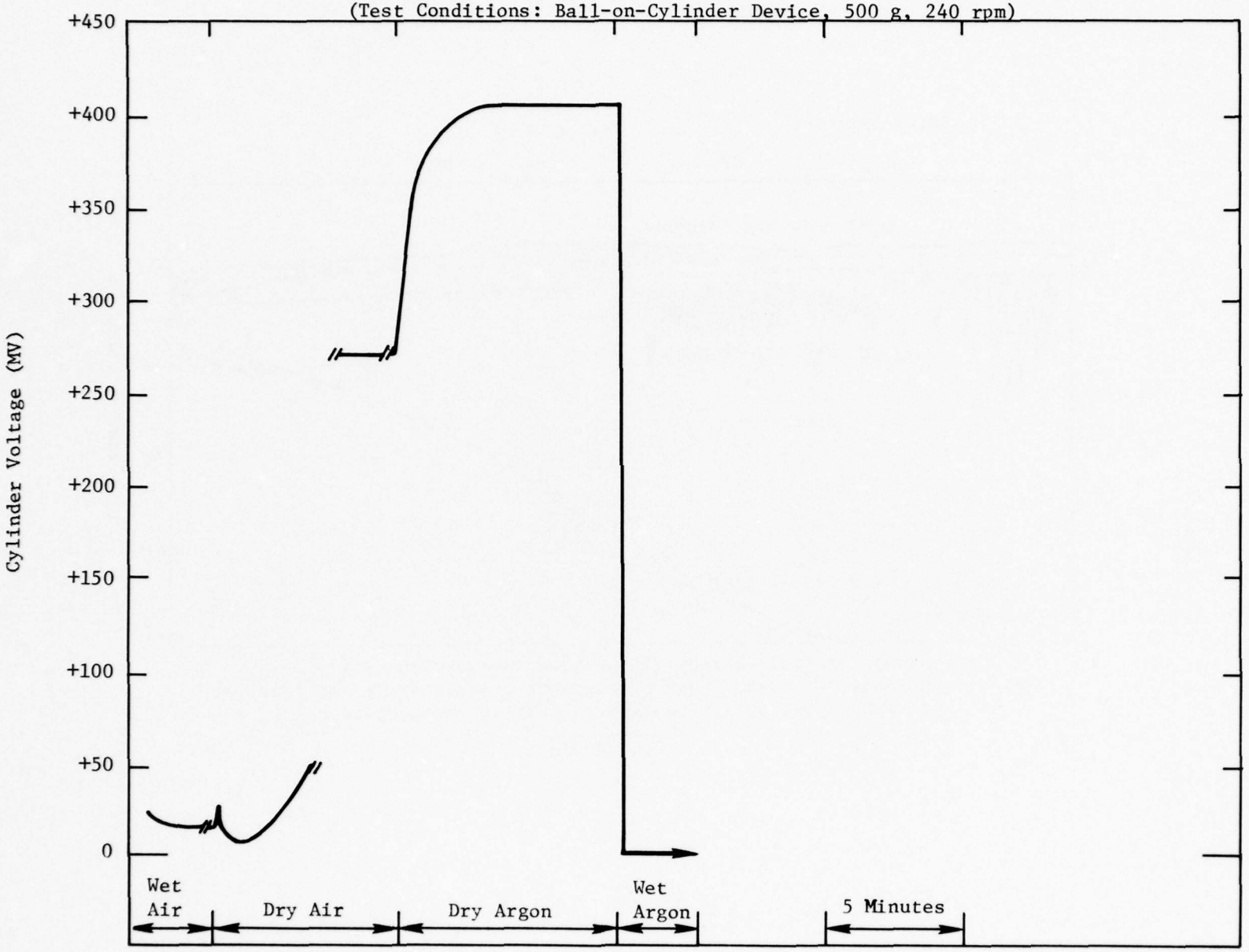

FIGURE 41B

Self-Generated Voltages as Measured for 3% Tricresyl Phosphate in HVLRO Under Various Blanketing Atmospheres (Test Conditions: Ball-on-Cylinder Device, 2000 g, 240 rpm)

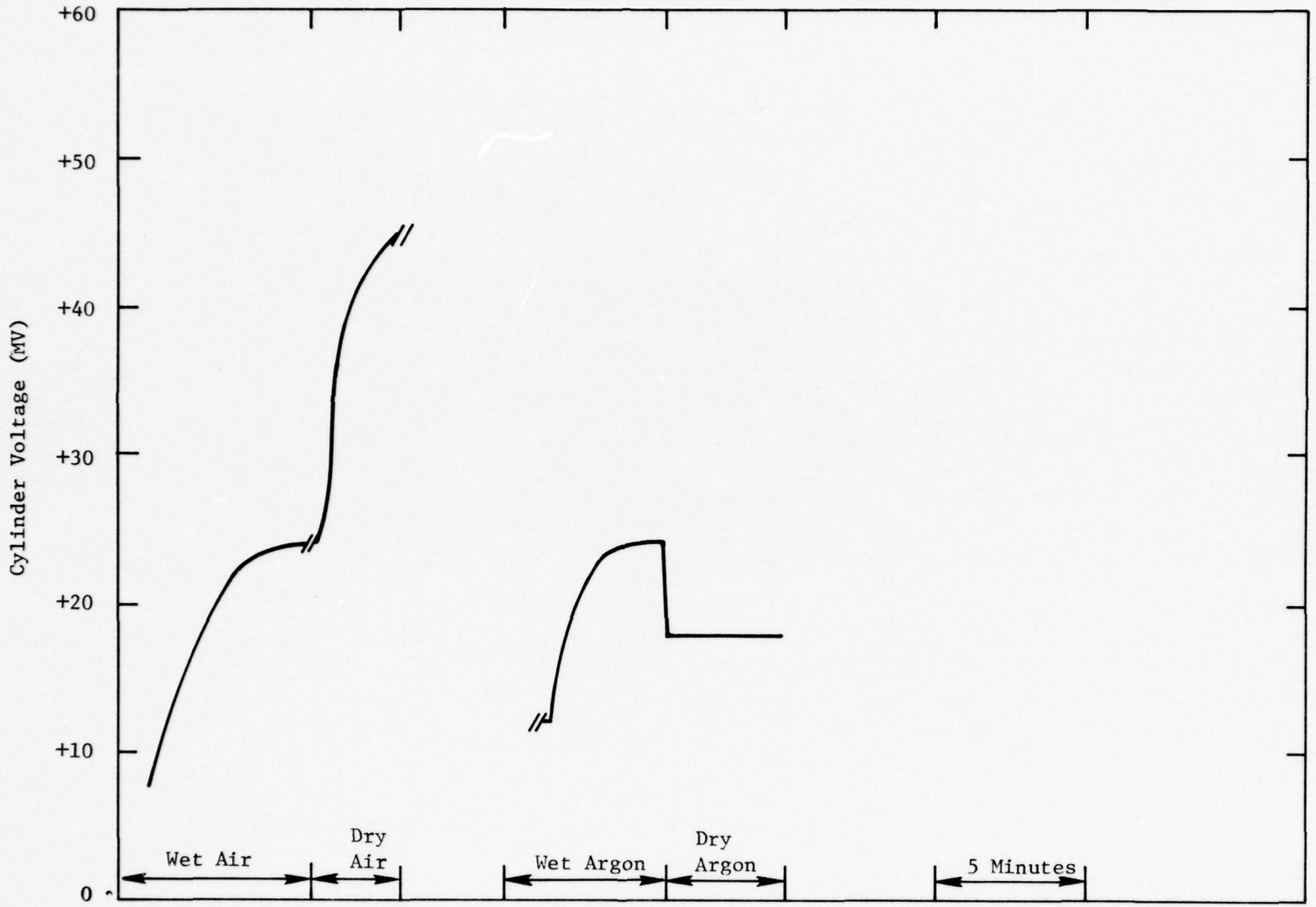

APPENDIX C

AN ANALYSIS OF THE NEAR SURFACE MICROSTRUCTURE PRODUCED BY WEAR

R. N. Pangborn and S. Weissmann
College of Engineering, Rutgers University
P. O. Box 909, Piscataway, N. J. 08854

Prepared for: I. L. Goldblatt
Products Research Division
EXXON Research and Engineering Company
P. O. Box 51, Linden, N. J. 07036

INTRODUCTION

The defect structure induced by wear in the near surface layers of aluminum was studied using an x-ray double crystal diffractometer method for polycrystalline materials. An aluminum disk was provided with wear tracks produced under various conditions: (1) steel-on-aluminum in dry air, HVLRO lubrication and 1 kg load, 1 min. and 30 min. duration; (2) same system with substitution of HVWO for 30 sec.; (3) same as initial system but in wet air for 30 min.; (4) aluminum-on-aluminum in wet air for 1 min.

The x-ray double crystal diffractometer is designed to measure both the lattice misalignment and internal strain induced in the near surface grains of a deformed material. X-ray rocking curves, indicating the range of reflection (i.e. wider angles of reflection are associated with higher degrees of imperfection), were taken in the parallel arrangement. A dislocation-free silicon single crystal in the (111) orientation was used to obtain monochromatized Cu K_{α} radiation. Exposures were taken at angular rotation positions (12 minutes of arc intervals of the specimen to generate

pictoral rocking curves for each grain on a cylindrical film. In this way, each reflecting grain of the specimen was considered to function independently as the second crystal of the double crystal diffractometer. Appropriate film shifts accompanying each angular setting produced an array of spots of rising and falling intensity as each grain was rotated through its range of reflection. The rocking curves, so manifested, were analyzed from each of the Debye-Scherrer rings having suitable Bragg angles, and treated statistically. (Fig. 1C)

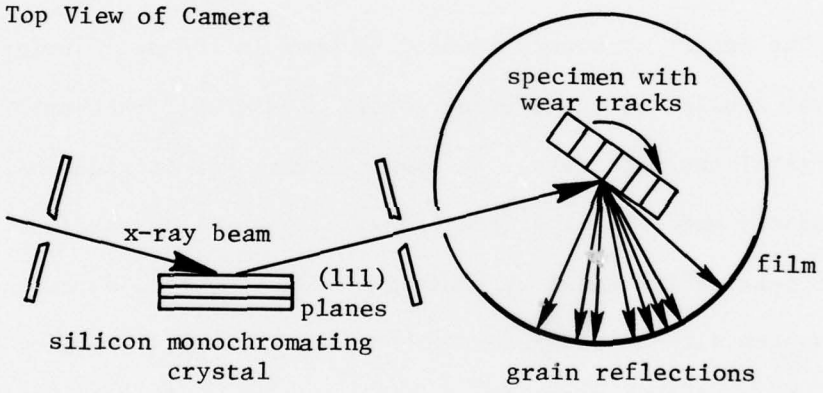

FIGURE 1C Schematic Diagram of an X-Ray Double Crystal Diffractometer

DISCUSSION OF X-RAY THEORY APPLIED

This x-ray method measures the lattice defects of each individual grain. When the lattice defects are introduced by deformation, the dislocations accumulated locally break up the grain into coherently reflecting lattice domains. The strain distribution derives principally from the accumulated dislocation configurations which determine the misorientation between coherently reflecting lattice domains. (Fig. 2C)

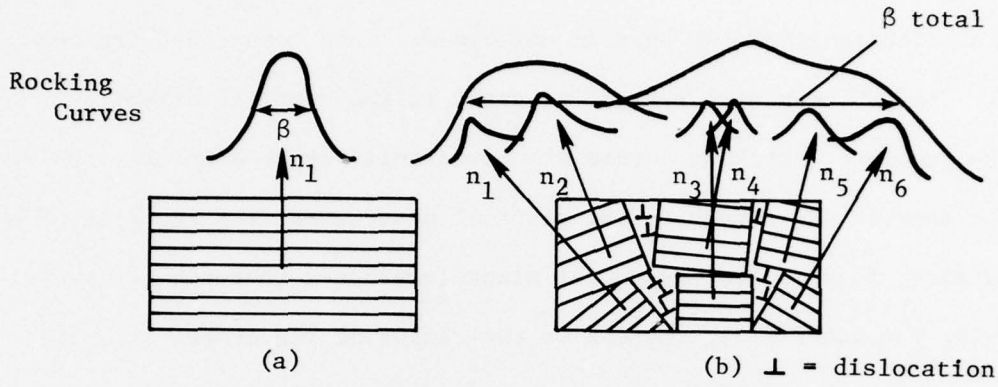

FIGURE 2C Lattice Misalignment and Associated Rocking Curves
(a) Before Deformation, (b) After Deformation

The misorientation is expressed by the respective normals n_1, n_2, . . ., n_6, . . ., n_n of the lattice domain. Each domain may also have defects accumulated internally, giving rise to smaller rocking curves which can be resolved at early stages or low degrees of deformation. This allows determination of the strains within the small domains or "particles," as they are called by Warren-Averbach (1C). The composite of the small rocking curves, technically their "convolution," is the overall rocking curve, β_{total}. As the domains become smaller and smaller as a result of deformation, the composite rocking curve becomes broader and smoother. Because of the advanced stage of deformation caused by wear processes, it is this overall rocking curve that is of interest (the break-up being too complete to allow interpretation of the individual spot sequence in terms of internal "particle" strains).

A second analytical tool furnished by the double crystal diffractometer method is the vertical break-up of the individual arrays. Although the x-ray beam is rigidly parallel in the plane of the diffractometer (the

horizontal plane) by reflection from the monochromatizing silicon crystal, the vertical divergence of the beam is unimpeded. This means that the beam effectively "rocks" over each reflecting grain in the vertical direction during each exposure. Rocking curves of this origin may be similarly analyzed, taking into account the change in the vertical divergence as a function of each spot's distance, Y, from the equatorial plane (expressed in terms of the azimuthal angle, $\Psi = \tan^{-1}(Y/R)$, where R is the radius of the camera (2C, 3C)). The azimuthal spread or vertical length of the spot expressed in degrees, $\Delta\Psi$, thus obtained should correspond favorably with the rocking curves obtained by controlled specimen rotation and application of a parallel x-ray beam.

RESULTS

In Table 1C are gathered the results obtained by analysis of five wear tracks and an undeformed (fresh surface, as mechanically polished) portion of the aluminum disk. Their interpretation is as follows:

(1) The overall rocking curve width, β, is the horizontal range of reflection, averaged for 25 to 40 grain reflections. The standard deviation, σ^2, of these values is on the order of 10 minutes of arc. (Fig. 3C)

(2) The median value of the rocking curve width, β_m, is indicative of the number of grains which, as a result of the wear process, have widths exceeding those typical of the undeformed material. This value is meaningful since it was experimentally imperative that the x-ray beam width was so set as to slightly exceed the wear track width, therefore impinging on both deformed and undeformed grains. The degree to which grains in the track are broadened with respect to the undeformed material at either side of the track included within the beam's span, is reflected by the median value.

TABLE 1C

Effect of Wear Upon the Build-Up of Near Surface Strain

Column 1	2	3	4	5	6
TEST	CONDITIONS UNDER WHICH WEAR WAS PERFORMED	VISIBLE DAMAGE	β	β_m	$\Delta\Psi$
			(minutes of arc)		
0	None Track Surface	undeformed (polishing scratches)	85.3	84	77.4
1	Steel/Aluminum load: 1 kg lubricant: HVLRO dry air duration: 30 min.	medium, shallow wear	110.6	108	117.6
2	Steel/Aluminum load: 1 kg lubricant: HVWO dry air duration: 30 sec.	medium, deep wear	115.1	120	126.6
3	Aluminum/Aluminum load: 1 kg lubricant: HVLRO wet air duration: 1 min.	heavy, deep wear grayish color	117.9	120	140.4
4	Steel/Aluminum load: 1 kg lubricant: HVLRO dry air duration: 1 min.	light, shallow wear	97.5	96	112.2
5	Steel/Aluminum load: 1 kg lubricant: HVLRO wet air duration: 30 min.	very light, shallow wear	89.4	90	99.1

(3) The azimuthal spread, $\Delta\Psi$, is the manifestation of the vertical break-up and is therefore informative with regard to the induced wear damage. It represents the mean value of 12 grain reflections, each adjusted for its deviation from the equatorial plane. For these values, σ^2 is on the order of 9 minutes of arc. (Fig. 3C)

$\Delta\Psi$ = azimuthal spread

β = rocking curve width from controlled specimen rotation using a parallel beam

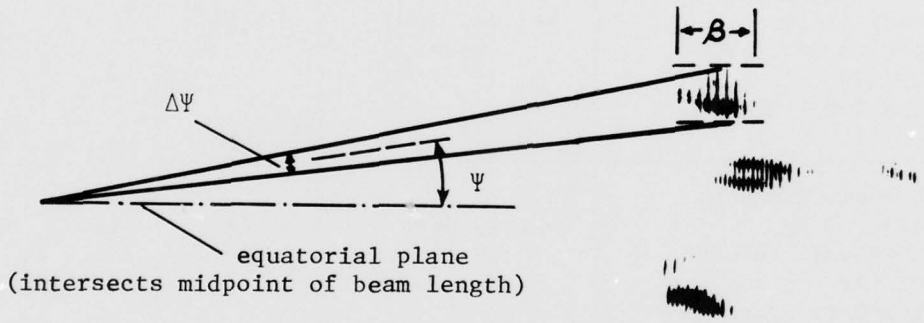

FIGURE 3C Enlargement of Typical Grain Reflections From a Deformed Aluminum Alloy Specimen

CONCLUSIONS

By comparing the mean rocking curve width, β (column 4 of Table 1C), and the median rocking curve width, β_m (column 5), with the azimuthal spread of the lattice misalignment, $\Delta\Psi$ (column 6) it may be seen that the results are self consistent. It may be observed also that the measured increase of lattice misalignment appears to be in good agreement with the magnitude of imposed wear produced under varied conditions.

SUGGESTIONS FOR FUTURE WORK

X-ray rocking curve studies are sensitive to disclosing the lattice distortions induced by different conditions of wear, and in addition can be used to obtain a quantitative assessment of the wear damage. It is suggested that the depth effect of wear can be elucidated by (a) step-wise removal of surface layers and subsequent x-ray analysis, and (b) application of x-rays with different wavelengths and thus different penetration characteristics.

REFERENCES

1C. Warren, B. E. X-ray Diffraction. (Reading, Mass: Addison-Wesley Publishing Co., 1969).

2C. Reis, A. J., Slade, J. J., and Weissmann, S., J. Applied Physics, 22, #5 665 (1951).

3C. Slade, J. J., Weissman, S., J. Applied Physics, 23, #3, 323 (1952).

DISTRIBUTION LIST

Recipient	Number of Copies
Office of Naval Research Code 473 Arlington, Virginia 22217 Attn: R. S. Miller	(3)
Defense Documentation Center Building 5 Cameron Station Alexandria, Virginia 22314	(12)
Naval Research Laboratory 4555 Overlook Avenue Washington, D. C. 20390 Attn: Technical Information Division	(1)
Code 2627	(6)
Code 2629	(6)
Code 6170	(1)
U. S. Naval Postgraduate School Monterey, California 93940 Attn: Dept. of Mechanical Engineering	
U. S. Naval Academy Annapolis, Maryland 21402 Attn: Dept. of Mechanical Engineering	(1)
Naval Air Systems Command Jefferson Plaza Washington, D. C. 20360 Attn: B. Poppert, Code 240E	(1)
Naval Sea Systems Command Crystal City, National Center #3 Washington, D. C. 20360 Attn: Code 033	(1)
Naval Ships Engineering Center Prince George's Center Hyattsville, Md. 20782 Attn: J. F. Dray, Code 6148D	(1)
Naval Ships R&D Center Annapolis, Md. 21402 Attn: Dr. R. McQuaide	(1)
Naval Air Engineering Center Lakehurst, New Jersey 08733 Attn: Mr. P. Senholzi	(1)

Recipient	Number of Copies
Naval Air Propulsion Test Center Trenton, New Jersey 08628 Attn: Mr. R. Valori	(1)
Naval Air Development Center Warminster, Pa. 18974 Attn: Mr. A. Conte	(1)
National Bureau of Standards Washington, D. C. 20234 Attn: Dr. W. Ruff	(1)
NASA Lewis Research Center 2100 Brookpark Road Cleveland, Ohio 44135 Attn: W. J. Anderson	(1)
Air Force Aeropropulsion Laboratory Wright-Patterson Air Force Base Ohio 45433 Attn: AFAPL/SFL	(1)
Army Research Office Durham, North Carolina 27706 Attn: Dr. E. A. Saibel	(1)
Office of Naval Research Branch Office 1030 East Green Street Pasadena, California 19906	(1)
Assistant Chief for Technology Office of Naval Research, Code 200 Arlington, Virginia 22217	(1)
Air Force Materials Lab/MBT WPAFB Ohio 45433	(1)
Goddard Space Flight Center Code 325 Greenbelt, Md. 20771 Attn: J. E. Stern	(1)
Office of Naval Research Branch Office 666 Summer Street Boston, Mass. 02210 Attn: Dr. F. S. Gardner	(1)
Commander, Defense Contract Administration Services District, Springfield 240 Route 22 Springfield, New Jersey 07081	(1)

Recipient	Number of Copies
Martin Marietta Laboratories 1450 South Rolling Road Baltimore, MD 21227 Attn: Mr. Jack S. Ahearn	(1)
Bell Laboratories 6200 East Broad Street Columbus, OH 43213 Attn: Dr. M. Antler	(1)
ALCAN Research Center P. O. Box 8400 Kingston, Ontario Canada K7L4Z4 Attn: Dr. Peter Ashley	(1)
Iowa State University of Science & Technology Department of Mechanical Engineering Ames, IA 50011 Attn: Professor Shyam Bahadur	(1)
Imperial College of Science and Technology Department of Mechanical Engineering Exhibition Road London, England SW7 Attn: Professor Alistair Cameron	(1)
Department of Mechanical Engineering University College of Swansea Singleton Park Swansea SA2 8PP, U. K. Attn: Professor F. T. Barwell	(1)
University of California at San Diego Energy Center 2836 Govat Avenue San Diego, CA 92122 Attn: Dr. Alan Beerbower Research Engineer	(1)
Department of Chemical Engineering Imperial College Prince Consort Road London SW7 2BY, U. K. Attn: Dr. B. J. Briscoe	(1)
NASA Lewis Research Center, M.S. 23-2 21000 Brookpark Road Cleveland, OH 44135 Attn: Dr. Donald H. Buckley Head, Fundamentals Section	(1)

Recipient	Number of Copies
Northwestern University Dept. of Mechanical Engineering and Astronautical Sciences The Technological Institute Evanston, IL 60201 Attn: Professor R. A. Burton	(1)
BAM (Federal Institute for Materials Testing) Unter den Eichen 87 1000 Berlin 45 West Germany Attn: Professor Horst Czichos	(1)
John Deere Waterloo, IA 50705 Attn: Mr. Pranab K. Das Engineering Specialist	(1)
Office of Naval Research Code 438 Arlington, VA 22217 Attn: Mr. Stanley W. Doroff	(1)
Virginia Polytechnic Institute Blacksburg, VA 24060 Attn: N. S. Eiss, Jr.	(1)
IBM Endicott Laboratories P. O. Box 6 Department E21 Endicott, NY 13760 Attn: Dr. P. Engel	(1)
Fundamental Research Section Research and Technical Department Texaco Research Center Beacon, NY Attn: R. Fein	(1)
Allegheny Ludlum Industries, Inc. 2000 Oliver Building Pittsburgh, PA 15222 Attn: Dr. Eugene F. Finkin Vice President	(1)
Battelle Columbus Laboratories 505 King Avenue Columbus, OH 43201 Attn: Dr. W. A. Glaeser	(1)

Recipient	Number of Copies
Chevron Research Company P. O. Box 1627 Richmond, CA 94802 Attn: Mr. Douglas Godfrey Senior Engineering Associate	(1)
Mechanical Technology, Inc. 968 Albany-Shaker Road Latham, NY 121100 Attn: Dr. Pradeep K. Gupta	(1)
Mechanical Development Department Research Laboratories General Motors Corporation Warren, MI 48090 Attn: D. F. Hays	(1)
Cornell University Sibley School of Mechanical and Aerospace Engineering Upson Hall Ithaca, NY 14853 Attn: Professor Said Jahanmir	(1)
DTNSRDC - ANNA Randallstown, MD 21402 Attn: Mr. Sidney A. Karpe Research Chemican Engineer	(1)
C. S. Draper Labs 555 Technology Square M. S. 42 Cambridge, MA 02139 Attn: Dr. E. Kingsbury Technical Staff	(1)
Pennsylvania State University 108 Chemical Engineering Building University Park, PA 15802 Attn: Professor E. E. Klaus	(1)
General Electric Co. Corporate Research Center P. O. Box 8 Schenectady, NY 12304 Attn: Dr. Ranga Komanduri	(1)
Texaco, Inc. P. O. Box 509 Beacon, NY 12508 Attn: Dr. Kenneth L. Kreuz Senior Research Associate	(1)

Recipient	Number of Copies
Department of Mechanical Engineering University of Hawaii 2540 Dole Street Honolulu, HI 96822 Attn: Professor Jorn Larsen-Basse	(1)
Department of Materials Science and Engineering M.I.T., Room 8-202 Cambridge, MA 02139 Attn: Professor Ronald M. Latanision	(1)
The Franklin Institute Philadelphia, PA 19103 Attn: Mr. L. Leonard	(1)
Renessaler Polytechnic Institute Department of Mechanical Engineering Troy, NY 12180 Attn: Professor Frederick F. Ling	(1)
Timken Company 1835 Dueber Avenue, S.W. Canton, Ohio 44706 Attn: W. E. Littmann	(1)
University of Michigan 2046 East Engineering Building Ann Arbor, MI 48104 Attn: Professor Kenneth Ludema	(1)
Mechanical Engineering Department Imperial College of Technology London, SW1, U.K. Attn: Dr. P. B. MacPherson	(1)
Mechanical Engineering Department M.I.T., Room 1-304C Cambridge, MA 02319 Attn: Professor Frank McClintock	(1)
Westinghouse R & D Center 1310 Beulah Road Pittsburgh, PA 05235 Attn: Dr. I. R. McNab	(1)
U. S. Army Watervilet Arsenal Benet Weapons Lab Watervilet, NY 12189 Dr. R. S. Montgomery Research Chemist	(1)

Recipient	Number of Copies
Wear Sciences, Inc. 925 Mallard Circle Arnold, MD 21012 Attn: Mr. Marshall Peterson President	(1)
University of Aston in Birmingham Gosta Green Birmingham B47ET, England Attn: Dr. T. F. J. Quinn Reader in Tribology	(1)
Department of Mechanical Engineering M.I.T., Room 35-010 Cambridge, MA 02139 Attn: Professor Ernest Rabinowicz	(1)
Westinghouse R & D Center Lubrication Mechanics 1310 Beulah Road Pittsburgh, PA 15235 Attn: Dr. A. A. Raimondi Manager	(1)
GM Research Labs GM Technical Center GM Corporation Warren, MI 48090 Attn: Mr. Fred G. Rounds	(1)
Mobil Research & Dev. Corp. Central Research Division P. O. Box 1025 Princeton, NJ 08540 Attn: Dr. C. N. Rowe	(1)
The Japan Petroleum Institute Nisseki Building 2-4, 3-Chome, Marunouchi Chiyodak-Ku Tokyo, Japan Attn: Dr. Toshio Sakurai Professor of Takai University	(1)
Department of Mechanical and Production Engineering Paisley College of Technology High Street Paisley PA1 2BE, UK Attn: Mr. Douglas Scott	(1)

Recipient	Number of Copies
Engineering Science Department Arizona State University Room ECG 247 Tempe, AZ 85281 Attn: Professor M. C. Shaw	(1)
Department of Mechanical Engineering Massachusetts Institute of Technology Room 35-136 Cambridge, MA 02139 Attn: Prof. Nam P. Suh	(1)
Department of Physics Cavendish Laboratory Madingley Road Cambridge University Cambridge CB3 OHE, U. K. Attn: Professor David Tabor	(1)
Fluid Power Research Center Oklahoma State University Stillwater, Oklahoma 74074 Attn: Dr. R. K. Tessman Program Manager	(1)
IIT Research Institute Department of Metallurgy 10 West 35th Street Chicago, IL 60616 Attn: Dr. Krishna C. Tripathi Manager	(1)
Department of Metallurgy and Materials Science University of Nottingham University Park Nottingham NG7 2RD, U. K. Attn: Professor R. B. Waterhouse	(1)
Foxboro/Trans-Sonics, Inc. P. O. Box 435 Burlington, MA 01803 Attn: Mr. Vernon C. Westcott	(1)
Mechanical Technology, Inc. 968 Albany, Shaker Road Latham, NY 12110 Attn: Dr. Donald Wilcock	(1)
Department of Mechanical Engineering Georgia Institute of Technology Atlanta, Georgia 30332 Attn: Prof. W. O. Winer	(1)

Recipient	Number of Copies
Department of Energy Division of Power Systems 20 Massachusetts Avenue, N. W. Mail Stop 2221C Washington, D. C. 20545 Attn: Mr. Martin Zlotnick	(1)